# Improving the filling jet schematisation through a lock door by taking into account the presence of a ship

O.D.M. van Loon

Delft University of Technology

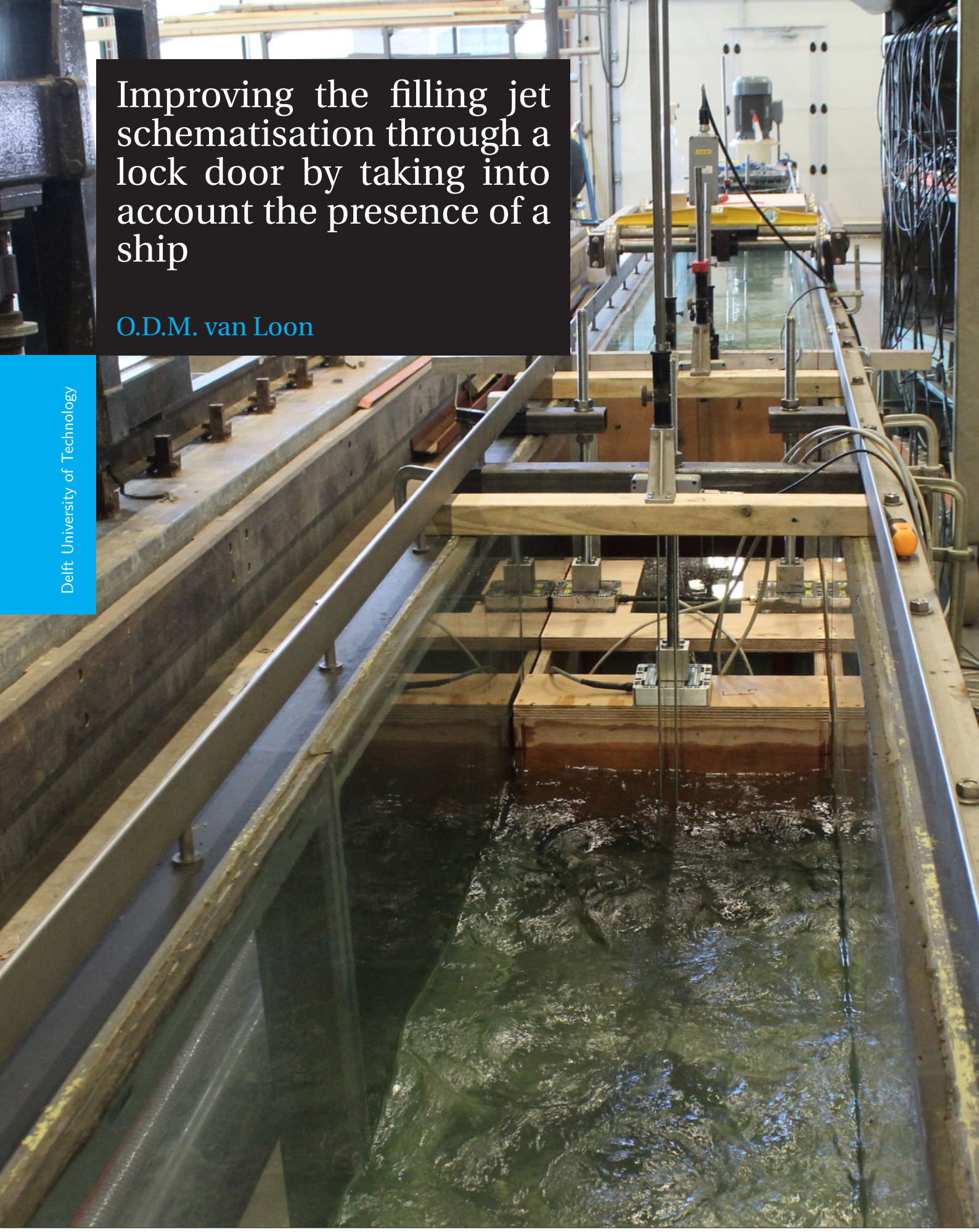

TU Delft Delft University of Technology

Challenge the future

# IMPROVING THE FILLING JET SCHEMATISATION THROUGH A LOCK DOOR BY TAKING INTO ACCOUNT THE PRESENCE OF A SHIP

by

**O.D.M. van Loon**

in partial fulfillment of the requirements for the degree of

**Master of Science**
in Hydraulic Engineering

at the Delft University of Technology,
to be defended publicly September 20th, 2017

| | | |
|---|---|---|
| Thesis committee: | Prof. ir. T. Vellinga | TU Delft |
| | Ir. P. P. D. van der Ven | Deltares |
| | Ir. H.J. Verheij | TU Delft |
| | Dr. ir. R.J. Labeur | TU Delft |

An electronic version of this thesis is available at `http://repository.tudelft.nl/`.

TU Delft Delft University of Technology

Deltares Enabling Delta Life

# PREFACE

This thesis is my graduation work for the master of science in hydraulic engineering at the Delft University of Technology. The research is performed in collaboration with Deltares and the subject was introduced by them. The thesis treats my efforts regarding the improvement of the filling jet schematisation in a lock. With the final goal a more optimised filling time in locks while still maintaining the needed safety levels. Even though I believe this research is a minor step within a larger study, I am proud to present my findings in this report.

A number of people deserve my thanks for their support during the research. First and foremost big thanks to Pepijn van der Ven, for his unwavering presence during the whole graduation process. Although bound by a tight schedule Pepijn always managed to find time to discuss the more difficult topics of my research. During every stage of the graduation he was able to assist where needed. The discussions we had almost always lead to new insights and in my opinion greatly improved the quality of the thesis.

I am grateful for the professional academic supervision that was available for my graduation, thanks to Tiedo Vellinga, Henk Verheij and Robert Jan Labeur. Our progress meetings gave direction towards the research when needed and I learnt a lot from the critical questions. Your supervision gave me confidence considering the relevance and progressiveness of the study.

A lot of different aspects where involved in this research, therefore quite a lot of people at Deltares were involved due to their varying specialities. Big thanks to all the colleagues at Deltares who assisted me during my time there. Special thanks to Arne van der Hout for helping me with the preparation, execution and processing of the scale model tests. Thanks to Marcel Busink and Marcel Grootenboer for realising the setup and help think of practical and realistic solutions for the problems faced during the weeks in the testing facility. Regarding the particle image velocimetry (PIV) measurements, thanks to Helena dos Santos Nogueira for her enthusiasm and expertise considering this difficult and advanced method of measuring. The PIV measurements with a ship were never performed before and could only be realised using the expertise available at Deltares, therefore also thanks to Paul Meys who helped with the calibration and installation of the laser. Although the scale model tests where a big highlight of this research, they where only this successful due to a good preparation made possible with a computational fluid dynamics (CFD) model. Tommaso Boschetti helped me a lot with realising this model. I would like to thank him for the extensive explanations which followed from his passion for this calculation method.

Last but not least I would like to thank my family who supported me during the graduation time. Special thanks to my mother who always motivated me during my study and amplifies my determination with her love and support. Thanks to my girlfriend and her parents for reviewing my report together, the different point of view was refreshing and useful. A final thanks to Ernst Vasbinder and Martsen Oostenbrug for improving the orthography of the report.

Orin van Loon,
Delft, August 18th, 2017

# ABSTRACT

Locks are used to enable ships to travel from one water body to another. Usually there is a water level difference between the two water bodies that needs to be overcome by levelling the water in the lock. This report treats the calculation of longitudinal forces on a ship in a lock chamber due to the levelling procedure. The focus will be on the force resulting from the filling jet through the levelling door in the lock. The main point of interest is the interaction between the ship and the flow resulting from the filling jet. To understand more about this interaction the following methods are used: the one-dimensional software model Lockfill, computational fluid dynamics (CFD) and scale model tests.

This study was initiated in the context of improving the accuracy and applicability of the software Lockfill. Lockfill is based on the conservation laws of mass and momentum, while schematising the flow using a two-dimensional parameterization of the filling jet. In previous studies conducted to improve Lockfill, the following problem was noticed: the current schematisation in Lockfill does not include an interaction between the flow pattern in the lock and the ship. In reality the ship will have a certain influence on the flow pattern induced by the filling jet. Therefore this research focuses on the schematisation of the filling jet in front of the ship. Two different effects will be considered which can hardly be treated separately because they are closely connected. The first effect is that of the ship on the flow pattern between the lock gate and the ship. The second effect is the influence of this flow pattern on the forces acting on the ship.

Theory considering the jet behaviour in the presence of a ship is not yet fully complete, therefore it was decided that additional scale model measurements were necessary. A two dimensional situation was created for the scale model, neglecting variations over the width of the lock. The prototype of the scale model is based on typical dimensions of locks and inland ships in the Netherlands. The scaled situation was tested using a CFD model to prepare for the scale model measurements. This preparation revealed that the jet attaches to the bottom for the chosen geometry. A normative position of the ship was defined based on the minimum keel clearance and minimum distance from the gate. The flow in the lock was measured for the situation with the ship in the normative position and the situation without ship. The flow measurements consist of multiple point measurements in the lock performed with an electromagnetic velocity meter (Dutch abbreviation: EMS) and particle image velocimetry (PIV) measurements just downstream of the gate. The longitudinal forces on the ship were measured for variations in: keel clearance, downstream position of the ship with respect to the gate and water level difference over the gate.

The EMS point measurements revealed vertical flow profiles that visually correspond to the expectations based on the CFD calculations. Although some small variations over the width were observed it was decided to maintain the two dimensional approach. Furthermore, a velocity profile found with the EMS measurements was compared to a velocity profile measured with PIV. These two different measurement methods correspond very well, emphasising the trustworthiness of both measurement methods. To determine forces on the ship from the velocity information the momentum flux in front of the ship must be determined. This was done for both the PIV measurements and the Lockfill jet schematisation. The measured momentum flux follows the same trends as the Lockfill jet schematisation, however the exact values can strongly deviate especially further from the gate.

The presence of the ship reduces the deflection of the jet towards the bottom. The reason for the reduced deflection is the interference of the ship's bow with the upper eddy limiting the fluid motion. This results in a reduction of pressure and therefore a deflection of the jet in the upward direction. This means that the momentum flux in the jet for the situation without ship decreases faster because it attaches to the bottom closer to the gate. Furthermore, the discharge in the jet with ship reaches a higher maximum since the lower eddy is bigger and thus provides a larger distance over which entrainment is possible.

The measured forces were compared to the forces Lockfill would predict for the same situation. For the normative situation forces calculated with CFD and the PIV flow field were compared to the measurements as

well. Both CFD and PIV overestimate the forces with a small relative error of less than +4%. Lockfill performs well when the ship is placed close to the gate but deviates significantly when the ship is placed further downstream. The reason for the strong deviation is the incorrect schematisation of the jet.

In conclusion, Lockfill determines the force on the ship accurately as long as the momentum flux can be determined successfully. Determining the momentum flux comes down to a correct schematisation of the filling jet. Variations in keel clearance and discharge are covered quite well by Lockfill. However an increase in distance from the gate reveals big differences compared to the measurements. This is caused by an overestimation of momentum flux dissipation in the Lockfill jet schematisation. The reason for this is that in reality the jet stays more attached to the bottom, therefore maintaining a higher momentum flux.

Taking into account the results from this study, the improvement of Lockfill should start with the schematisation of the filling jet. Preferably it should be improved in such a way that the momentum flux in front of the bow of the ship is determined accurately for every position of the ship in the lock. A start can be made by implementing the tendency of the jet to attach to a boundary.

# CONTENTS

# LIST OF SYMBOLS

| | | |
|---|---|---|
| $a$ | $[m]$ | Distance from the bottom to the opening in the gate |
| $\vec{a}$ | $[m/s^2]$ | Acceleration |
| $A$ | $[m^2]$ | Area |
| $2b_0$ | $[m]$ | Size of the opening in the gate |
| $C$ | $[m^{\frac{1}{2}}/s]$ | Chézy coefficient |
| $C_d$ | $[-]$ | Discharge coefficient |
| $C_1$ | $[-]$ | Coefficient for pressure reduction in front of the bow |
| $C_2$ | $[-]$ | Coefficient for the area of the jet hitting the bow |
| $C_3$ | $[-]$ | Coefficient for boundary layer development |
| $d$ | $[m]$ | Draught of the ship |
| $dt$ | $[s]$ | Time between laser pulses |
| $D$ | $[m]$ | Distance between the centre line of the jet and the bottom |
| $F$ | $[N]$ | Force (specifics denoted in subscript) |
| $g$ | $[m/s^2]$ | Gravitational acceleration |
| $h$ | $[m]$ | Water depth (position denoted in subscript) |
| $H$ | $[m]$ | Distance between the centre line of the jet and the water surface |
| $h_s$ | $[m]$ | Height of the ship |
| $i$ | $[m/m]$ | Slope of the water surface |
| $k_c$ | $[m]$ | Keel clearance |
| $k_s$ | $[m]$ | Nikuradse surface roughness |
| $L$ | $[m]$ | Length scale |
| $l$ | $[m]$ | Length (object denoted in subscript) |
| $m$ | $[kg]$ | Mass |
| $n$ | $[s/m^{\frac{1}{3}}]$ | Manning roughness |
| $N$ | $[-]$ | Number of data values |
| $Q$ | $[m^3/s]$ | Discharge (specifics denoted in subscript) |
| $R$ | $[m]$ | Hydraulic radius |
| $Re$ | $[-]$ | Reynolds number |
| $S$ | $[kgm/s^2]$ | Momentum flux (specifics denoted in subscript) |
| $S_{block}$ | $[-]$ | Blockage factor |
| $t$ | $[m]$ | Thickness of the gate |
| $U$ | $[m/s]$ | Velocity (specifics denoted in subscript) |
| $w$ | $[m]$ | Width (object denoted in subscript) |
| $x_b$ | $[m]$ | Distance between the gate and the ship |
| $x_i$ | $[-]$ | Value of $x$ at entry point $i$ |
| $x_1$ | $[m]$ | Distance between the gate and the front most part of the ship |
| $\bar{x}$ | $[-]$ | Average of all $x$ values |
| $X_{bow}$ | $[m]$ | Distance between the gate and the bottom of the ship |
| $\alpha$ | $[^\circ]$ | Angle of the jet |
| $\beta$ | $[^\circ]$ | Angle of the bow |
| $\lambda$ | $[-]$ | Scale factor |
| $\mu$ | $[Ns/m^2]$ | Dynamic viscosity |
| $\nu$ | $[m^2/s]$ | Kinematic viscosity |
| $\rho$ | $[m^3/s]$ | Density (fluid denoted in subscript) |
| $\sigma$ | $[-]$ | Population standard deviation |

# 1

# INTRODUCTION

This report treats the calculation of longitudinal forces on a ship in a lock chamber due to levelling the water in the lock. The focus will be on the force resulting from the filling jet through the levelling door in the lock. The main point of interest is the interaction between the ship and the flow resulting from the filling jet. To learn more about this interaction the following methods are used: the one dimensional software Lockfill, computational fluid dynamics and scale model tests.

In this chapter the reader will become familiar with the following topics: the context of the research and existing calculation methods for the longitudinal forces on a ship in a lock. Once these topics are explained the problem description for this research is given, whereby the schematisation of the force in the program Lockfill is chosen as main point of interest. The problem description leads to the definition of the objectives and the methodology for successfully completing these objectives. At the end of the introduction a reading guide can be found in which the different phases of the study are explained step by step.

## 1.1. ENGINEERING CONTEXT

Locks are used to enable ships to travel from one water body to another. Usually there will be a water level and/or salinity difference between the two water bodies that needs to be overcome. Two main concepts need to be considered when optimising the design of the levelling procedure: the time it takes for ships to pass the lock and the safety level that needs to be maintained during this procedure. For economical reasons it is important that ships experience as little delay as possible when passing a lock. Minimising the time it takes to complete a locking cycle will benefit the number of ships that can pass the lock per day. Additionally, the average waiting time of each individual ship will be shorter. A shorter delay results in less time lost while passing the lock and will thus save money. Although the lock ideally operates as quickly as possible, safety levels need to be taken into account. A high safety level implies a low chance on accidents during the locking cycle. Locks are therefore designed to cause as little delay as possible, while still operating within the safety guidelines.

An important factor that contributes to the time it takes to complete a locking cycle is, the filling/emptying time of the lock. The filling/emptying time is greatly influenced by the amount of water that can safely be let into or out of the lock. Part of these safety restrictions are the occurring longitudinal forces on the ship(s) in the lock. The total longitudinal force can be split into different components. The following five main contributors to the net longitudinal force on a ship in the lock can be distinguished:

1. A translatory wave will be formed while filling through a lock gate. Caused by the variation of discharge into the lock over time. The translatory wave will result in an oscillating force on the ship.

2. The discharge decreases over the length of the lock, this is a direct result of the increasing part of the lock which is already filled. The constantly decreasing discharge means a momentum decrease in longitudinal direction. The momentum decrease results in a water level slope and thus a force directed towards the active lock gate.

3. Friction between the hull and the flow around the ship results in a longitudinal force component in the same direction as the flow. A secondary effect is that the friction on the ship and the bottom/walls of the lock induces a slope in the water level, resulting in an additional component directed away from the active lock gate.

4. When present, the filling jet can have a direct flow force on the ship. The filling jet is the result of the concentrated flow into the lock. It is common to reduce this effect by implementing breaking bars, the bars will ensure that the flow is spread out over the wet cross-section of the lock. This induces a less concentrated flow profile and thus lower forces against the ship.

5. Density differences result in a density driven flow and thus in an additional force on the ship. Of course there needs to be a density difference between the water in the lock chamber and the approach channel, otherwise this force component will be zero.

## 1.2. CALCULATION METHODS FOR THE LONGITUDINAL FORCES

There are a number of different types of numerical models available to calculate the longitudinal forces on a ship in a lock. These models range from highly schematised zero-dimensional approximations to complex three-dimensional models where the flow and fluid-structure interaction are calculated in detail. Increasing the complexity will also increase the computation time and expertise required by the user. The degree of complexity that is needed often depends on the design stage of the lock. For the initial design or a rough estimate a simple model often provides enough information, while having the benefit of requiring little computation time.

An example of a relatively simple model is the program Lockfill, which is developed by Deltares. This is a validated one-dimensional program that uses cross-sectional averages to determine the force on the ship. The validation of the program is mainly done using scale model measurements of existing shipping locks in the Netherlands. The fast computational process can describe various levelling systems. Starting with the difference in initial water level over the lock head, the water level variation and flow in the lock chamber over time can be determined. From these two parameters the longitudinal force components can be derived using the conservation laws for momentum and mass.

Because of the high level of schematisation and the one-dimensional calculation principles used in Lockfill, the calculation time is very short (order of seconds). Especially when compared to the calculation time of more complex alternatives. For example, a three-dimensional finite element calculation methods like CFD, which has a calculation time in the order of several hours or days. This makes Lockfill very useful for calculations during the initial design phase of projects, where often calculation speed is equally important to the accuracy of the results. However, in the past years the demand for higher accuracy in the schematised calculations increased significantly. Therefore, Deltares is looking to improve the accuracy and applicability of Lockfill.

## 1.3. PROBLEM DESCRIPTION

In the context of improving the accuracy of the calculated longitudinal forces on a ship in a lock using the Lockfill schematisation, the following problem was noticed. The current schematisation in Lockfill does not include an interaction between the flow pattern in the lock and the ship. In reality the ship will have a certain influence on the flow pattern induced by the filling jet. This problem was already noticed during the development of the program. In Vrijburcht et al. (1988) is mentioned that, the current theory cannot determine the degree of influence that the ship has on the flow pattern. In a later study (De Loor 2012), meant to analyse the performance of the software, is mentioned that the schematisation of the filling jet, with the presence of the ship, can still be improved a lot. Especially, because the filling jet is often a significant component of the longitudinal force.

This research will focus on the schematisation of the filling jet in front of the ship. Considering two different effects which can hardly be treated separately, because they are closely connected. The first effect is that of the ship on the flow pattern between the lock gate and the ship. The second effect is the influence of this flow pattern on the forces acting on the ship. During the analysis of the Lockfill calculation method some other possible improvements were noticed, these will be discussed in section 2.4.4.

## 1.4. OBJECTIVE AND RESEARCH QUESTIONS

The main goal for this study will be to establish an understanding of the interaction between the jet flow and a ship in the lock. This includes both the effect of the ship on the flow and the resulting forces on the ship due to the flow. The location of the ship is of great import considering the magnitude and direction of the forces on the ship. This is a consequence of the flow in the lock, which changes due to the position of the ship. In this research the focus will be on the flow pattern in front of the ship and the forces resulting from different positions of the ship.

To ensure that the stated goal is reached the following main research question is formulated:

*"To what extend does a ship in a lock influence the flow pattern in front of the ship and how does the position of the ship influence the longitudinal forces on the ship?"*

Additional sub questions which help to solve the main question are:

1. *"How are the longitudinal forces on the ship determined in Lockfill?"*
2. *"What differences can be noticed when looking at the flow pattern in the lock, with and without a ship in the lock and can this be quantified by means of the momentum flux?"*
3. *"How do the forces determined with Lockfill and the scale model measurements compare to each other?"*

## 1.5. METHODOLOGY

In this section a step by step methodology for this thesis project is formalised. The presented methodology will be used to answer the formulated research questions and consequently reach the project goal. Each sub question will be mentioned at the research activity, in which they are expected to be answered. The following research activities are part of this methodology and can be seen as the research program:

1. Study relevant literature to get a better understanding of the problem and possible solutions. This includes an extensive analysis of Lockfill and liquid jet behaviour.
2. Use a CFD model to prepare for scale model measurements.
3. Perform scale model tests where both the flow in the lock and the forces on the ship will be measured.
4. Compare the results of Lockfill, CFD and scale model measurements with each other.

### 1.5.1. LITERATURE STUDY

In order to understand the Lockfill calculation methods, which are used to determine the forces, the sub question: "How are the longitudinal forces on the ship determined in Lockfill?" must be answered. This can be achieved by studying the derivations of the different force components in Lockfill. By knowing how the forces in Lockfill are determined, possible improvements can be suggested and further researched.

To understand the flow in the lock due to the incoming filling jet, a better understanding of filling jet behaviour is needed. For this purpose literature about liquid jet behaviour will be studied extensively. Furthermore the relevant force contributions will be calculated using a momentum balance. Although commonly known in the field of engineering, an explanation and derivation of the momentum equations will be provided in the report because it is such an important part of this research.

### 1.5.2. PREPARATIONS FOR THE SCALE MODEL TESTS INCLUDING CFD CALCULATIONS

In preparation of scale model tests a two-dimensional CFD model can be set up. Important to note is that the CFD model will simulate stationary flow. The discharge and water level will not vary in time. For clarification, the model does not simulate the levelling process but only the initial flow into the lock. This corresponds with the scale model measurements that will be performed. A non-stationary model is not required when looking at the schematisation of the filling jet. The purpose of the CFD model is mainly to detect unexpected features of the flow and forces before the scale model is realised. This will prevent mistakes in the scale model setup which will be way more time consuming and expensive to fix.

### 1.5.3. SCALE MODEL MEASUREMENTS

The scale model measurements will be performed at the water-soil flume at Deltares. Before the measurements can be performed, a lot of preparation is required. Fortunately comparable scale model tests were

already performed at Deltares, see Van Velzen & Dos Santos Nogueira (2015). The report of the tests can serve as a reference for this study. Different measurement techniques were used to determine the flow velocities in the scale model. For the scale model measurements that will be performed as part of this study, the EMS and PIV measurement techniques will be used. This gives the possibility for local velocity measurements and a good impression of the entire flow field. The laser doppler velocimetry (LDV) technique used in Van Velzen & Dos Santos Nogueira (2015) is also valuable but it does not provide additional information nor accuracy and is thus not used in the present study.

Two different measurements will be performed. First the forces on the vessel for different positions in the lock will be measured. When the forces on the ship for different positions are known the flow pattern just downstream of the gate will be recorded using a PIV setup. This will be done for a case without a ship in the lock and a case with a ship in the lock. This means that it will be possible to answer the sub question: "What differences can be noticed when looking at the flow pattern in the lock, with and without a ship in the lock and can this be quantified by means of the momentum flux?".

### 1.5.4. COMPARISON OF THE RESULTS OBTAINED WITH DIFFERENT METHODS

After the scale model test the required data will be available and different comparisons can be made. While analysing the results from the scale model tests the sub question, "How do the forces determined with Lockfill and the scale model measurements compare to each other?" can be answered. It will be interesting to see if the measured forces correspond to the forces Lockfill would calculate in the same conditions. The key here is to understand the differences and agreements between the tests and Lockfill.

Furthermore the flow pattern with and without ship can be compared to each other to see if the presence of the ship influences the flow. This can be approached in two ways, qualitatively and quantitatively. With a qualitative analysis the spreading and direction of the jet are visualised and compared for the different methods. For the quantitative analysis the momentum in the jet for a number of cross-sections is determined, giving an indication of the momentum flux it contains.

## 1.6. READING GUIDE

Figure 1.1 gives an overview of the different aspects included in this study. On the right the four main phases of the project structure are presented. Then on the left the subsequent steps and their expected results are visualised. The interactions between the different aspects are explained by means of arrows. The end results of this research are placed in the bottom left.

First, a literature study regarding fluid motion and methods to determine forces on an object in the fluid is conducted. Within the subject of fluid motion the main interest lies within the behaviour of turbulent jets. Furthermore, an analysis of the program Lockfill will be performed to get a better understanding of the problem introduced in Section 1.3. The combination of the knowledge gained from the literature study and the analysis of Lockfill will help to find possible improvements for the force predictions in Lockfill. This will be described in Chapter 2.

In Chapter 3 the prototype for the scale model tests is elaborated. The prototype is based on average dimensions for ships and locks in the Netherlands, while the position of the ship is taken to be as extreme as possible resulting in a normative situation. The scaling of the prototype to normative model conditions will be discussed. Before the scale tests are performed a relatively small CFD study is performed to support the scale model tests.

Chapter 4 covers the scale model tests. The setup, equipment and measurement details are discussed. Three types of measurements will be performed: velocity point measurements to map the velocity in the flume and check if it corresponds to the expectations, force measurements on the ship at different locations in the flume and PIV measurements to get an accurate two-dimensional flow field just after the gate. The PIV measurements will be performed for both the situation with ship in the flume and without ship in the flume.

The results of the scale model tests are given in Chapter 5. The results in this chapter are raw results and thus not edited in any way. Just like the measurements the results are subdivided into three parts. First the flow

in the flume is discussed based on point measurements at strategic positions in the flume. Then the force measurements for the ship at different positions in the flume are elaborated. Lastly the results from the PIV measurements are presented. All the measurement results are made available at http://researchdata.4tu.nl, the DOI of the dataset is 10.4121/uuid:0aff8af7-9baa-40be-8f4f-45bed1b31062.

In Chapter 6 the data gathered from the measurements is compared to the existing knowledge in the form of the calculation method of Lockfill. The momentum flux in the jet is studied extensively since this is found to be one of the main contributors to the force on the ship. Once the momentum flux can be determined and also predicted, the force on the ship can be found based on the flow.

The conclusions of this research are presented in Chapter 7. This chapter also covers recommendations for further research.

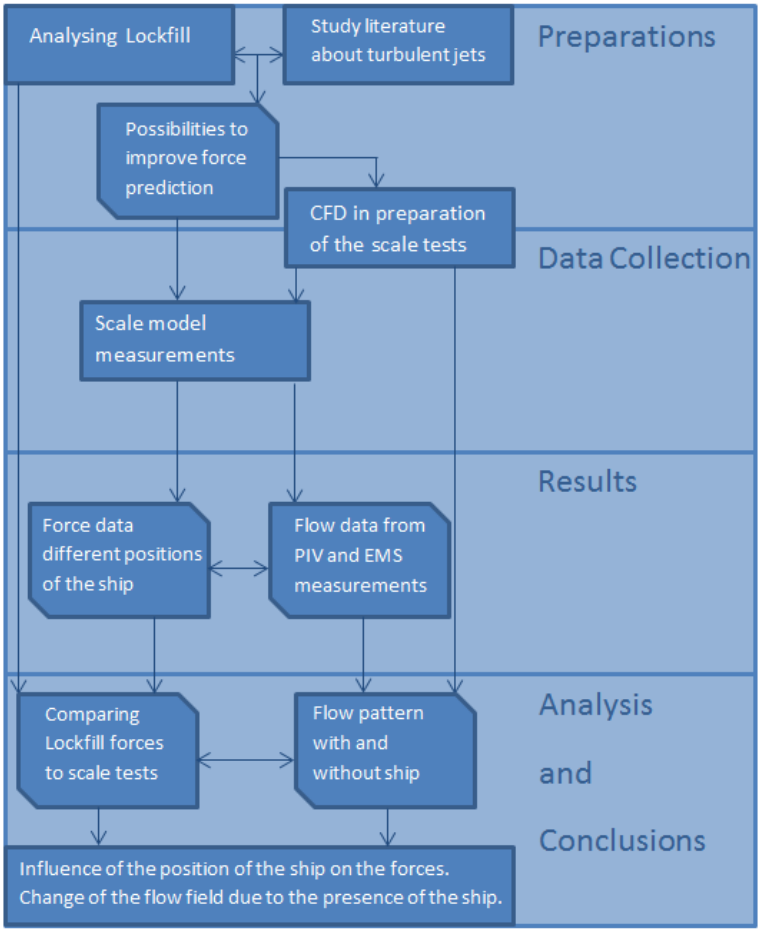


Figure 1.1: Flow chart explaining the different aspects and their interaction

# 2

# THEORETICAL BACKGROUND

In this chapter some theoretical background that is essential for this study is presented. As part of the literature study the following subjects are considered:

1. Relevant theory and equations to describe the fluid motion.
2. Determining the longitudinal force on a ship in a lock.
3. Behaviour of turbulent water jets.
4. Force schematisation in Lockfill.
5. Computational fluid dynamics and the software Star-CCM+

For the subjects mentioned above the information needed to understand the content of this report is provided as much as possible. Some aspects are elaborated in depth because they play a major role in this study. Other aspects are discussed only briefly because a basic understanding of those aspects is sufficient for the reader of this thesis. For additional information about a specific subject the reader is sometimes referred to an appendix.

## 2.1. DESCRIBING FLUID MOTION

It is essential to understand how fluid in motion is behaving and how forces on an object in the fluid can be determined using the flow velocity. Therefore the following topics were researched: mass balance, momentum balance and turbulence. Turbulence was not studied in great detail, because it will not play a huge role in answering the research questions and the influence of turbulence on the jet behaviour will be addressed when studying jet behaviour.

### 2.1.1. MASS BALANCE

The mass balance is a very important concept in fluid mechanics. It basically states that the net inflow of mass into an elementary control volume over time should be equal to the mass outflow over that same time. This assumes that the fluid is incompressible, in other words the density of the fluid is constant over time, which is a valid assumption for water. The derivation of the mass balance and the resulting continuity equation are elaborated in Appendix A. Here the continuity equation for one dimensional steady flow is displayed, see Equation 2.1. This equation states that the mass of water flowing into an certain area of interest, denoted with subscript 1, is equal to the mass flowing out of the area, denoted by subscript 2.

$$\rho * A_1 * U_1 = \rho * A_2 * U_2 \tag{2.1}$$

Where:

$A$ = the area over which the flow enters or leaves the area of interest $[m^2]$
$U$ = the velocity of the fluid entering or leaving the area of interest $[m/s]$
$\rho$ = the density of the fluid $[kg/m^3]$

### 2.1.2. MOMENTUM BALANCE

The balance of momentum formalised for fluid mechanics finds its origin in the second law of Newton. The net force acting on a given mass is proportional to the time rate of change of linear momentum of that mass. For a constant mass this can be written as $\vec{F} = m * \vec{a}$. When considering a fluid with free surface between two sections, the momentum balance can be formulated as in Equation 2.2. For additional information the reader is referred to Appendix A or for the complete derivation to Van Rijn (2011). For the cases treated in this study there will be no density difference, so $\rho_1 = \rho_2$. If there is a salinity difference over the lock the density will not be constant between the two sections. In Figure 2.1 the momentum balance is illustrated.

$$\frac{1}{2}\rho_1 g h_1^2 - \frac{1}{2}\rho_2 g h_2^2 + \rho_1 h_1 U_1^2 - \rho_2 h_2 U_2^2 - F_{sink} = 0 \tag{2.2}$$

Where:

$h$ = the water depth at the section defined in the subscript $[m]$
$U$ = the velocity at the section defined in the subscript $[m/s]$
$F_{sink}$ = the force sink between the two sections $[N]$


Figure 2.1: Sketch of the momentum balance as described in Equation 2.2

### 2.1.3. TURBULENCE

Almost every flow in nature is turbulent, however it is very difficult to give an exact definition of turbulence. In Van Rijn (2011) it is stated that, "Turbulence is an irregular fluid motion in which the variables show random variation in space and time". The most important characteristics of turbulence are:

1. Irregularity or randomness requiring a stochastic approach when solving turbulent problems.
2. Diffusivity resulting in rapid mixing of mass, heat and momentum.
3. Fluctuations in all directions making it three-dimensional.
4. Kinetic energy is dissipated due to viscous action.

A common way to check if a flow is turbulent is with the Reynolds number $Re = (UL)/\nu$). For high Reynolds numbers ($Re > 3500$) the flow is characterised as turbulent and for low Reynolds numbers as laminar ($Re < 2300$). This is mainly true for flow in pipelines. For flow with a free water surface the degree of turbulence depends on the geometry and hydrodynamic conditions. A source for turbulent fluctuations can be shear in the mean flow. This is the case when velocity gradients are present in the flow. In case of turbulence due to velocity gradients, but without the presence of a fixed wall or boundary the turbulence is called free turbulence. The faster moving fluid particles will accelerate the slower particles, which in turn decelerate the faster moving particles. In other words, along the shear plane between the water bodies with different velocities energy is transferred from the faster particles to the slower particles. This process continues until both bodies have the same velocity.

In this study mainly time averaged situations are studied. Averaging over time will diminish the importance of turbulence since it is characterised as random and will average out over time if the conditions remain constant. However, it is still an important mechanism that determines the spreading of a jet entering a stagnant fluid body. This will be treated further in Section 2.3.

## 2.2. RELEVANT LONGITUDINAL FORCES

Five different force components on the ship in the lock during levelling are mentioned in Chapter 1. For this study a stationary situation will be considered i.e. the discharge and water level will not vary over time. A stationary flow can be assumed because the full locking cycle will not be considered and each small time step within the locking cycle can be schematised as a stationary situation. Due to the assumption that the considered situation is stationary, no translatory wave will be generated. This force component will therefore not be considered. Furthermore, there will be no density differences between the water in the lock chamber and the water in the approach channel. The density driven force is therefore also irrelevant to consider. The components that are still relevant are:

1. The force resulting from momentum decrease over the length of the lock.
2. The direct force from the filling jet on the bow of the ship.
3. The friction between the water flow and the hull, wall and chamber floor.

### 2.2.1. FORCE RESULTING FROM MOMENTUM DECREASE

Two separate components result in a momentum decrease over the length of the lock. Firstly, the velocities from the concentrated filling jet decrease in the longitudinal direction, because of the filling jet is spreading over the water body. Secondly, the discharge decreases in the longitudinal direction because the part of the lock that still needs to be filled gets increasingly smaller. The decrease in discharge results in a decrease in average flow velocity, assuming the wet cross-section remains constant. Lower discharge and velocity means a decrease in momentum over the length of the lock. The momentum decrease results in a water level difference between the bow and the stern and thus a force in the direction of the lock head. This is visualised in Figure 2.2.

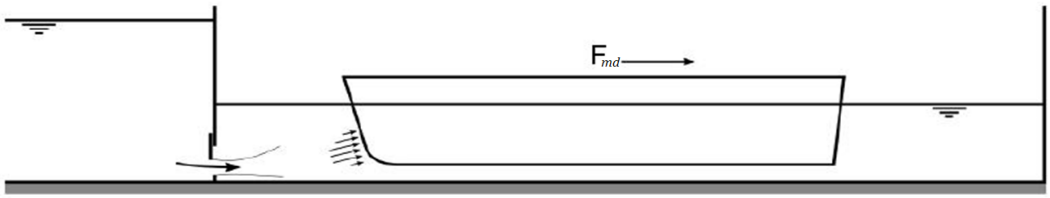


Figure 2.2: Schematic of the force due to momentum decrease during filling (Deltares 2016)

The presence of the ship is not yet taken into account. A ship will make the wet cross section locally smaller and therefore increase the flow velocity, consequently decreasing the water level. This effect can be included by means of a ratio between the wet cross-section with the ship and the wet cross-section without the ship, using the principle of mass conservation in longitudinal direction.

### 2.2.2. FORCE DUE TO THE IMPACT OF THE FILLING JET

When the ship is deep enough in the water the filling jet will collide with the bow of the ship. The resulting positive force component, schematised in Figure 2.3, can be calculated using a formulation that considers the flow pressure against the bow (Samson 1972). It is possible to implement a hull angle that corresponds with the dimensions of the ship. In that case the component perpendicular to the bow should be calculated to determine the force. When the ship is positioned high in the water column, the jet will pass under the ship without a collision and this force component will then equal zero.

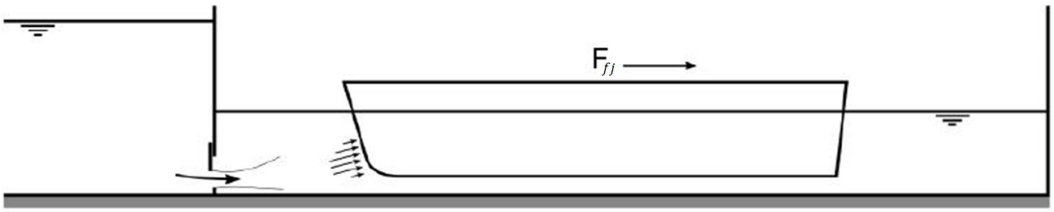


Figure 2.3: Schematic of the force from the filling jet (Deltares 2016)

### 2.2.3. FORCE DUE TO FRICTION

The friction force in a lock is not a direct effect of the filling jet but from the mean flow in the lock. The friction force has two components:

1. The friction between the hull and the water flow around the ship, causing a force in the flow direction.
2. The flow along the lock chamber floor and walls causes a friction force. Due to the energy dissipation associated with this friction a water level difference will occur, this is visualised in Figure 2.4.

The resulting friction effect can be calculated using the Chézy formula and the formulas of Stickler and White-Colebrook.

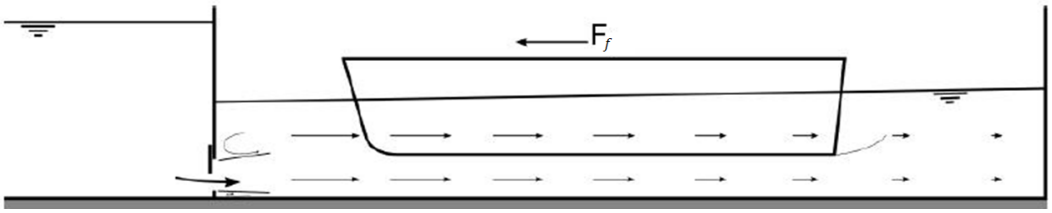


Figure 2.4: Schematic of the force due to friction (Deltares 2016)

## 2.3. TURBULENT JETS

During the levelling procedure water flows from one water body to another as a consequence of opening the locking gate and the water level difference over the gate. In the lower water body a turbulent jet is formed starting at the entry point. When filling the lock the jet will be inside the lock chamber, dominating the flow pattern close to the gate and influencing the flow pattern in the entire lock. In the coming subsections a lock with only one gate and thus one turbulent jet is considered, but in theory every opening will have its own jet. These jets can, depending on the geometry, either merge or continue solitary. Gates close to each other produce jets who are likely to merge and at gates with a significant distance between each other solitary jets will likely be observed. This is mostly a transverse effect and in this study the physics in the vertical and longitudinal direction are most important, since the focus lies on improving Lockfill in which the transverse direction is not taken into account. Including the transverse direction in Lockfill can be an improvement made in the future, but for now a two-dimensional approach is preferred. Therefore, spreading over the width of the lock is assumed to be uniform for most of the cases. The right terminology for a two dimensional jet is plane jet.

The subject turbulent jets will be explained step-by-step. Starting with a plane free jet in infinite water, which is a theoretical jet that is not influenced by any boundary conditions. Introducing upper and lower boundaries will result in a plane jet in confined water. By implementing a boundary perpendicular on the stream an impinging jet is formed. Finally, some findings about other geometrical effects will be elaborated also introducing the Coanda effect.

### 2.3.1. PLANE FREE JET IN INFINITE WATER

In this subsection a free jet is considered, this implies a jet which is not influenced by any boundary effects. In other words a jet in a semi infinite volume. Like mentioned before only the behaviour of the jet in longitudinal and vertical direction are considered, resulting in a two-dimensional approach. In theory effects like spreading should be comparable in the transverse direction, but are less important in this study since the aim is not to improve Lockfill in transverse direction.

When considering a jet in infinite stationary water, the jet will start spreading as soon as it leaves the entry point. The angle at which the jet spreads relative to the centre line is determined experimentally and was found to be 1:6 (9.46 degrees), see Figure 2.5. The physical mechanism that induces this spreading is a turbulent mixing at the shear layer between the jet and the stagnant fluid. These so called mixing layers are found on both sides of the yet and do not only penetrate outwards but also inwards, see Figure 2.5. The inward penetration has a smaller angle 1:12, resulting in a region between the upper and lower mixing layer. This region is called the potential core and in the potential core the original velocity is preserved. Due to the given angle, the length of the potential core is found to be 6 times the height of the jet nozzle. The area in which the

potential core is still present is called the flow development region (Rajaratnam 1976). After the flow development region a second region starts, called the fully developed flow region. In this region no potential core is present and the outer spreading angle of the mixing layer increases to 1:4.

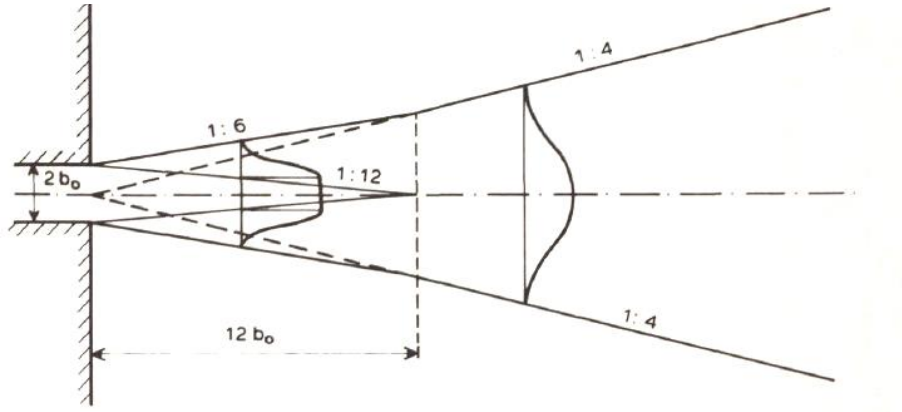


Figure 2.5: Geometry of a free jet in infinite water (Vrijburcht et al. 1988)

Now that the boundaries of the free jet are defined the velocity profiles within the jet will be elaborated. The velocity profile in the potential core is rectangular because the initial velocity is preserved and assumed uniform. In the fully developed region the velocity is maximum at the centre line and at the outer edges of the jet boundaries the velocity is zero. The transition between the maximum and the outer edge is described by a smooth Gaussian curve. In the fully developed region the velocity profile is self similar, meaning that the shape of the profile remains the same if the length scale changes. Due to energy dissipation the maximum velocity in the jet will slowly decrease in longitudinal direction. However, the free jet in open water is a theoretical example with no boundaries. Looking at the limit state, at an infinite distance from the point of entry, the jet will be infinitely wide, with an infinitely small velocity. The energy will thus be fully dissipated.

The net momentum of the jet is constant in longitudinal direction, because there is no pressure gradient that can compensate for the momentum loss. Basically, the momentum should remain constant because there is no mechanism which can induce a momentum loss. However, the velocity does decrease, so there must be a mechanism keeping the momentum constant. This mechanism can be found in the entrainment of the surrounding water, the free jet will entrain water from the surrounding fluid body increasing the amount of water transported by the jet. This means that the surrounding fluid is in slow motion towards the active jet. The discharge increase in the jet in longitudinal direction combined with simultaneous velocity decrease results in a constant momentum in the jet.

### 2.3.2. PLANE JET IN CONFINED WATER

This subsection treats the influence of the water surface and the bottom of the lock on the jet. Due to these boundary restrictions the jet is no longer a free jet. There are two main differences, compared to the free jet. One, the pressure gradient due to the flow can be translated to a change in free water surface, in the sense that the water surface can react on the pressure by changing its position in the vertical. Two, it is no longer possible to entrain water unrestrictedly. These differences can be noticed even before the jet flow reaches the boundaries and are mainly important for the conservation of momentum.

The presence of the free water surface and its adaptation to the flow conditions make it possible for the confined jet to lose momentum in the the longitudinal direction. Whereas, the free jet could never lose momentum this way. The boundaries restrict the water entrainment, due to these restrictions eddies will be formed under and above the jet. The size of these eddies is determined by the available space between the jet and the boundary. Within the eddies there is no net loss of fluid, so the water that is entrained from an eddy by the jet will later on be returned.

Taking the introduced effects of the water surface and the formed eddies into account, the following can be argued considering the momentum in the jet:

1. Within the transition area the momentum is constant. The effect of withdrawing discharge from the eddies and the effect of dispersion of the velocity field cancel out.
2. After the transition area the momentum will decrease significantly. The discharge will decrease because the filling jet will yield water back to the eddies and the flow velocity will decrease even further due to dispersion.

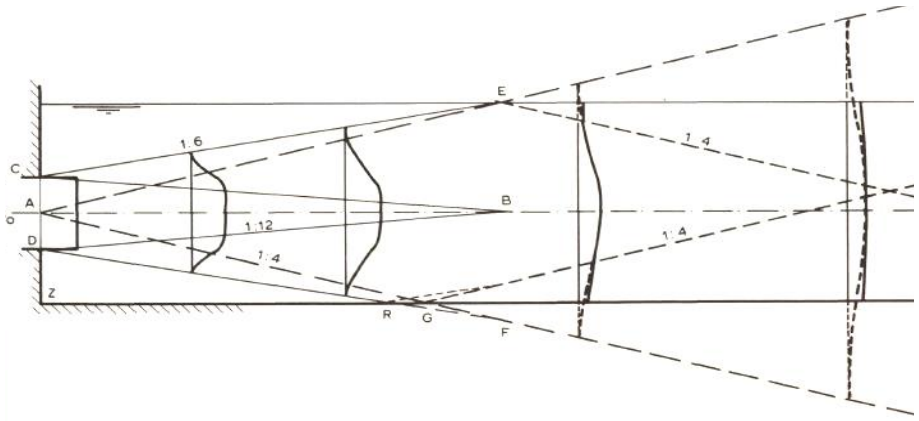


Figure 2.6: Geometry of a confined jet, including the reflection at the boundaries (Vrijburcht et al. 1988)

Although the development of momentum in the confined jet differs significantly from the free jet, the velocity profiles can be described in a similar way. However, when the jet reaches a boundary the velocity profile will change. When one of the outer edges of the mixing layer reaches a boundary, at point R in Figure 2.6, the velocity profile will be influenced instantly. The following method can be used to determine the changed shape of the velocity profile. First, an influence area from the wall into the jet will be defined. It is assumed that this influence area is equal to the vertical distance the jet would have spread, if the boundary did not prevent it. The next step is, to reflect the part of the velocity profile that cannot exist due to the boundary. This ensures that the continuity law is taken into account. The reflection plane is the boundary, this induces that the discharge blocked by the boundary progresses like a wall jet. This approach results in an acceptable velocity profile when compared to measurements in Vrijburcht (1988).

### 2.3.3. SUBMERGED IMPINGING JET

In this subsection a submerged free turbulent jet that impinges against a solid surface is considered. The theory presented here is mainly based on Samson (1972). For simplicity a case with orthogonal impingement is considered here. In reality the bow of a ship often has a certain angle with respect to the jet. It is assumed that the theory presented here can also be used for the impingement under an angle after compensating with geometry rules.

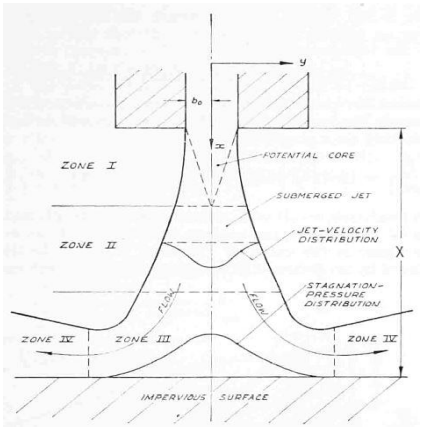


Figure 2.7: Submerged plane free turbulent jet impinging onto a surface (Samson 1972)

Consider a free jet approaching a solid surface and colliding with it. After impingement two equal wall jets are formed having a 90° angle with respect to the initial free jet. Wall jets will be described in the next subsection. Due to the deflection of the flow on the surface the direction of momentum is changed, resulting in a distribution of pressure on the deflection surface. The shape of the pressure distribution corresponds to the shape of the velocity profile in the impinging jet and is related to the velocity squared. An impinging jet is basically a free jet before impinging, therefore the velocity profile can be described by a Gaussian curve. The pressure force should be equal to the momentum deflected. The actual force on the impingement surface is therefore strongly dependent on the distance between the starting point of the jet and the impingement surface (X), since the velocity in the jet decreases with the distance travelled.

### 2.3.4. PLANE TURBULENT WALL JET

A jet can remain attached to a certain solid boundary, either after impingement (Samson 1972) or due to the initial conditions (Rajaratnam 1976), literature refers to this yet type as a wall jet. The properties of a wall jet are slightly different from a free jet, although the approach in describing the shape of the jet and the velocity profiles are almost identical. The most important difference is that only one shear layer is formed on the fluid side, see Figure 2.8. On the other side, where the solid boundary is present, a boundary layer develops. The potential core of the jet is defined similarly as for the free jet, when the boundary layer meets the penetrating shear layer, the potential core is consumed. When the potential core is no longer present the flow state is fully developed.

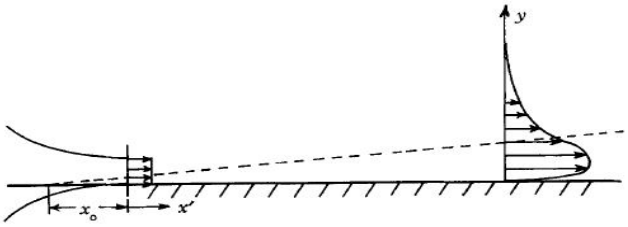


Figure 2.8: Plane turbulent wall jet (Schwarz & Cosart 1960)

Looking at the velocity profiles of the wall jet, it was found that the shape of the velocity profiles, over the distance travelled, is self similar. Note that the same can be said about the velocity profiles of the free turbulent jet. This knowledge makes it easier to describe the velocity profile in different parts of the jet, since its development is only dependent on the distance travelled by the jet. The velocity profile deviates from the Gaussian curve that was found for the free jet. Instead the maximum velocity is closer to the wall and propagates away from the wall, as the jet flow gets further from the point of origin.

### 2.3.5. COANDA EFFECT

The situation of a ship in a lock during levelling can be simplified to an object partially blocking the turbulent jet. In literature there are very little examples of this specific situation. However, what can be found is the so called Coanda effect on a jet. This effect basically describes the tendency of the jet to attach to a boundary. In the case of a plane jet into a lock with no ship, the available attachment boundaries are the water surface or the bottom of the lock. When a ship is present the jet can also attach to the hull of the ship.

The boundary on which the jet most likely attaches is very much dependent on the location of the jet inlet, this was studied in Shimada et al. (2004). If the jet inlet is close to the bottom it most likely attaches there, the same holds for the free water surface. Typical flow patterns for these different modes are shown in Figure 2.9. The deflection direction based on the point of entry and Reynolds number is shown on the right of Figure 2.9. Here, $h$ is the diameter of the entry point, $H$ is the distance between the centre line of the jet and the average water surface and $D$ is the distance between the centre line of the jet and the bottom. It was found that the dependency on the Reynolds number for the type of deflection is negligible. According to this diagram the flow can be categorised into three types:

1. When $H$ is sufficiently larger than $D$, the jet will deflect to the channel bed. The found condition for this type is $H/h \geq 2.2D/h$.
2. When $H$ is sufficiently smaller than $D$, the jet will deflect to the water surface. The found condition for this type is $H/h \leq (0.27D/h + 4.2)$.

3. Between the mentioned conditions the deflection is not fixed. This does not necessarily mean that the jet will not deflect. The prediction of the deflection direction just can not be made with enough certainty.

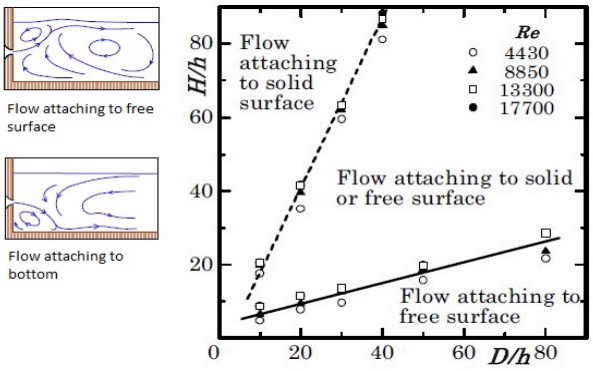


Figure 2.9: Different modes of jet attachment (left) and the influence of point of entrance on the deflection direction (right) (Shimada et al. 2004)

A few things need to be adjusted to make the presented formulas useful for this research. First the parameters will be described with symbols commonly used in this report. The following conversions will be made $h = 2b_0$, $H = h_1 - a - b_0$ and $D = a + b_0$. Secondly the constant 4.2 has to be neglected, otherwise scale effects are not taken into account properly, because this constant does not scale. When looking at Figure 2.9 neglecting the constant 4.2 has very little effect and is therefore justified. These adjustments lead to Equation 2.3, which describes the range of jet heights in which it is not certain where the jet will deflect to. In this area it is most common to assume the jet will deflect to the closest boundary.

$$0.27\frac{(a+b_0)}{2b_0} \leq \frac{(h_1-a-b_0)}{2b_0} \leq 2.2\frac{(a+b_0)}{2b_0} \tag{2.3}$$

Where:

$a$ = the distance from the bottom to the beginning of the opening $[m]$
$2b_0$ = the size of the opening $[m]$
$h_1$ = the water depth $[m]$

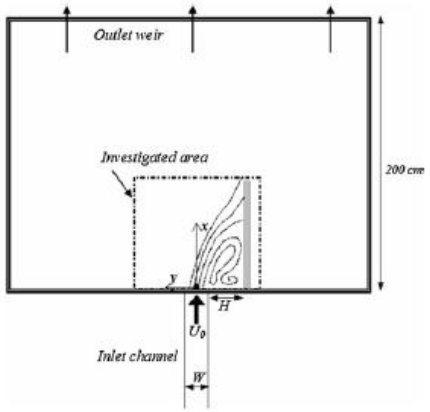


Figure 2.10: Experimental setup for the Coanda jet experiments (Miozzi et al. 2010)

Further simplified the range of jet heights in which it is not certain where the jet will deflect to is given by Equation 2.4.

$$1.27 \leq \frac{h_1}{a+b_0} \leq 3.2 \tag{2.4}$$

In Miozzi et al. (2010) the deviation of a jet from the straight direction, due to the presence of a lateral wall is investigated. This deviation in the flow condition of the free jet is known as the Coanda jet or offset jet. The underlying mechanism of the flow deflection is investigated using experimental observations. Figure 2.10 shows the setup for these experimental observations. Water is let into a stagnant basin resulting in a water jet, which is consequently deflected by the lateral wall. Within the experiments the presence of the lateral wall clearly resulted in a velocity field which is expected from a Coanda jet, implying a strong deflection of the flow in the direction of the lateral wall. This phenomenon takes place due to the non-symmetric pressure fields at the boundaries. The asymmetry in the pressure field is a result of the lateral wall limiting the entrainment on that side of the jet, creating a lower pressure than on the other side of the jet. It was found that the distance at which the lateral wall is placed, $H$, strongly influences the exact flow field and the attachment point to the lateral wall. In the sense that a higher $H$ gives a attachment point further from the jet entrance.

## 2.4. ANALYSIS OF LOCKFILL

In this section the calculation method that is used in Lockfill will be elaborated. This will provide an understanding of the computational steps that are taken to determine the longitudinal forces on the ship. It is important to fully understand how the forces are determined, so flaws can be detected and possibly improved. The version of the program on which the analysis is performed is: Lockfill version 5.3, July 2016.

### 2.4.1. JET SCHEMATISATION IN LOCKFILL

The shape of the filling jet and the corresponding velocity profile are schematised using the theory presented in note six from Vrijburcht et al. (1988). A free jet in infinite water is used as starting point for the schematisation. The influence of the water surface boundary and lock bottom boundary are included using reflection of the velocity profile. Reflection on the boundaries will transform the free jet in infinite water into a free jet in confined water. Both jet types are discussed in Section 2.3. The jet schematisation in Lockfill is a two-dimensional approximation in which the presence of a ship is not included. The friction interaction with the bottom and the walls are neglected, this implies that the jet will not change due to friction with the boundaries. To prevent confusion, there is a friction force on the ship, but this friction force results from the main flow and not from the jet. The jet starts expanding as soon as it leaves the gate entrance, at an angle of 1:6, this part is called the transition area. After a distance of 6 times the entrance diameter the angle increases to 1:4. At this point the velocity profile fits the description of a Gaussian curve, see Figure 2.5 in Section 2.3.1. Outside of the jet boundaries the velocity is assumed to be zero, therefore possible effects of the return flow are not included in the calculation.

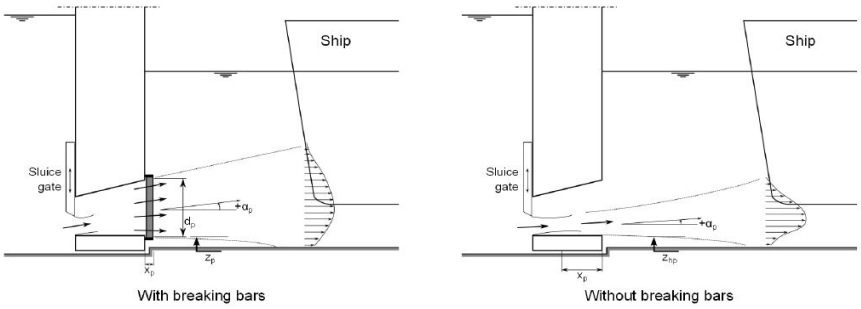


Figure 2.11: Schematic of the filling jet entering the lock: with breaking bars (left) and without breaking bars (right) (Deltares 2016)

When defining the starting position of the filling jet, three parameters are important: starting position with respect to the vertical, starting height and the angle with respect to the horizontal. Within Lockfill there are two options available, a schematisation with breaking bars or a schematisation without breaking bars, see Figure 2.11. The situation with breaking bars has a flow pattern that is dispersed over a greater area, while the situation without breaking bars has a more concentrated flow field. Furthermore, the starting position of the jet is different for both situations. In the case with the breaking bars it is assumed that the filling jet starts just behind the breaking bars. When there are no breaking bars present the filling jet will start between the

gate and the entrance to the lock chamber. This should be the point where the jet has its lowest diameter as a result of the venturi effect.

### 2.4.2. DISPERSION ANGLE OF THE JET

Due to some new developments in the Lockfill software it is possible to change the dispersion angle after the transition area, this is elaborated in Van der Ven (2015). This gives more possibilities for the schematisation of the boundaries of the filling jet. For example it is now possible to determine the expansion angle using CFD and then implement that in Lockfill. Using this method the standard filling jet schematisation can be adjusted for specific cases. This gives for example the option to include the Coanda effect in the Lockfill schematisation, as long as a CFD study will be done before the Lockfill calculations.

### 2.4.3. LOCKFILL CALCULATION METHOD

In the following subsections the methods and assumptions used to obtain the longitudinal forces in Lockfill will be discussed. Each case presented here will assume that the bow of the ship is faced towards the lock gate. For a complete derivation of the expressions of the force components the reader is referred to Vrijburcht (1988). The equations are explained in more detail in Appendix B. The expressions that are derived for the force components elaborated in Appendix B can also be found in the Lockfill manual (Deltares 2016).

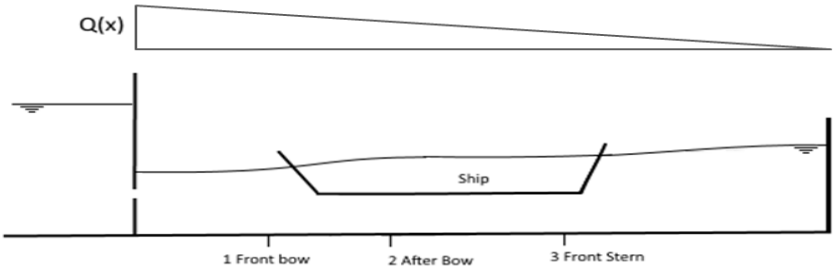


Figure 2.12: Locations for the momentum balance in Lockfill and the decrease of the discharge in horizontal direction

All three force components mentioned earlier are derived from the one-dimensional momentum and continuity equation at the bow, along the hull and at the stern of the ship, see Figure 2.12. An expression is written for the water level difference between point 1 and point 2. The same is done for the water level difference between points 2 and 3. Using these expressions the separate forces on the ship can be determined. The last step is adding the forces and rewriting them in a manageable form. The force is defined to be positive if directed away from the active lock head. To make a one-dimensional formulation possible variations in the width are not taken into account. It is assumed that the jet is active over 80% of the width of the lock, i.e. 20% of the width is assumed to have zero velocity.

#### MOMENTUM BALANCE AT THE BOW OF THE SHIP

The momentum balance is used to find an expression for the difference in water level in front of the ship and just after the bow, while simultaneously formulating an expression for the direct force against the ship due to the filling jet. The following assumptions are made in the derivation:

1. At the bow a concentrated filling jet is present, with a momentum $\rho U Q_1$ calculated with the jet schematisation based on the theory of a free jet in confined water.
2. The momentum of the filling jet at the bow is corrected with a coefficient $C_2$. This coefficient is defined as the area of the filling jet that hits the bow divided by the total area of the filling jet in front of the bow. Basically it determines the percentage of the filling jet that actually hits the ship.
3. The direct force against the bow is defined as a jet against a plate under an angle.
4. At the bow, the pressure is hydrostatic for a water level in front of the bow, with a deviation for the jet pressure and flow along the bow. The flow along the bow is corrected using a coefficient $C_1$, which scales the force. The origin of this factor could not be traced in literature, in Lockfill a default value of 0.9 is used.
5. The difference in water level is small compared to the average water depth in the lock.

Using the momentum balance at the bow and the assumptions elaborated above an expression for the water level difference over the bow is found. With the water level difference the net hydrostatic pressure against the bow can be quantified. Furthermore, the force due to the filling jet against the bow is determined using the formulation for a jet against an inclined plate. It is important to note that the jet also influences the momentum at the bow and thus the difference in water level over the bow. For example, a concentrated filling jet with higher velocities will result in a bigger water level difference.

#### MOMENTUM BALANCE ALONG THE HULL OF THE SHIP

Another momentum balance is formulated between just after the bow of the ship and just in front of the stern of the ship. Again the intention is to determine a water level difference between the two locations. Simultaneously the friction force along the hull of the ship can be determined. The following assumptions are made during the derivation of the force components:

1. Between the bow and the stern, the flow has a uniform distribution over the wet cross-section.
2. The formulations of Chézy and Stickler and White-Colebrook are applicable to determine the friction force.
3. Between the bow and the stern the flow along the solid materials induces a friction force, resulting in a water level difference between the bow and the stern.
4. The discharge decreases linearly over the length of the lock, see Figure 2.12.

#### FORCE AT THE STERN OF THE SHIP

It is assumed that the pressure against the stern of the ship is hydrostatic. This is a direct result from the assumption that there is complete flow separation at the stern.

#### COMBINING THE FORCES

Combining the forces from the bow, hull and stern makes it possible to rewrite them in a convenient way. To simplify the problem it is assumed that the water level terms still in the equation are equal to the average water level in the lock. The forces are rewritten in a form that categorises them by the mechanism instead of the location. The mechanisms were introduced in Section 2.2.

Reproducing the derivation for the Lockfill calculation method, it was found that the presence of the ship is taken into account, in the sense that the filling jet collides with the ship. The force of the jet on the ship is taken into account in the momentum equation. However, the ship does not interact with the flow pattern itself, i.e. the presence of the ship does not influence the assumed flow pattern. The interaction between water and ship is therefore not complete. Furthermore, it is very important to understand that the filling jet influences two force components. Firstly, the direct force against the bow, which is a function of: the local jet momentum, the geometrical angles and the percentage of the jet that hits the ship. Secondly, the water level drop in front of the ship due to high longitudinal velocity. The water level drop is also a function of the momentum of the jet, but in the current schematisation not of the surrounding geometry.

### 2.4.4. POSSIBLE IMPROVEMENTS TO THE LOCKFILL CALCULATION METHOD

Although the results from the program Lockfill are sufficiently accurate for the initial design of a lock according to Vrijburcht et al. (1988), there are still improvements to be made. These improvements can result in an even higher accuracy or a bigger scope of application. A number of different assumptions from the Lockfill calculation method, which are influenced by the presence of the ship, will be discussed here. In this study the focus will be on the influence of the location of the ship on the forces on the ship. This makes the filling jet in front of the ship the most logical subject to study first. However, for the purpose of further research it is useful to give an overview of other things which can be improved.

By including the 3D-effect of the filling jet the schematisation can be made more accurate. Currently it is assumed that the flow is evenly distributed over 80% of the width of the lock. With some filling mechanisms this might be the case, but in most situations the jet will not be evenly distributed or the distribution is a function of the distance from the door. Introducing a 3D effect in Lockfill will benefit the accuracy of the program a lot and Deltares is already making plans to realise this. This will however not be included in this research, because the main problem addressed here can be schematised in 2D very well.

It is assumed that the force against the stern of the ship is solely hydrostatic. This follows from the assumption that the flow will not stick to the stern and is freely released, i.e. there is complete flow separation at the stern of the ship. In reality this is almost never the case, especially considering many different ship shapes. It is hard to predict how significant the assumption of hydrostatic pressure is on the total force on the ship. If there is a lot of energy loss due to flow separation at the stern, a coefficient correcting the pressure at the stern might be required.

## 2.5. INTRODUCTION TO CFD AND STAR-CCM+

CFD stands for Computational Fluid Dynamics, which entails the numerical calculation of fluid behaviour. In Anderson (1995) an excellent description about what CFD entails is given. It is explained that the physical aspects of any fluid flow are governed by three fundamental principles: conservation of mass, conservation of momentum and conservation of energy. CFD software uses these three conservation laws to obtain a solution in the form of numbers for the flow field, at discrete points in space and time. This can be realised by replacing the integral and partial differential equations, which describe the three fundamental physical principles, by equations with discretized algebraic forms. The exact manner in which these equations are derived and transformed to serve CFD purposes will not be included in this report.

The CFD software package that is used for this report is Star-CCM+. This software package is especially suitable for calculating fluid motion close to stationary structures. Additionally it provides one environment to execute the different steps within a CFD calculation. These steps being:

1. Making the geometry of the model domain.
2. Dividing the model domain into a numerical grid.
3. Selecting the right numerical schemes and mathematical models to describe the physics.

The geometry can be made in a 3D CAD environment, which makes accurate modelling of the desired structures and computational domain possible. For the generation of the grid a number of different shapes and sizes are available, each with their advantages and disadvantages. Furthermore, local refinements are possible for locations where more detailed physical process take place, like flow separation, or where simply more information is needed. The transition from larger to smaller cells should not exceed a factor 2, i.e. the smaller cells should not have less then half of the dimensions compared to the adjacent ones. Otherwise, this could lead to numerical errors in the calculation, (O'Mahoney et al. 2015). Star-CCM+ has a wide platform with different equations to solve physical processes. The most important processes for this study are: fluid mechanics, turbulence and multiphase-flow. To determine which physical models are best the user has to know what kind of flow will be found. Therefore extensive knowledge about fluid behaviour is definitely a requirement when using the software. The version of Star CCM+ that is used for this study is: STAR-CCM+ 11.04.010.

## 2.6. CONCLUSIONS CONSIDERING THE THEORETICAL BACKGROUND

At the moment two different approaches are available when calculating forces on a ship in a lock. CFD can be used to solve the flow and based on the calculated flow resulting forces on the ship can be found. This method requires high computational power, expertise and time. By using a parameterization of the fluid motion a program like Lockfill can determine the forces faster while still maintaining sufficient accuracy.

For this study three relevant longitudinal forces on a ship in a lock must be considered:

1. The force resulting from the momentum decrease over the length of the lock.
2. The direct force from the filling jet on the bow of the ship.
3. The friction between the water flow and the hull, wall and chamber floor.

These are all physical processes that can be accounted for when the jet schematisation is accurate. The current schematisation of the flow in Lockfill does not take into account the influence of the presence of the ship on the flow and is based on a free jet with addition of reflection on the water surface and bottom of the lock. Although jets are extensively researched in available literature, the influence of the ship on the jet is not. Therefore additional data needs to be obtained to study the behaviour of the jet with and without ship. Furthermore the position of the ship will change the flow, therefore multiple positions of the ship in the lock should examined further.

# 3

# PREPARATIONS FOR THE SCALE MODEL TESTS USING A CFD MODEL

In this chapter an overview of the different parameters which are relevant for this research will be given first. Then a prototype for the scale tests will be defined. The prototype is made as generic as possible to describe typical locks in the Netherlands. The prototype will be scaled to the size used in the scale model measurements and CFD model. Most geometrical distances can be scaled using a single scale factor. Thereafter, a description is given about how the CFD software is used to provide insight in the flow patterns in the lock. The main goal of the CFD calculations is to study the flow behaviour and to prepare adequately for the scale tests. The CFD model is therefore not validated within this study, considering its main purpose is to provide an order of magnitude and not exact results. The reason for including the CFD calculations and not fully depending on scale measurements alone is that the scale measurements can be performed only once. This means that mistakes in the scale model setup have a significant impact on the quality of the data. While mistakes in the CFD model can be corrected more easily and additional calculations are possible at any time. Therefore, it could be argued that the purpose of the CFD calculations is mainly to prevent possible mistakes in the scale model setup.

There are a lot of different variables that need to be considered for the test setup. Not all can be varied during the course of the tests. Therefore it is important to decide and motivate which parameters will remain constant and which will be varied. To further reduce the number of different situations only one parameter will be varied at a time. The other parameters will remain constant while the parameter which is of interest will be changed. Hereby a definition of the expected normative condition is provided. This normative condition is the starting point of each set of variations.

An important note for the dimensions given in this chapter: the actual dimensions are not of a specific interest for this research since it is not one case that will be tested. The general reactions of the force when changing one of the parameters, while the others remains constant is important. The definition of the prototype and the scaling to model scale is only done to make the case as realistic as possible. But one might say that any arbitrary set of dimensions will suffice as long as the important parameters are varied in different test so that trends can be detected.

## 3.1. DEFINITION OF THE DIFFERENT VARIABLES

When considering a ship in a lock there are quite a lot of variables that can have an influence on the longitudinal forces on the ship. In Figure 3.1 these variables are visualised. The influence of the shape of the opening in the gate and the possible presence of breaking bars are already left out of the scope of this research. Furthermore, the ship is schematised as a box with a bow under a certain angle relative to the horizontal axis. The width of the lock ($w$) is not considered since the experiments will be performed in a two-dimensional setup, neglecting all influences over the width.

Each variable will be elaborated briefly. The water depth in the approach channel is denoted as $h_1$ and the

water depth in the lock $h_2$. The difference in water height between the two water bodies is called $\triangle h$. The position of the ship is determined by means of two parameters, the distance between the gate and the point where the bow meets the bottom of the ship $X_{bow}$ and the keel clearance $k_c$. Resulting automatically in the draught of the ship $d$. For the gate three parameters are most important: the thickness of the gate $t$, the size of the opening $2b_0$ and the position of the opening with respect to the bottom $a$. The dimensions of the ship are described by: the length of the bottom of the ship $l_s$, the height of the ship $h_s$ and the angle of the bow $\beta$. Lastly, $x_1$ is defined as the distance between the gate and the front most point of the ship.

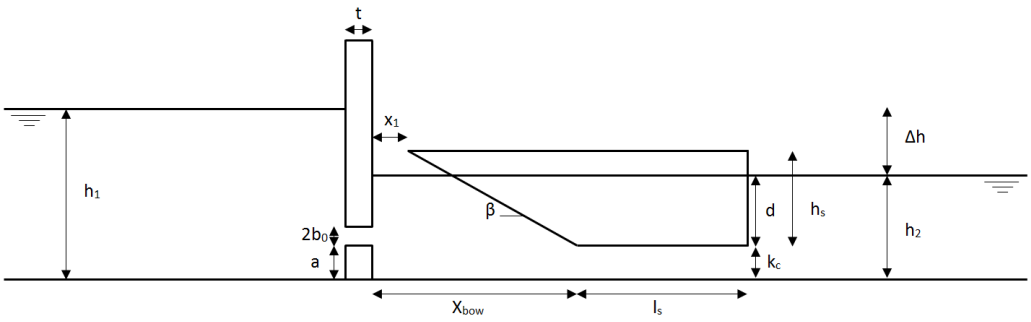


Figure 3.1: Important parameters for this study

## 3.2. PROTOTYPE

The description of the prototype is divided into four parts. The first part gives a description of the prototype for the ship. In the second part the normative position of the ship is determined. The third part treats the hydrodynamic conditions for the normative situation. In the fourth part an elaboration about the prototype for the lock and the gate is provided.

### 3.2.1. PROTOTYPE OF THE SHIP

For the ship prototype a combination is made between the most common inland ship CEMT Va and a pushing barge. The general dimensions of the CEMT Va ship are considered to be most generic for this research and the shape of the bow of an average pushing barge is chosen because it is uniform over the width. The uniformity is preferred, because both the scale model measurements and the CFD model are schematised in 2D, neglecting all deviations over the width. The loaded draught of the CEMT Va ship is 3.50 meter according to Rijkswaterstaat (2011). The width and length of the ship are 11.4 meter and 110 – 135 meter respectively. The angle of the bow ($\beta$) of the ship is assumed to be 30 degrees, corresponding to an average pushing barge according to Deltares (2016).

### 3.2.2. NORMATIVE POSITION OF THE SHIP

The normative position of the ship is determined by placing the ship as close to the gate as possible and creating the highest amount of blockage, by reducing the keel clearance to the minimum. With this approach the longitudinal forces on the ship are expected to be on their maximum, while still maintaining a realistic situation. The minimal keel clearance for a ship with class IV or higher is 0.70 meter and the minimum distance between the gate and the tip of the bow is 2.0 meter (Deltares 2016). To convert this into the defined $X_{bow}$ the horizontal length of the bow needs to be added to the minimum distance, this results in approximately 8.4 meter. With an assumed freeboard of 1.6 meters.

### 3.2.3. HYDRODYNAMIC CONDITIONS

The water level in the lock for the normative situation can be determined using the draught of the prototype ship and the minimum keel clearance. Both values added together give a water depth $h_2$ of 4.2 meter. A reasonable water level difference is considered to determine $h_1$. Hereby the following considerations need to be taken into account:

1. Not the water level difference is the main point of interest, but rather the discharge through the gate resulting from the water level difference. Especially the maximum discharge is interesting because then the highest forces on the ship are expected.

2. During the filling cycle of the lock the gates will be opened slowly, increasing the discharge through them. Meanwhile the discharge decreases due to the reduction in water level difference. This means that the maximum discharge does not occur simultaneously with the maximum water level difference. At the time that the discharge is at its maximum the water level difference can already be halved.

A suitable water level difference at maximum discharge ($\triangle h$) is 2.8 meter. The maximum water level difference that the lock overcomes is then 5.6 meter, assuming that the maximum water level difference is two times the water level difference at maximum discharge. This is of course highly dependent on the filling mechanism and is very lock specific. Now that both $h_2$ and $\triangle h$ are determined, $h_1$ can be found. $h_1$ will have a value of 7 meter for $\triangle h = 2.8$ meter. Note that during the levelling procedure $\triangle h$ and $h_2$ are changing while $h_1$ remains constant. Due to the increase in $h_2$, $k_c$ will increase as well therefore the normative keel clearance of 0.70 meter does not occur simultaneously with the maximum discharge through the gate. This is therefore an excessive situation for the purpose of the present study.

### 3.2.4. PROTOTYPE OF THE LOCK AND GATE

The thickness of the locking door is copied from the scale measurements which were performed in 2015 at Deltares, Van Velzen & Dos Santos Nogueira (2015). This is a prototype thickness of 1.05 meter, averaging a number of different locks in the Netherlands. In Rijkswaterstaat (2000) it is stated that the location of the opening is almost always placed in the lower half of the lower water body. This prevents concentrated flows near the surface which would lead to high forces against ships in the lock. For the normative situation the gate opening should therefore be situated in the lower half but as close to the surface as possible, because this will result in a significant force due to the filling jet on the bow, which is the focus of the present study. This means that the upper side of the opening is situated exactly in the centre of the lower water body.

Using Equation 2.4, provided in Subsection 2.3.5, a check can be performed to see if the jet has a specific tendency to attach to the bottom or surface. The result is inconclusive, in the sense that, for the chosen parameters the requirements of Equation 2.3 are met ($1.27 \leq 2.4 \leq 3.2$). This entails that the jet originating from the opening has no clear tendency to deflect towards the bottom or the surface. However, this does not mean that the jet will not deflect. It is logical to assume that the jet will attach to the closest boundary, in this case the bottom.

The size of the opening can be scaled using the starting point that the area of a 3D lock opening must be equal to the 2D schematisation. The area for a lock opening is prescribed in Rijkswaterstaat (2000), which is 8.4 square meter, based on 6 openings with a width of 1.4 meter and a height of 1 meter. Because the lock opening in the 2D case is over the entire width, the height can be determined by dividing 8.4 square meter by 12.5 meter, resulting in a opening height of 0.7 meter.

## 3.3. FROM PROTOTYPE TO CFD MODEL DIMENSIONS

The CFD model dimensions correspond to the dimensions that will be used for the scale measurements. This ensures that the CFD results are applicable when designing the scale measurements. Furthermore, the results of the scale measurements and the CFD calculations can be compared to each other more easily. In this section the physical dimensions of the CFD model are elaborated. The dimensions are based on a prototype lock and ship, scaled in such a way that it can be build in the test facility that is available. First a base model is determined from what is expected to be the normative situation. This means a ship close to the lock with a large draught and small keel clearance.

Similar tests were performed at Deltares in which a scale factor of 1 : 7 was used, (Van Velzen & Dos Santos Nogueira 2015). Not exactly the same dimensions are applicable but it can serve as a good reference. Since the maximum water depth in the flume that is available for this research is roughly two times smaller than the maximum water depth of the other experiments a scale factor of 1 : 14 is chosen.

The prototype needs to be scaled to a fitting scale model. For most parameters which represent a distance this simply comes down to dividing by 14, which is the scale factor. However, two exceptions can be recognised. First, the width of the scaled lock is restricted by the width of the flume. The flume is 0.5 meter wide and therefore insufficient to cover the entire width of the prototype lock. It can be argued that, because a 2D schematisation is used this does not influence any results. Secondly, the length of the ship in prototype

is at least 110 meter, scaled this will result in a ship of almost 8 meter long. Since the ship needs to be easily movable in the scale test setup, the length of the ship is reduced to 0.50 meter on scale. Note that this is the length of the bottom of the ship, in other words the total length minus the horizontal length of the bow. Fortunately it is not strictly necessary to scale the length of the ship, since the main interest of this research is the behaviour of the jet in front of the ship and the length of the ship only influences the friction term. The friction on the bottom of the ship will however be underestimated. In Table 3.1 the dimensions of the prototype and the CFD scale model are listed. The scale factor is listed in the last column.

Table 3.1: Dimensions of the prototype and CFD scale model (normative situation)

| Parameter | Prototype [m] | CFD scale model [m] | Scale factor |
|---|---|---|---|
| $h_1$ | 7.00 | 0.50 | normal scale factor 14 |
| $h_2$ | 4.20 | 0.30 | normal scale factor 14 |
| $\triangle h$ | 2.80 | 0.20 | normal scale factor 14 |
| $d$ | 3.50 | 0.25 | normal scale factor 14 |
| $l_s$ | 110 | 0.5 | not correctly scaled factor 220 |
| $k_c$ | 0.70 | 0.05 | normal scale factor 14 |
| $x_1$ | 2.00 | 0.14 | normal scale factor 14 |
| $a$ | 1.4 | 0.1 | normal scale factor 14 |
| $2b_0$ | 0.7 | 0.05 | normal scale factor 14 |
| $t$ | 1.05 | 0.08 | normal scale factor 14 |
| $w$ | 12.5 | 0.50 | not necessary, 2D schematisation |

## 3.4. SCALE EFFECTS

For these type of scale models Froude scaling is suitable, because the flow is inertia dominated. The Froude number describes the ratio between inertia and gravity (Chanson 2004) and is often notated in the following manner $\frac{Inertiaforce}{Gravityforce} = \frac{U^2}{gL}$. Another scaling method is Reynolds scaling, which is used to scale viscous dominated flows. Reynold scaling is in this case impossible, because the viscosity can not be scaled and for correct scaling the velocities will become unrealistically large. However a check should be performed to see if the prototype and the scale model are in the same turbulent regime. To perform this check the Reynolds numbers of both the prototype and the scale model are calculated using equation 3.1. The Reynolds number for the scale model is 100,000, with $l$ being the height of the gate opening and $U$ the expected velocity of 2.0 m/s. The Reynolds number prototype is 7,500,000 with a scaled velocity of 7.5 m/s and $l$ being the gate height. Both are in the same turbulent ($Re > 4000$) regime and therefore the check is successful.

$$Re = \frac{\rho U l}{\mu} \tag{3.1}$$

Where:

$Re$ = the Reynolds number $[-]$
$U$ = the relative speed of the fluid $[m/s]$
$l$ = the characteristic length $[m]$
$\mu$ = the dynamic viscosity of the fluid $[Ns/m^2]$

Froude scaling requires dynamic similarity between the model and reality. In this case this means that the scaling should meet the requirement following from Equation 3.2. The subscript $p$ stands for prototype and the subscript $s$ for scale model.

$$\frac{U_p^2}{gL_p} = \frac{U_s^2}{gL_s} \tag{3.2}$$

Where:

$U$ = the velocity of the fluid $[m/s]$
$L$ = the characteristic length $[m]$

Introducing the scale factor $\lambda$, a formulation can be found for the linear dimensions. Linear dimensions can be scaled directly with $\lambda$ because the relation between the scale size and reality is linear. The scaling of all the linear dimensions, in this case especially geometrical distances, should meet the requirements of Equation 3.3. The linear scale factor between prototype and scale model was introduced earlier. A scale factor of 14 was found to be most suitable, so $\lambda = 14$.

$$L_p = \lambda L_s \tag{3.3}$$

Combining Equation 3.2 and 3.3 will result in Equation 3.4. This equation describes the relation between the velocity in prototype and the velocity in the scale model.

$$U_p = \sqrt{U_s} \tag{3.4}$$

Now that Equation 3.4 is established the scaling relations for other physical parameters can be derived just from the physical units. The multiplication factors that can be used to transform model scale to prototype scale, are given in Table 3.2. Note that $\frac{\rho_p}{\rho_s} = 1$ so the density will have no influence on the scaling.

Table 3.2: Multiplication factors for the physical parameters

| Physical parameter | Unit | Multiplication factor [m] |
|---|---|---|
| Length | $[m]$ | $\lambda$ |
| Velocity | $[m/s]$ | $\sqrt{\lambda}$ |
| Discharge | $[m^3/s]$ | $\lambda^{2.5}$ |
| Force | $[N]$ | $\lambda^3$ |
| Pressure | $[N/m^2]$ | $\lambda$ |
| Time | $[s]$ | $\sqrt{\lambda}$ |

## 3.5. SETUP OF THE CFD MODEL

Initially a three-dimensional CFD model was preferred over the two-dimensional variant. An additional benefit of including the third dimension in the model is that variations of the flow velocity over the width can be analysed. However, the calculation time of the 3D model was unacceptably long. Furthermore, even if a calculation was finished in a reasonable amount of time the available hardware had trouble displaying the results. Therefore it was decided to neglect the width of the lock and model in two dimensions. This decision does not have a major impact on the quality of the results since the schematisation of the gate and ship are constant over the width anyway. In this section a brief explanation is given about the setup of the 2D CFD model. More detail about specific settings will be provided in Appendix C.

### 3.5.1. GEOMETRY AND MESH

The dimensions given in the third column of Table 3.1 are used for the initial model. Furthermore, the downstream side of the modelled flume is 10 meter long and the upstream side is 5 meter long. The boundaries should be located far enough from the area of interest to prevent any unwanted influence.

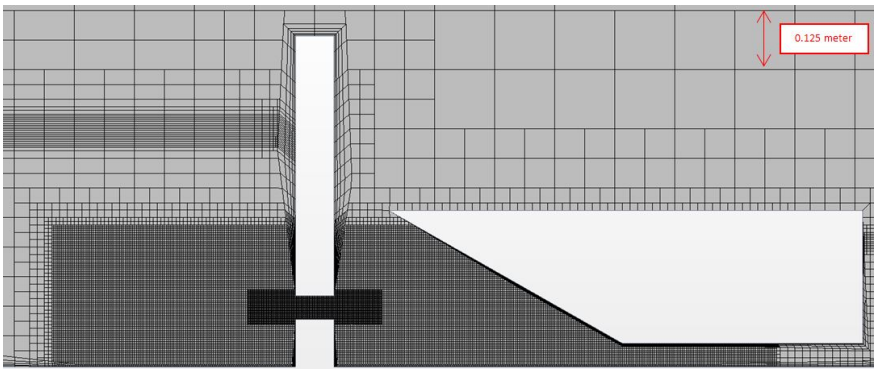


Figure 3.2: The mesh around the gate and the ship for the CFD model

The grid surrounding the gate and the ship is visualised in Figure 3.2. To generate a mesh the trimmed cell mesher is used, creating a rectangular shaped main mesh. This mesher is selected because it works well with the modelling of a water surface. The rectangular shape of the grid results in less unwanted irregularities around the water surface than for example a polyhedral mesh. The mesh is generated with a base size of 0.25 meter, with a refinement of the mesh where the water is expected to be. Additional vertical refinements are implemented around the interface between water and air. This will allow for a better prediction where the exact water surface is and result in an overall more stable solution. Furthermore, additional cells are required between the gate and the ship, because this is the main area of interest when looking at the flow. Finally, the mesh will be most detailed in the opening of the gate, because correctly capturing the separation that occurs here requires a very fine grid.

### 3.5.2. PHYSICS AND SOLUTION METHOD

There are a number of settings for the physics and calculation method of the model which need to be discussed. Two phases, water and air, are defined using a volume of fluids (VoF) model. With this model the percentage of each phase is calculated in every cell. The interface between the phases, in other words the water surface, can be found at the cells in which 50% of each phase is present. In principal a stationary solution is required, however the initial conditions can not be defined accurately enough in combination with the VoF, resulting in an unstable solution which does not converge. Therefore, an implicit unsteady solution method is implemented, which then can be run until a steady state is achieved. The time that is required to reach the stationary situation can be determined by monitoring a certain variable, like the discharge through the gate. It was found that the discharge does not fluctuate, with an accuracy of $< 0.1\%$, after running the model for 180 seconds. From this point on the solution is considered to be stationary. The results from the calculation before the stationary situation is reached are not considered in the analysis. These results are not representative for the stationary situation which is the main point of interest. However all the results after the stationary situation is established are usable.

The segregated turbulent flow is calculated using the Reynolds-Averaged Navier-Stokes equations. This finite element method is best suited to solve for the complex flow patterns that are expected. Turbulence in the flow can be solved using a turbulence model, two examples are Large Eddy Simulations (LES) and Reynolds-Averaged Navier-Stokes (RANS). The LES model requires more calculation time and therefore the RANS model is preferred. The well known $k-\epsilon$ model can be used as closure model for the RANS equations. It is common practice to try different turbulent models and determine the best by analysing the results. In O'Mahoney et al. (2015) this was studied and concluded that the $k-\epsilon$ is the best option to solve for turbulence in Star-CCM+. Therefore no new turbulent model analysis is performed in the present study.

A numerical scheme needs to be selected to solve the mathematical equations describing the physics. In this case a first order implicit scheme is sufficient since there is no significant variation over time. Enough iterations for each time step are essential, since the solution should converge before the end of each time step. A maximum of five inner iterations is selected, this should be sufficient for the situation which is relatively stable over time. A time step of 0.25 seconds is used which is short enough to include the necessary physics and long enough to not escalate the calculation time.

### 3.5.3. BOUNDARY AND INITIAL CONDITIONS

The boundary conditions at the upstream side of the gate is set to be a water level of 0.5 meter. This is achieved by implementing a pressure condition and a phase definition at this location. The same is done at the downstream side of the gate, however at this location the water level is set to be 0.3 meter. This differs slightly from the actual scale test because there the flow is driven by a discharge. However the same result will be achieved. The top boundary consist of a free air phase, i.e. stationary atmospheric pressure. All walls are considered to be no-slip boundaries. This implies that the velocity exactly at the wall is equal to $0 m/s$ and that a boundary layer will be formed. Table C.2 in the appendix displays the selected boundary conditions for the domain.

The initial condition is defined as the full field of variables at the start of the simulation ($t = 0$). It is most efficient to choose the initial condition in such a way that the stationary situation is reached as soon as possible. This can best be achieved by defining the water levels on both sides of the gate to be equal to their respective boundary condition. The initial velocity will be set to zero and the pressure is hydrostatic. Any turbulence variables are initially very small and will develop during the calculation.

## 3.6. ADJUSTMENT TO THE NORMATIVE KEEL CLEARANCE IN THE MODEL

A problem is noticed when looking at the water surface in the model. The water level between the gate and the ship is higher then expected. This can be explained by the fact that the opening under the ship is relatively small. The size of the gate opening is equal to the keel clearance and therefore the flow passing the ship will experience a resistance resulting in a water level setup. This setup is of such significance that the water level exceeds the bow of the scale model ship. In case of the actual scale tests the ship would overflow. The situation seems unrealistic, because in reality this large setup in front of the ship would never occur as the setup will disappear through the space between the side of the ship and the wall of the lock.

A solution can be found when revisiting the scaling of the keel clearance of the ship. Initially the scaling was based only on the keel clearance of the prototype ship. On closer inspection it seems better to scale the blockage of the ship. The schematisation is two dimensional and therefore the space between the ship and the wall will be neglected if only the keel clearance is taken into account. The blockage is defined as the ratio between the wet cross-section of the ship and the wet cross-section of the lock, see Equation 3.5 (Barrass 2004).

$$S_{block} = \frac{A_s}{A_l} \tag{3.5}$$

Where:

$S_{block}$ = the blockage factor [−]
$A_s$ = the wet cross-section of the ship [$m^2$]
$A_l$ = the wet cross-section of the lock [$m^2$]

The width ($w$) of the prototype lock for a CEMT Va ship should be at least 12.5 meter. Furthermore, taking into account the geometrical distances given in Section 3.2 the following calculation can be made for the alternative normative keel clearance. With as starting point the blockage on prototype scale should be equal to the blockage on model scale, an improved keel clearance can be determined. The wet cross-section of the lock, is equal to the width of the lock times the water level in the lock $h_2$. The wet cross-section of the ship being equal to the width of the ship times the draught of the ship. Resulting in a prototype blockage factor of 0.76. Since the width of the ship in the scale model is approximately the same as the width of the lock, the draught for the scale model can be calculated by multiplying the blockage factor times the scaled water depth. Finally the draught can be subtracted from the water depth to obtain the keel clearance. This results in a model scale keel clearance of 0.07 meter and a draught of 0.23 meter. All other parameters will remain the same. This new keel clearance will replace the earlier keel clearance of 0.05 meter.

## 3.7. CFD RESULTS

After adjusting the keel clearance to 0.07 meter two CFD calculations are performed. One without a ship in the lock and one with the ship in the normative position. In preparation of the scale tests the following questions should be answered studying the flow in the lock:

1. How does the jet behave in terms of attachment to boundaries and dispersion?
2. Is there an energy loss over the gate and can this be expressed in terms of a discharge coefficient?
3. At what distance from the gate can the flow in the lock be considered fully spread over the depth?
4. What forces can be expected on the ship?

### 3.7.1. JET BEHAVIOUR

A qualitative description of the jet with and without ship will be given on the basis of instantaneous velocity fields from CFD. Since the velocity fields are stored when the model has reached an equilibrium they represent the stationary situation and thus no time average is needed. The information can be used to place the point measurements for the scale tests strategically and determine the correct window size for the PIV. Furthermore the tendency for the jet to attach to a certain boundary can be checked since the results from the literature were inconclusive. The jet can be best visualised by plotting only the positive flow velocities. This is realised by visualising the velocities larger than 0.025 m/s to ensure a smooth view. So Figures 3.3 and 3.4 do not display the water surfaces but the positive velocities in the flume.

When there is no ship in the lock the jet will behave as visualised in Figure 3.3. It attaches to the bottom which is expected as explained in Subsection 3.2.4. For the PIV it will be interesting to include the collision with the bottom, which comes down to a vertical window of at least 0.5 meter after the gate. Since the bottom of the ship is located 0.6 meter from the gate this seems like a logical boundary.

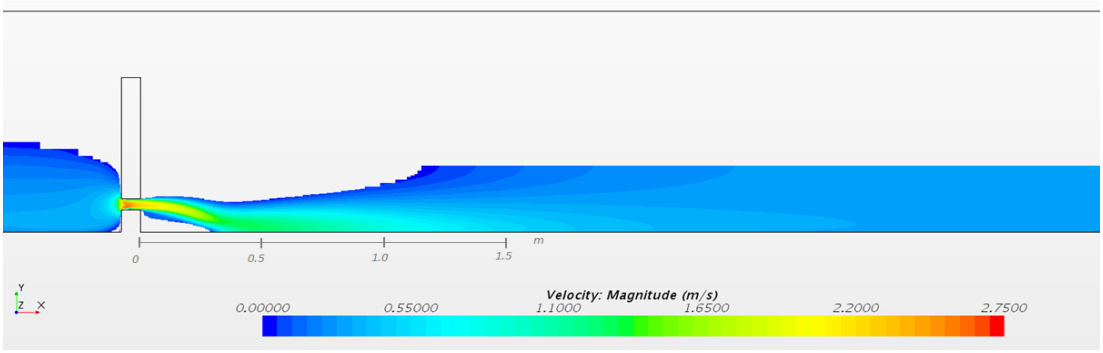


Figure 3.3: Visualisation of the jet calculated using CFD, without a ship in the lock

With ship in the normative position the jet will behave as visualised in Figure 3.4. Again the jet attaches to the bottom, however due to the presence of the ship high velocities at the bottom are maintained longer up to $x = 2$ meter. This is the typical wall jet behaviour explained in Section 2.3.4. The eddy behind the ship, caused by flow separation at the end of the ship, ensures that the jet remains attached to the bottom longer. Due to the circulation the jet is pressed against the bottom. It will be important to place any reference water surface meters in the scale model outside of its effect area.

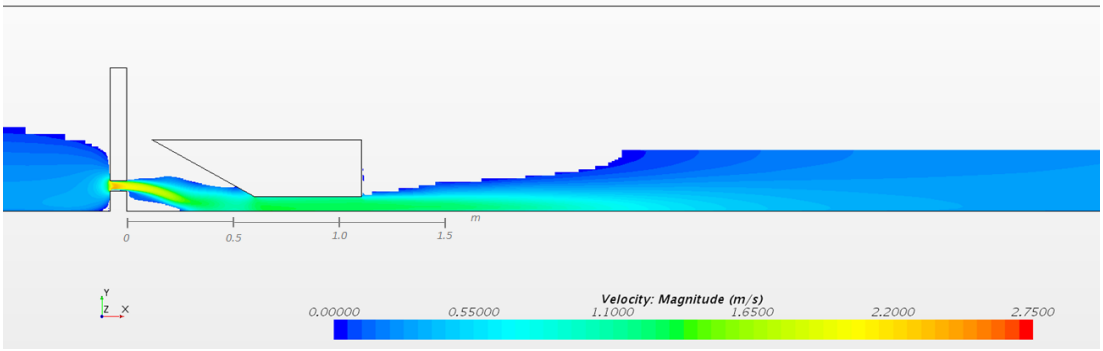


Figure 3.4: Visualisation of the jet calculated using CFD, with ship in the lock

Some interesting positions for scale test point measurements follow from the calculated jet behaviour. Without ship two positions seem valuable to get an idea of the flow in the flume of the scale test. The position where the jet starts attaching to the bottom, approximately 0.3 meter after the gate and where the jet seems fully attached approximately 0.8 meter after the gate. With ship also two positions seem interesting. In front of the ship and after the ship.

### 3.7.2. DISCHARGE COEFFICIENT

The water level difference over the gate and the discharge can be related to each other with Equation 3.6. For the scale tests the discharge will be leading when comparing different situations, because the water level difference is very much dependent on the location of measurement, since the water level downstream is not constant. Therefore if a water level difference is defined the location of measurement will always be given.

$$Q = C_d A_g \sqrt{2g\triangle h} \tag{3.6}$$

Where:

$Q$ = the discharge through the gate $[m^3/s]$
$C_d$ = the discharge coefficient $[-]$
$A_g$ = the cross-sectional area of the gate $[m^2]$
$\triangle h$ = the water level difference over the gate $[m]$

According to Van der Ven et al. (2015) the discharge coefficient can be estimated reasonably well using a CFD calculation. The calculated water level difference over the gate and discharge through the gate can be the input of Equation 3.6. The water level difference is defined as the difference between the water level just upstream of the gate and just downstream of the gate. This will result in an estimation of the discharge coefficient $C_d$. Using the CFD model a discharge coefficient of 0.87 is found for the situation without ship and a coefficient of 0.86 for the situation with ship. Apparently the presence of the ship has some influence on the coefficient. This is not surprising since the discharge found for the situation with ship is smaller then the discharge for the situation without ship. The discharge is smaller because the presence of the ship creates additional flow resistance. Now Equation 3.6 can be used again to give an estimate of the discharge needed for a certain water level difference during the scale tests. This will be an indication and the exact discharge needed to realise a certain water level difference must be determined during the scale tests. This is however valuable information for the selection of the pump capacity needed. The highest water level difference needed during the scale tests will be 0.20 meter which comes down to a discharge of 43 l/s.

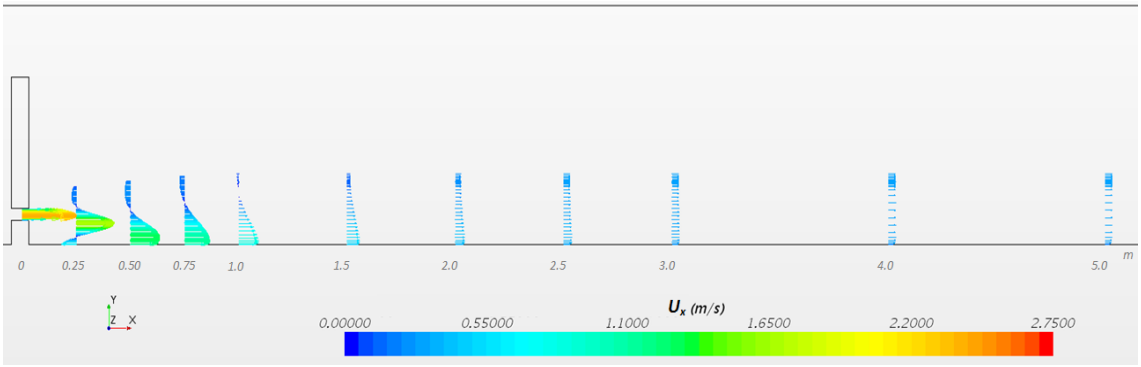


Figure 3.5: Visualisation of the vertical $U_x$ velocity profiles with no ship in the lock

### 3.7.3. VELOCITY PROFILES OVER THE LENGTH OF THE LOCK

Figure 3.5 and Figure 3.6 display the $U_x$ velocity profiles at some distances from the gate. Note that the actual CFD model is longer then displayed in the figures, the boundary in the model is at $x = 10$ meter. It is clear that under and above the opening in the gate eddies are formed, this can be concluded from the visible return flow. Furthermore, the tendency of the jet towards the bottom can be confirmed. However what needs to be learned from these images is where the flow reaches some kind of equilibrium profile. This information is required for the downstream position of a measurement instrument that measures the reference water level. Furthermore, it can give an estimate of the minimum length of the flume after the gate. Since the end of the flume should be far away enough to generate minimum boundary effects. The distance it takes to get an equilibrium flow will be a good start for this estimation.

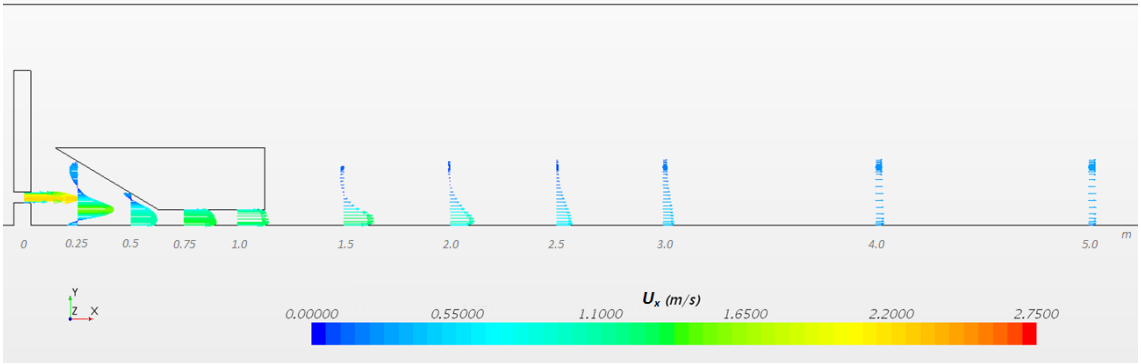


Figure 3.6: Visualisation of the vertical $U_x$ velocity profiles with ship in the lock

For for both situations the uniform flow is not yet reached at 3.0 meter after the gate, since the velocity of the jet still has a certain influence near the bottom. Especially for the situation with the ship in the lock, where

the influence of the jet reaches further then without the ship. At 4.0 meter from the gate an almost straight velocity profile is found for the situation with ship. Only after 5.0 meter the velocity profile is developed far enough that it can be called almost in equilibrium, which is satisfactory in this case.

### 3.7.4. FORCES ON THE SHIP

The forces on the ship can be determined in the model, by integrating the pressure on the surface of the element representing the ship. A distinction can be made between the forces in the horizontal x-direction and the vertical y-direction. Since the the longitudinal forces are of interest for this study only the forces in the x-direction will be calculated. It is important to get an estimation of the forces for the selection of the force measurement instruments. The force in the x-direction ($F_x$) was found to be 48 Newton, $F_x$ can be interpreted directly for being the resulting force due to the fluid motion. It is important to notice that the ship is assumed to be fixed when the forces are determined. In reality the ship will move and adjust its position based on the forces acting on it. However, since this study is performed to understand the influence of the ship on the flow, the exact forces that occur in reality are not important.

## 3.8. CONCLUSIONS FROM THE SCALE MODEL TEST PREPARATIONS

Based on typical dimensions of locks and inland ships in the Netherlands a prototype for the scale model is defined. Furthermore, using regulations a normative position of the ship in the lock could be found. On prototype scale this comes down to a keel clearance of 0.7 meter and a distance from the gate of 2.0 meter. With the scaling rules explained in Section 3.4 the prototype can be scaled to scale model conditions.

In preparation of the scale model tests a CFD calculation is performed for the situation without ship in the lock and the situation with ship in the normative position. Due to an unrealistic setup in front of the ship, the keel clearance is recalculated based on the blockage of the prototype ship. This leads to the final dimensions for the scale model, summarised in Table 3.3.

Table 3.3: Final dimensions for the scale model (normative situation)

| Parameter | Prototype [m] | Scale model [m] |
|---|---|---|
| $h_1$ | 7.00 | 0.50 |
| $h_2$ | 4.20 | 0.30 |
| $\triangle h$ | 2.80 | 0.20 |
| $d$ | 3.22 | 0.23 |
| $l_s$ | 110 | 0.5 |
| $k_c$ | 0.98 | 0.07 |
| $X_{bow}$ | 8.4 | 0.6 |
| $a$ | 1.4 | 0.1 |
| $2b_0$ | 0.7 | 0.05 |
| $t$ | 1.05 | 0.08 |
| $w$ | 12.5 | 0.50 |

The following could be learned from the CFD calculations:

1. The jet attaches to the bottom and when the ship is present the wall jet exists for a larger distance downstream of the gate. To capture the attachment to the bottom the full area between the gate and the ship should be covered with PIV. Furthermore a few interesting locations for point measurements were found. Without ship two positions seem valuable, 0.3 meter and 0.8 meter after the gate. With ship also two positions seem interesting, one in front of the ship and the other after the ship.
2. The discharge coefficient was found to be 0.87 without ship in the lock and 0.86 with ship in the lock. With these discharge coefficients a discharge of approximately 43 l/s is needed to realise a water level difference over the gate of 0.2 meter.
3. Analysing the velocity profiles calculated with CFD it was found that the velocity is nearly uniform at 5.0 meter downstream of the gate. This will therefore be a good location to measure the reference water level.
4. The longitudinal force on the ship calculated with CFD was found to be 48 Newton. This is a force ($F_x$) in the positive x-direction.

# 4

# SETUP FOR THE SCALE TESTS

The scale model measurements as described in this chapter were realised in the water-soil hall at Deltares. The prototypes of the gate and the ship are described in Chapter 3. Chapter 3 also covers the scaling from prototype size to scale model size. The dimensions for the normative situation are summarised in Table 3.3 in Section 3.8. In addition to the normative situation some different variations for the ship its position will be introduced. These tests will then be used to find a relation between the varying parameter and the forces on the ship. For a visual impression of the scale tests the reader is regularly referred to Appendix D.

The model setup will be covered in this chapter. First a description of the general model setup will be given. Thereafter, the research program will be elaborated. A distinction will be made between three measurement types performed. For each of these measurements the setup changes slightly to create the optimum circumstances for the tests and to ensure that the right parameters are measured. The measurement types are:

1. Velocity point measurements to get an impression of the flow and ensure that the flow corresponds to the expectations.
2. Force measurements for different positions of the ship.
3. PIV measurements to capture the two dimensional flow pattern just after the gate.

## 4.1. THE FLUME

The flume available for the scale measurements is 19.2 meter long, 0.5 meter wide and 0.70 meter high. The entire flume is made of four segments with a length of 4.8 meter each. The walls of these segments are made out of glass with steel construction bars every 1.2 meter. The flume upstream of the gate will function as the entrance channel to the lock and the flume downstream of the gate is the lock itself. There are a number of important structures present in the flume, each of these structures will be elaborated in the subsections below.

### 4.1.1. GATE AND PIV WINDOW

The scale gate is a wooden structure with an opening over the entire width of the flume, see Figure 4.1 in Appendix D. The opening is located 0.1 meter above the bottom of the flume and is 0.05 meter high. The gate is 0.08 meter thick and is situated approximately in the center of the flume to ensure that the boundary effects from both sides influence the area of interest as little as possible, with the area of influence being the water body directly after the gate. Ideally the gate would be situated a bit further in the upstream direction to place the area of interest exactly in the center. Unfortunately some significant damage to the glass wall at this location was observed. The damage to the glass will have a negative impact on the images for the PIV measurements. Therefore the next window was taken as PIV window. This resulted in the gate being positioned 9.7 meter after the water inlet and thus 9.5 meter before the end of the flume, see Figure 4.2. The area of interest is still sufficiently far upstream of the downstream end of the flume to ensure that there are no boundary effects (verified with CFD, 5 meter minimum, see Subsection 3.7.3). With the placement of the gate the position of the steel bars along the side of the flume is taken into account. To ensure a clear visual on the flow through the opening the gate is placed 0.1 meter after a bar.

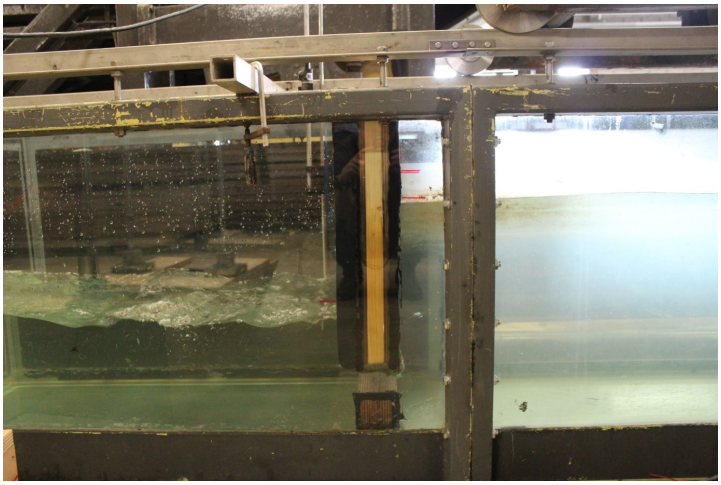

Figure 4.1: Scale model gate with a water level difference of approximately 0.2 meter

The boundary effects at the area of interest should of course be as little as possible. Using a standard free jet dispersion angle of 9.46 degrees (Section 2.3.2), the distance that is needed to get to a fully spread velocity profile can be estimated. Assuming that the jet needs to spread over half the water depth the distance until the jet reaches the boundaries can be calculated using $x = \tan(9.46)/0.15$. With x being the horizontal distance from the gate. The fully developed flow is realised over twice this distance, assuming that the reflection occurs at the same angle as the spreading of the jet. This comes down to a distance of 2.25 meter. Comparing this quick estimation to the 5 meter found in CFD (Subsection 3.7.3) quite a large difference is found. This is caused by the fact that the jet is attaching to the bottom and thus not behaves like a free jet. Since the prediction in CFD is more accurate the 5 meter will be taken into account. Meaning that the area of interest should be at least 5 meter from any boundary.

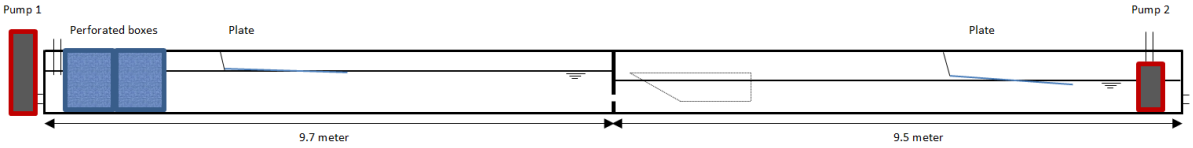


Figure 4.2: Overview of the scale model test setup

### 4.1.2. PUMPING SYSTEM

To realise a water level difference over the gate water is pumped through a circulating closed system. Water is extracted from the end of the flume and enters the flume again upstream of the gate. A pump with variable discharge was deployed, see Figure D.1a in Appendix D. With this pump the discharge can be regulated with an accuracy of approximately 1 l/s. Once a constant discharge is reached the set discharge will remain the same for long enough to perform multiple tests. Initially one pump was located at the upstream side, the connection realised using a pipeline with a diameter of 0.1 meter. Unfortunately no single pump was available that could handle the required discharge already estimated with CFD. Therefore an additional pump with a separate pipeline was installed, see Figure D.1b in Appendix D. The diameter of the pipeline is the same, the location of the second pump however was most convenient at the downstream side. Furthermore, the discharge of this pump is constant and could not be regulated. To operate the scale model the second pump could be switched on to deliver the bulk of the discharge, thereafter the first pump could be used to regulate the additional discharge needed. Both the pipelines were equipped with a discharge meter to measure the circulating discharge.

### 4.1.3. REGULATING THE HYDRODYNAMIC CONDITIONS

To ensure a well spread flow at the upstream side of the gate, perforated boxes are placed directly after the inlet, see Figure D.2a in Appendix D. The grid in these boxes spreads the water more evenly across the flume. Due to the concentrated inlet of water at the start of the flume waves are formed, the waves propagate in the direction of the gate. To prevent the surface upstream of the gate from fluctuating, a wooden plate is placed

floating on the surface 4 meter after the inlet, see Figure 4.2. The plate ensures that the water surface becomes more smooth and reduces the propagation of waves in the downstream direction significantly. The surface fluctuations are reduced to such extend that they are almost non existent when arriving at the gate. A similar structure is implemented downstream, 3 meters before the end of the flume. Here the purpose of the plate is to prevent waves which reflect at the end of the flume from reentering the area of interest, see Figure D.2b.

Ideally the situation downstream of the gate corresponds to the situation found in a real lock. There are however two differences between a real lock and the scale model which need to be addressed. One, there is no filling of the lock over time since a stationary situation is tested. This is not a problem for the purpose of the tests, since the interest lies not in the behaviour over time but in the relevant positions of the ship. Two, since the water is pumped in a closed system a water level difference can be expected between the gate and the end of the flume. An alternative would be to construct a weir at the end of the flume to force a constant water level. This is however more difficult to construct and possibly not needed. An estimation needs to be made considering the slope of the water surface. The estimation will be provided using the Chézy formulation, see Equation 4.1.

$$i = \frac{1}{R}(\frac{U}{C})^2 \tag{4.1}$$

Where:

$i$ = the slope of the water surface $[m/m]$
$R$ = the hydraulic radius $[m]$
$U$ = the average flow velocity $[m/s]$
$C$ = the Chézy coefficient $[m^{\frac{1}{2}}/s]$

The Chézy coefficient can be calculated using Equation 4.2. The Manning roughness for glass walls, with some additional roughness due to the connections, is estimated to be 0.014 based on the information provided in Chow (1959).

$$C = \frac{1}{n}R^{\frac{1}{6}} \tag{4.2}$$

Where:

$n$ = the Manning roughness of the walls $[s/m^{\frac{1}{3}}]$

With the two equations the water surface slope can be estimated. To determine the average flow velocity and hydraulic radius a water depth of 0.30 meter is assumed. Furthermore a maximum discharge of 43 l/s is expected, see Subsection 3.7.2. This results in a surface slope of $2.3{\cdot}10^{-4}$ and thus a total water level difference over the flume after the gate of $9.5 * 0.00025 * 1000 = 2.2$ mm. The surface slope will also be measured to see if the calculated estimate is correct.

## 4.2. THE MODEL SHIP

The model ship is made entirely from wood except the bow, which is made from perspex. The reasoning behind this, is that for the PIV measurements in front of the ship, the bow needs to be transparent to enable lighting in the area in front of the bow. On the top of the ship three force sensors are installed, which are placed in a triangular shape to ensure that the ship stays fixed in every degree of freedom. Two are placed in front of the ship and one on the back. On top of each force sensor a steel cylinder is placed, which is connected to a steel beam fixed to the flume wall. The height at which the ship is placed can be regulated using screwing-bolts, for every cylinder two bolts are used. One of the bolts is placed on top of the beam and one is placed under the beam. A photo of the ship in normative position is included in Figure 4.3.

To compensate for the upward pressure of the water, weights can be placed in the ship. By carefully placing the right amount of weights the draught of the ship can be regulated without overloading the force sensors. For clarity, the ship can be moved in both the vertical and the horizontal direction between the different measurements. However, during a measurement the ship will remain in a fixed position. To ensure that there is no friction between the wall of the flume and the ship some space needs to be left open. This space should however be as small as possible to maintain the 2D schematisation. A tolerance of 3.5 millimeter on each side

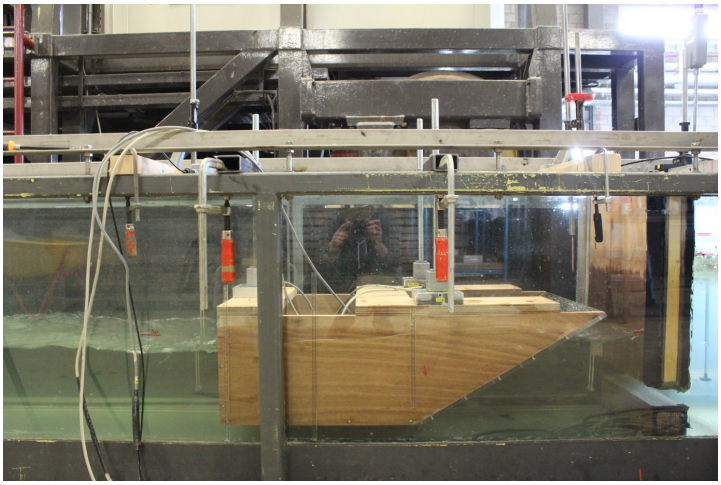

Figure 4.3: Scale model ship with a water level difference of approximately 0.2 meter

was chosen considering many different factors, e.g. expansion of the wood due to the water, the accuracy on which the ship can be placed in the flume and irregularities in the wall of the flume at the locations where different segments are connected to each other. Before each measurement, during the installation of the ship, a check was performed to ensure that the ship did not make contact with the wall at any point.

## 4.3. DEFINITION OF THE COORDINATE SYSTEM

For the experiments a Cartesian (x,y,z) coordinate system is defined. With x in the longitudinal direction, y in the cross direction and z in the vertical. The origin of the coordinate system is chosen at the right downstream side of the gate when facing in the flow direction. The origin for the z-axis is placed on the bottom of the flume. The directions of the axis are displayed in Figure 4.4. The flow directions (u,v,w) correspond to the directions of the (x,y,z) axis within this coordinate system.

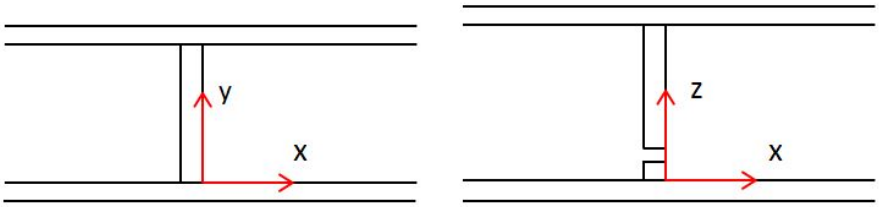


Figure 4.4: Top view of the coordinate system (left) and side view of the coordinate system (right)

## 4.4. MEASUREMENT INSTRUMENTS

In this section the measurement instruments available for the tests will be discussed. This includes some detailed information about the operation and accuracy of the wave height meter, the electromagnetic velocity meter and the force sensors. Furthermore, the main position of the instruments will be elaborated. The main position is defined as the default location of the measurement instrument. The location can however change since multiple different measurements were performed. The following measurement instruments where used:

1. 4x Wave height meter (WHM).
2. 1x Electromagnetic velocity meter (EMS).
3. 3x Force sensors.
4. 2x Discharge meter.
5. A complete PIV measurement setup.

### 4.4.1. WAVE HEIGHT METER

The wave height meter is developed to measure dynamically varying liquid levels and thus excellent for the measurement of a free surface. The wave height meter consist of two parallel stainless steel rods with a plat-

inum reference electrode to compensate the surface elevation measurement for the effect of varying electrical conductivity of the fluid. The output signal is linearly proportional to the liquid level between the sensor rods. The response frequency is 15 Hz and the accuracy is 0.5% of the measurement range, which is 0.5 meter. To determine the zero value of the wave height meters a ruler is used. With the ruler the stationary water level is measured simultaneously with the wave height meters. Consequently the wave height meters can be adjusted to correspond with the manual measurements. Since the water level is constant in the horizontal the wave height meters are calibrated very well with respect to each other. The absolute water level is however subject to the accuracy of measuring with a ruler, approximately 1 millimeter.

### 4.4.2. ELECTROMAGNETIC VELOCITY METER

With an electromagnetic velocity meter, in Dutch 'Elektro Magnetische Snelheidsmeter' (EMS), the water velocity in two perpendicular directions can be measured. The EMS consist of a steel rod with a probe at the tip. The measurement principle is based on liquid moving through the magnetic field created underneath the tip of the probe. Two pairs of platinum electrodes inside the probe sense the induced voltages produced by the flow passing the probe. The probe has been designed in such a way that these voltages are proportional to the liquid velocity parallel to the plane of the electrodes. The dynamic response of the electromagnetic velocity meter is 7 Hz. The range is set to 5.0 m/s and the accuracy is 0.01 m/s plus 1% of the measured value. The measured volume under the probe depend on the homogeneity of the flow field. When the flow is homogeneous 95% of the signal is measured in a layer thickness of 5 mm. However if the flow has multiple layers with different velocities this layer thickness can increase up to 10 mm. To ensure the right zero value for the measurement an automatic method is developed. In stationary water ten seconds of data is collected, then an average is taken over the ten seconds and this will function as the zero point for the rest of the measurements.

### 4.4.3. FORCE SENSORS

The force sensors that need to be used can be selected based on the expected force calculated with CFD. The force in the x-direction according to the CFD model, described in Chapter 3, is equal to 48 Newton. Three force sensors with a maximum capacity of 50 Newton should suffice. There would be very little chance that one sensor reaches its maximum capacity, since the force is divided over the three sensors. Even in the case of one sensor recording significantly more force than the other two, no sensor will reach its maximum capacity. Only two 50 Newton force sensors were available at the time. As an alternative one sensor with a larger measurement range of 200 Newton was taken. To maintain symmetry the two 50 Newton sensors where placed in the front and the third with the capacity of 200 Newton in the back. The accuracy of the 50 Newton sensors is 0.20 Newton and the accuracy of the 200 Newton sensor is 0.50 Newton. In the most unfavourable situation, all three inaccuracies are measured in the same direction, the uncertainty will therefore be smaller than 0.9 Newton. The force sensors placed on the ship measure forces in three directions, i.e. x, y and z. The main interest lies in the longitudinal forces on the ship, the forces in the x-direction. Forces in the other directions will also be measured but only to see if there are extreme results, which can have a negative impact on the parameter of interest. For example, when extreme forces in the z-direction are measured the forces in the x-direction will possibly be influenced by the extreme results. In such a situation it is unlikely that the forces in the x-direction are measured correctly.

### 4.4.4. MAIN POSITION OF THE MEASUREMENT INSTRUMENTS

The main position of the EMS is in the center of the flume, 0.10 meter after the gate and 0.125 meter above the bottom, see Figure 4.5. This is in the center of the opening, where the highest velocities are expected. In terms of coordinates defined in Section 4.3 the position is (0.10,0.25,0.125).

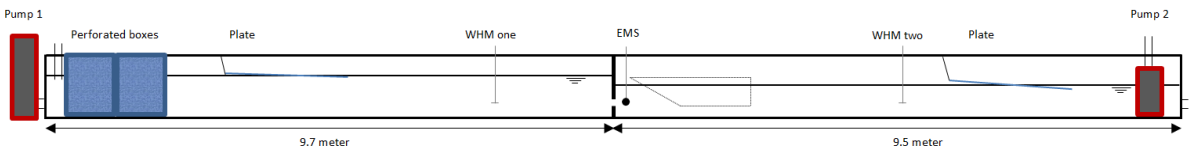


Figure 4.5: Overview of the scale model test setup for the main position of the measurement instruments

The discharge measurement instruments are each placed on a pipeline. Discharge meter one is placed on the pipeline with the pump that can vary the discharge and discharge meter two is installed on the constant

pump. The total discharge can be determined by a summation of the two. This is not indicated in the figure because it is trivial.

Two wave height meters have a fixed position and serve as a reference for the water level difference over the gate. Wave height meter one is placed 3.5 meter in upstream of the gate and wave height meter two is placed 5.1 meter downstream of the gate. Both are placed at some distance from the gate to minimise the influence of the flow in the area of the gate. Therefore the measured water levels are assumed to be representative for the average water level in, the entrance channel (in front of the gate) and the lock (after the gate). The third wave height meter can be deployed where needed for the specific measurement.

## 4.5. MEASUREMENT TIME

The time needed to reach the stationary condition after turning on the pumps must be determined. During this time the actual measurement can not be started yet, since the flow will not be a good representation of the stationary condition. The time needed to reach the stationary condition can be found by measuring for a long time and determining from the data, after what amount of time the signals remain relatively constant. Because there is always some fluctuating noise in a measurement signal, relatively constant means that a signal fluctuates around a certain value. In this case it was found that the flow reaches its stationary condition 20 minutes after turning on the pumps.

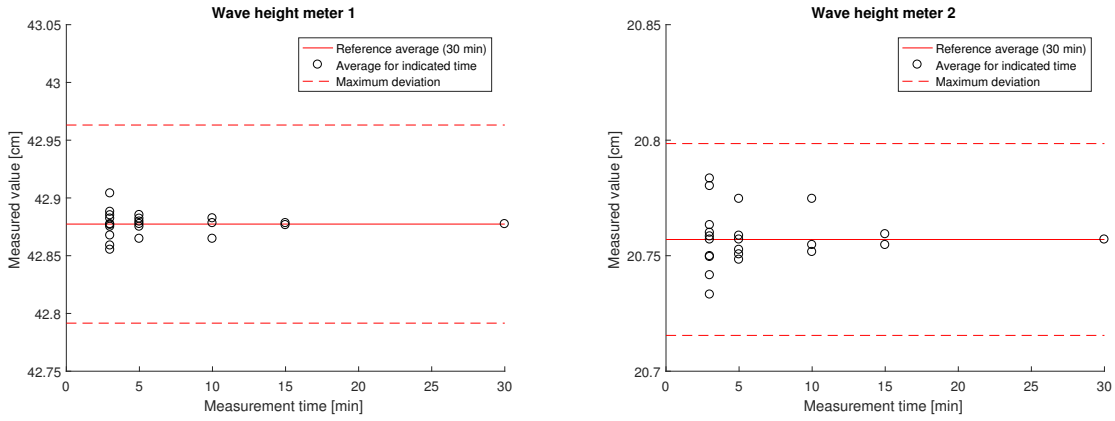


Figure 4.6: Deviations of the average of different measurement times with respect to the reference average, for the wave height meters

Besides the time it takes to reach a stationary condition another time period must be determined. The minimum time needed for each measurement, to ensure a good representation of the average flow is captured. The following method is used to determine the measurement time. First a measurement is performed with a time long enough to be sure that the average flow is measured and no low frequency oscillations are neglected. The time for this measurement was taken to be 30 minutes. Three parameters where measured: the water level upstream, the water level downstream and flow velocity just after the gate. The position of the measurement instruments is given in Section 4.4. The discharge was set to be 46.8 l/s to create a water level difference of 0.22 meter between the two measurement points. Initially was aimed for an water level difference of 0.2 meter, corresponding to the normative condition. However to set a discharge accurately with the two available pumps was harder than expected. Fortunately the exact discharge does not matter for the purpose of determining the needed measurement time.

An average over the 30 minutes of each parameter is determined to serve as a reference value. Then the data from the whole time series is subdived into smaller time series. The following situations are considered: two times 15 minutes, three times 10 minutes, six times 5 minutes and ten times 3 minutes. First the results from the wave height meters are considered. The deviation of the average from each smaller time series compared to the average over 30 minutes is plotted in a figure, see Figure 4.6. It is clear that even for a measurement time of 3 minutes the deviation of the reference average is not large. Considering a maximum deviation of 0.5% of the reference average value indicated in the figures with the dashed line. When looking at the velocity data, see Figure 4.7, the optimum measurement time was found to be 5 minutes, since the maximum deviation is exceeded with the measurement time of 3 minutes.

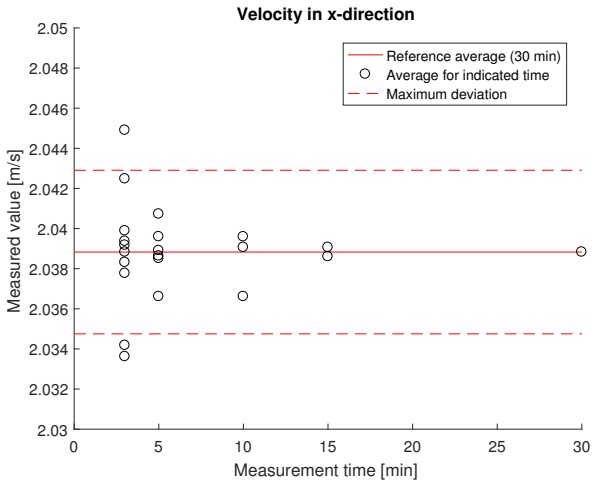


Figure 4.7: Deviations of the average of different measurement times with respect to the reference average, for the EMS

## 4.6. VELOCITY POINT MEASUREMENTS

EMS point measurements will be done to see if the flow in the flume behaves as expected, simultaneously measurements will be performed to test the water surface slope on the downstream side of the lock. First the adjustments to the base setup will be elaborated and then the measurements that were performed are described.

### 4.6.1. SETUP FOR THE VELOCITY POINT MEASUREMENTS

Before the velocity measurements were performed only one perforated box was present in the flume. The second one was installed after analysing the results of the point measurements in order to improve the flow distribution upstream of the gate. To test the surface slope an additional wave height meter (wave height meter three) is installed 8.5 meter after the gate, see Figure 4.8. With this wave height meter an estimation of the surface slope in the flume can be made. For example if a large difference between the newly installed wave height meter and the wave height meter at 5.1 meter is measured, a large water surface slope can be expected. This will only give an indication, if the surface needs to be measured more accurately multiple wave height meters need to be installed.

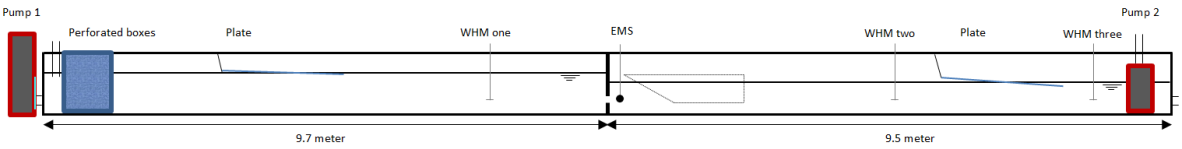


Figure 4.8: Overview of the scale model test setup for the EMS measurements and location of the wave height meters

### 4.6.2. VELOCITY POINT MEASUREMENTS TO BE PERFORMED

A consideration must be made about the number of point measurements performed. It takes too much time to measure everywhere and therefore the most important locations must be selected. In Subsection 3.7.1 some suggestions were made about possible locations to validate the flow. These options will be taken into account when determining the most important points to measure.

The velocity measurements will be performed without ship in the flume and with the ship in the normative position. For the situation without the ship, the pumps are set to a combined discharge of 45 l/s and for the situation with ship 43 l/s. Once the flow can be considered stationary the first measurement can start. Each measurement will have a duration of 5 minutes and the following parameters will be measured: the discharge, the water level upstream, the water level downstream, the water level near the end of the flume and the velocity at various positions. Both horizontal and vertical velocities will be measured. However mainly the horizontal velocities (velocities in x-direction) will be used, since these give the best impression of the

behaviour of the jet and are most important for the longitudinal forces on the ship.

For the case without ship four positions are selected to measure the flow profile in the vertical. The first position is 0.1 meter after the gate. This is still within the potential core of the jet and will therefore give an indication of the maximum velocities in the jet. The second position is 0.3 meter after the gate, this is where the jet attaches to the bottom according to the CFD calculation. The third position is 0.8 meter after the gate, where the jet should be fully attached to the bottom. The first three positions will provide information about the behaviour of the jet. The fourth point will be 4.8 meter from the gate, here a nearly fully developed flow profile is expected. On each position four points will be measured. The middle of the gate opening will be taken as reference point, which is 0.125 meter above the bottom. The rest of the water depth is sampled equally with 0.05 meter between each point. Resulting in 0.075, 0.125, 0.175 and 0.225 meter measured from the bottom. Close to the bottom and the water surface the EMS is known not to perform sufficiently accurate therefore no measurements will be performed here. Finally, a measurement over the width of the lock will be done to validate the two dimensional behaviour of the jet. This measurement will be 0.1 meter after the gate in the middle of the opening. Five points over the width are selected with the center of the flume as reference point and a distance of 0.1 meter between each point.

For the case with ship the same measurements will be performed. However position two and three are impossible since the ship blocks the possibility to place the EMS. Instead an alternative position 0.1 meter behind the ship is selected. The points also deviate slightly, since on this position the points higher in the water column are less interesting. Furthermore, an additional point is taken in the middle of the opening between the bottom and the ship. The following points are measured at this location 0.035, 0.075 and 0.125 meter from the bottom. In Table 4.1 the performed EMS measurements are summarised. Each position is indicated and the number of points over the depth or the width.

Table 4.1: Point measurements for the velocity

| Measurement and position | Ship | Number of points over the width | Number of points over the depth |
|---|---|---|---|
| One $x = 0.1$m | no | 5 | 4 |
| Two $x = 0.3$m | no | - | 4 |
| Three $x = 0.8$m | no | - | 4 |
| Four $x = 4.8$m | no | - | 4 |
| Five $x = 0.1$m | yes | 5 | 4 |
| Six $x = 1.2$m | yes | - | 3 |
| Seven $x = 4.8$m | yes | - | 4 |

## 4.7. FORCE MEASUREMENTS

The optimal research program for the force measurements delivers the needed data and is realistically executable in the available time. Therefore, a strategic decision needs to be made concerning the high number of variables displayed in Figure 3.1. Not all can be varied to measure their influence on the force against the ship. Some must remain constant to make the tests practically realisable and reduce the number of different variations. The normative situation defined earlier will function as starting position for these variations. When varying one parameter the others will maintain the same value as the normative situation. The following three parameters will be varied:

1. The keel clearance of the ship ($k_c$) (and subsequently the draught).
2. The distance between the ship and the gate ($X_{bow}$).
3. The water level difference ($\triangle h$), which is a function of the discharge ($Q$).

All the parameters directly related to the gate are kept constant, because the main interest lies in the interaction between the ship and the jet. The size, position and geometry of the gate opening do influence the behaviour of the jet and thus the force on the ship. However, if the gate remains constant, parameters directly related to the ship can be researched more efficiently. Varying parameters concerning the door will benefit the knowledge about the interaction between the jet and the ship less then varying the position of the ship. The ship itself is also kept constant for better understanding of the physics. If the influence of the ship's po-

sition on the force can be understood for a specific geometry, the step to understand it for other geometries can be made in a later study.

### 4.7.1. SETUP FOR THE FORCE MEASUREMENTS

Two additional wave height meters are installed besides the two reference wave height meters discussed in Section 4.4. The wave height meter near the end of the flume is removed since it is not needed to determined the water surface slope again. Wave height meter three is installed 0.1 meter downstream of the gate and wave height meter four 0.1 meter after the ship. The position of wave height meter four will thus change if the ship is moved. Wave height meters one and three make it possible to measure the water level difference over the gate accurately. Furthermore the average water level around the ship can be determined using wave height meters three and four, except when the distance between the ship and the gate is varied. Being able to measure the water level difference over the gate was found to be more important then the water level around the ship, otherwise wave height meter three would have been moved together with the ship.

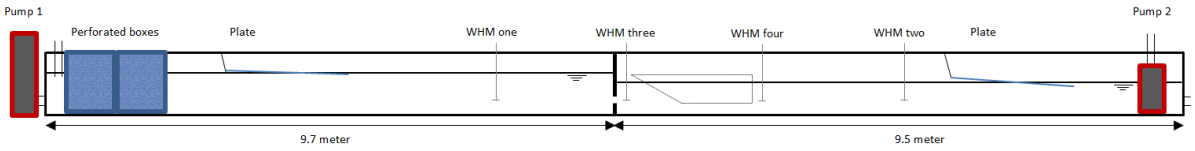


Figure 4.9: Position of the wave height meters during the force measurements

### 4.7.2. FORCE MEASUREMENTS TO BE PERFORMED

Six variations for $k_c$ will be tested. For each variation $X_{bow}$ will be 0.6 meter and the $\triangle h$ 0.2 meter, corresponding to the normative situation. The first variation is the normative situation, then for each variation the keel clearance will increase. The first steps will be small because a large effect on the force is expected, i.e. a strong gradient in the relation between force and keel clearance is expected. This is caused by the fact that the jet will be stronger near the bottom due to its tendency to attach to the bottom. Once the ship's bottom is on the same level as the top of the opening, the effect of the jet on the force will decrease significantly, because the jet can easily move under the ship. Thereafter one more position is taken just above the opening. This results in the following values for the keel clearance to be considered: 0.07 meter, 0.08 meter, 0.09 meter, 0.10 meter, 0.15 meter and 0.17 meter.

Five variations for $X_{bow}$ will be tested while $k_c$ and $\triangle h$ remain constant. Again the normative situation is the starting point from which $X_{bow}$ will be increased with each variation. The following values for the distance to the gate will be considered: 0.6 meter, 0.8 meter, 1.05 meter, 1.55 meter and 2.05 meter. The difference between each variation is smaller close to the gate because here a larger effect on the force is expected. The choice of these distances also takes into account the positions where it is not possible to install the ship due to the geometry of the flume. For example if a distance of 1.0 meter was chosen a beam would preclude the possibility of fixing the ship to the flume.

Three variations for $\triangle h$ will be tested while $k_c$ and $X_{bow}$ remain constant. Only three variations are chosen because a linear relation is expected between the water level difference and the force on the ship, this expectation can be confirmed with three points. The relation is expected to be linear because $U \propto \sqrt{\triangle h}$ see Equation 3.6 in Chapter 3 and $F \propto U^2$ see Equation A.2 in Appendix A. The square root cancels out the square resulting in a linear relation $F \propto \triangle h$. The normative situation has the highest water level difference realisable in the flume, therefore $\triangle h$ will be lower in the other two variations. The water level differences that will be considered are: 0.2 meter, 0.15 meter and 0.1 meter. A different water level difference is realised by adjusting the discharge and altering the starting volume of water in the flume to maintain a constant $h_2$. For a lower water level difference less water is needed in the flume.

## 4.8. PIV MEASUREMENTS

Since PIV is a rather advanced measurement method, some additional information about the technique is required. The abbreviation PIV stands for Particle Image Velocimetry. Simply stated small particles in the flow are traced using a camera and based on their displacement a two dimensional velocity field can be determined. Unlike for example EMS measurements, the PIV technique is non-intrusive, this implies that the

technique itself does not influence the flow in any manner. Furthermore PIV provides a full velocity field instead of single points. In the following paragraph the different aspects of the PIV measurement technique will be elaborated, the information is based on Van Velzen & Dos Santos Nogueira (2015).

A light source is installed that illuminates a single sheet in the area of interest. Meanwhile, a camera perpendicular to the plane of light and synchronised with the light source will capture images. For the light source a double pulsed laser is used. This laser illuminates the area of interest two times with a time difference of *dt*. For each laser pulse an image is made by the camera. On the frames captured by the camera the particles present in the flow will be visible. The frames will then be split into a grid of interrogation areas. At all interrogation areas a cross-correlation function will be used to determine the most probable displacement of a group of particles, resulting in an instantaneous two-dimensional vector map describing the flow for the time interval *dt*.

### 4.8.1. SETUP OF THE PIV MEASUREMENTS

A number of adjustments to the setup must be made to realise the PIV measurements. For safety reasons the entire flume has to be covered. This was realised using a combination of wooden plates and thick cloths, see Figure D.3a in Appendix D. Most of the other measurement instruments were removed to not interfere with the PIV measurements. Only the discharge meters and the reference wave height meters were kept in position. The laser is installed as indicated in Figure 4.10. To fully capture the area of interest and make the angle with the perspex as perpendicular as possible, the laser is aimed perpendicular to the plane between the bottom of the bow and the intersection between the water surface and the gate. The aim of the laser has a 21° degree offset with the vertical. The height at which the laser is installed is determined by the angle at which the laser light diverges which is approximately 10° degrees to both sides.

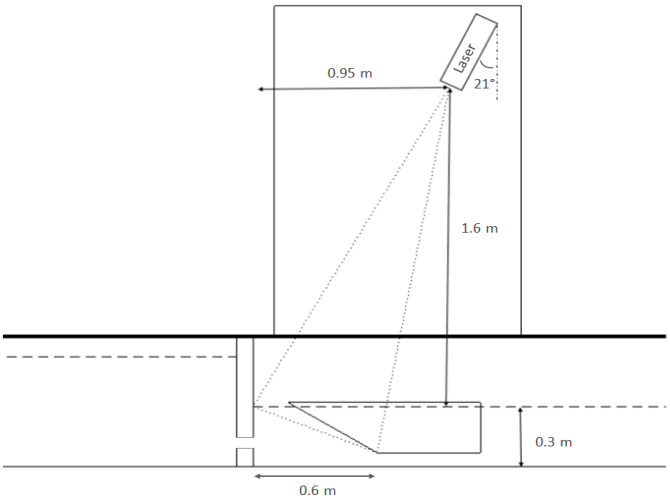


Figure 4.10: Laser position for the PIV measurements

The camera is positioned such that the area of water just after the gate can be captured, see Figure D.3b. The distance from the flume is determined by the area that needs to be captured. In this case about 1 meter from the flume to capture an area of 0.3 x 0.6 meter. The camera is placed on the same height as the center of the fluid that needs to be measured. This ensures that the perspective is correct and that the image is not distorted.

The water just after the gate needs to be stabilised, otherwise the surface instabilities caused by the flow will reflect the laser light, which will negatively impact the quality of the images. To realise a stable surface a special structure is made from perspex, see Figure D.4a. The structure can be best described as a small boat which is held in place by steel bars. The edges of the perspex structures are made higher with tape to avoid splashes of water into the structure. For the situation with the ship in the flume a similar structure is made. This structure is however attached to the ship to avoid a shade area, see Figure D.4b. In both cases the width of the structure is kept as small as possible to avoid any effect on the flow (or on the ship) as much as possible.

### 4.8.2. DETAILS ABOUT THE PIV MEASUREMENTS

The following main aspects determine the accuracy of the PIV data acquisition:

1. Time between laser pulses ($dt$).
2. Diameter and number of particles in the flow.
3. Size of the interrogation areas.

The time between laser pulses is dependent on the flow velocity in the area of interest. The time step should be large enough to capture the displacement of particles over the time $dt$. But also be small enough to maintain the needed precision. The cross-correlation algorithm should still be able to detect most of the particles within the interrogation area. For the measurements performed within this research the $dt$ was varied from 1500 up to 2000 microseconds.

The particles in the water, also referred to as seeding, need to meet some requirements. First of all, the density of the seeding should be equivalent to that of the host fluid. Secondly, the size of the seeding is important. The particles must be small enough to not influence the flow and large enough to cover 3-5 pixels to ensure detection by the camera. For these PIV tests the optimal size of the seeding particles was found to be 100 micrometer. Furthermore, the fluid should contain enough particles and they should be spread in the fluid evenly. About 9 particles per interrogation area is commonly used as reference quantity. To realise this 20 grams of seeding was added to the water in the flume. Since it is a closed system no additional seeding has to be added once the seeding is in the water.

The size of the interrogation areas must be determined based on the flow velocity, time between pulses and the concentration of seeding present in the flow. The resolution of the vector field is determined by the size of the interrogation areas. Two options for the size of the interrogation areas where considered, 64 x 64 pixels and 32 x 32 pixels. The results are very similar, however more vectors are displayed when using the smaller interrogation area giving an easier to interpret impression of the flow. Therefore the 32 x 32 pixels interrogation areas are used for the processing of the images.

The laser and camera are set to capture the double frames with a certain frequency. This implies that a specific amount of two-dimensional vector fields can be determined in a given time period. From these instantaneous vector maps a mean flow field can be determined. A frequency of 5 Hz was chosen over a time period of 5 minutes, resulting in 1500 instantaneous velocity fields.

### 4.8.3. CALIBRATION OF THE PIV SETUP

The first step for the calibration of the camera is positioning the camera in such a way that the entire area of interest fits on the image that is taken. The area of interest is defined from the middle of the gate to 0.6 meter downstream of the gate and from the bottom to the water surface. An additional 0.02 meter on all sides is taken as a buffer to ensure that the whole area of interest is in the picture. The next step is to take the calibration picture. For the picture the calibration plate is required, this is a black plate with a roster of white dots. These white dots are positioned exactly 0.02 meter apart from each other. The calibration picture must be taken with the calibration plate positioned at the location where the measurement will be performed, which is in the center of the flume. The flume must be filled with water when the picture is taken because the breaking index of water differs from the breaking index of air. Furthermore enough light must be present when taking the calibration image. Once the calibration image is successfully taken the conversion from pixels to engineering units can be made since the exact distance between dots is known.

The laser sheet needs to be centred as accurately as possible, because any deviation in the laser sheet will result in an error regarding the measured position and an error regarding the camera calibration. To ensure that the laser is focused correctly a structure is paced in the flume with a line indicating the exact center of the flume. Using safety glasses and illuminating the structure with low intensity of the laser, the lens can be adjusted to focus the sheet and position it correctly.

### 4.8.4. PIV MEASUREMENTS TO BE PERFORMED

Two cases will be measured with the PIV measurement system. The first case is without ship in the flume and the normative water level difference of 0.2 meter. The second case is with ship in the normative position and

the same water level difference. Testing these two situations will make a comparison between the flow profile without ship and with ship possible. Both cases will be measured four times with slight deviations in the *dt* settings. After finishing the measurements one measurement series of each case will be selected for further processing.

### 4.8.5. ADDITIONAL EMS MEASUREMENTS FOR A COMPARISON WITH PIV

In order compare the flow measured with PIV to the flow measured with the EMS a higher resolution of the EMS measurements is required. Therefore additional EMS measurements were performed after the PIV measurements. Only the situation without ship is considered in the comparison between measurement methods. Exactly the same discharge that was used for the PIV measurements is used for the additional EMS measurements, making a direct comparison possible. Eight additional points where measured over the vertical 0.1 meter downstream of the gate. The points where picked around the maximum measured earlier with the point measurements. The following distances from the bottom where measured: 0.05, 0.07, 0.09, 0.11, 0.122, 0.13, 0.15 and 0.17 meter.

## 4.9. CONCLUSION: MEASUREMENT PROGRAM

In this section an overview will be given of the measurements that were treated extensively in Sections 4.6, 4.7 and 4.8. In Table 4.2 all the measurement variations are summarised. In case of the EMS measurements not all the individual tests are displayed to keep the table clear.

Table 4.2: Measurement program

| Type of measurement | Variations | Total measurements |
|---|---|---|
| EMS measurements without ship | one, two, three and four | 21 |
| EMS measurements with ship | five, six and seven | 16 |
| Force measurements with varying $k_c$ | 0.07, 0.08, 0.09, 0.1, 0.15 and 0.17 meter | 6 |
| Force measurements with varying $X_{bow}$ | 0.6, 0.8, 1.05, 1.55 and 2.05 meter | 5 |
| Force measurements with varying $\triangle h$ | 0.2, 0.15 and 0.1 meter | 3 |
| PIV measurements | with ship and without ship | 2 |
| Additional EMS measurements for PIV | eight positions in z direction | 8 |

# 5

# RESULTS OF THE SCALE MODEL TESTS

In this chapter the results from the scale model measurements are discussed. First the velocity point measurements are elaborated, then the force measurements and finally the PIV measurements. The results in this chapter are raw results and thus not edited in any way. To give an indication of fluctuations in the measured signal the standard deviation is often calculated. The force measurements are also displayed in dimensionless values to make them generally applicable. The PIV results are provided both with ship and without ship in front of the gate. Furthermore a comparison is made between the PIV results and the point measurements.

## 5.1. REPRESENTATION OF THE DATA

The results presented in this chapter are averages over the measured time unless stated otherwise. To give an indication of the fluctuations in the signal the so called population standard deviation of the measurement signal is often provided. The population standard deviation is defined in Equation 5.1.

$$\sigma = \sqrt{\frac{1}{N}\sum_{i=1}^{N}(x_i - \bar{x})^2} \tag{5.1}$$

Where:

$\sigma$ = the population standard deviation [−]
$N$ = the number of data values [−]
$x_i$ = $x$ value at entry point $i$ [−]
$\bar{x}$ = average of all $x$ values [−]

## 5.2. EMS POINT MEASUREMENTS

The EMS measurements that were performed are described in Section 4.6. First the results without ship are discussed, followed by the results with ship. The main aim of the velocity point measurements is to capture the flow in the flume and determine if the flow is similar to the flow found with the CFD calculations. Similar in the sense that the behaviour of the jet corresponds, since the exact values of the velocity profiles will not be compared to each other in the present study. The purpose of the velocity measurements over the width is to validate the two-dimensional assumption. This means that the velocity gradients over the width must be low and the cross-sectional velocity profile should be predominantly uniform and symmetrical. The velocity measurements over the depth provide information about the velocity profiles at different points in the flume. These can be used to check the behaviour of the jet and give an indication of the position in the flume where the flow can be considered uniformly spread over the depth. Which is important information to validate the position of the reference wave height meter (wave height meter two).

### 5.2.1. WITHOUT SHIP

Figure 5.1 displays the average measured velocity profiles without the ship in the flume with $h_1$ = 0.5 meter and $h_2$ = 0.3 meter. The standard deviation of each measurement point is indicated with the blue bar. This gives an indication of the fluctuations within the measurement signal. The velocity profiles are measured at

different distances from the gate. The measurements will be discussed in the downstream direction, starting with a distance 0.1 meter from the gate.

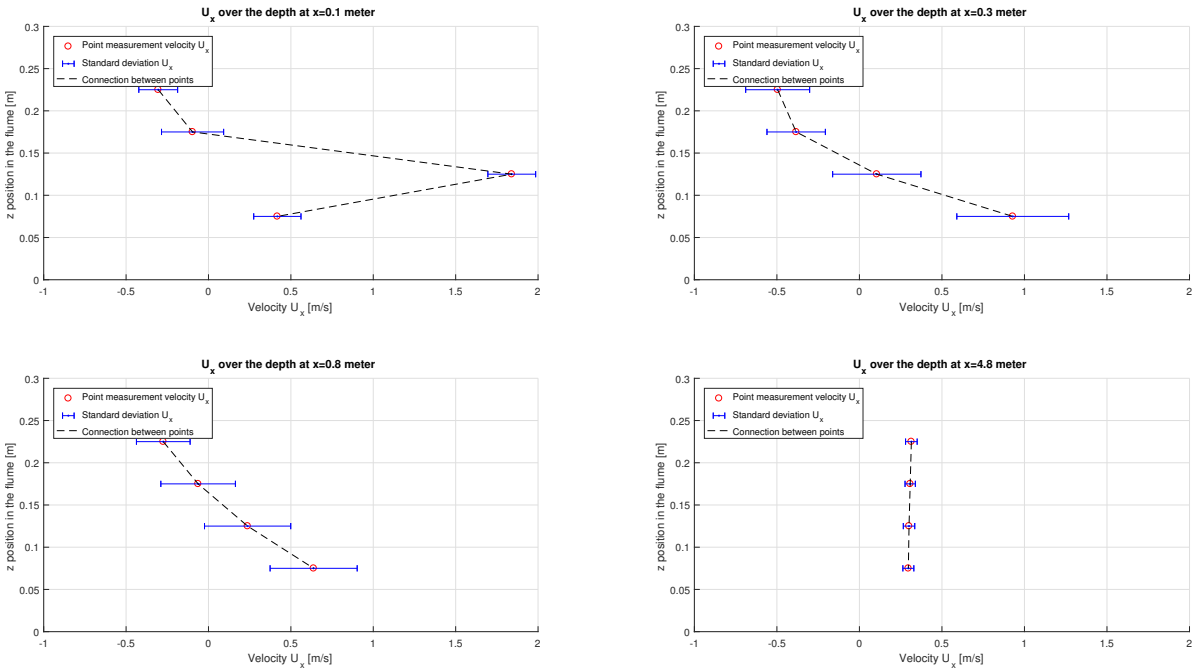


Figure 5.1: Point measurements without ship, over the depth, 0.1, 0.3, 0.8 and 4.8 meter downstream of the gate

At 0.1 meter the presence of the jet and the return flow above the jet is clearly noticeable. In the results from the CFD calculation an eddy under the jet was observed, this eddy is not captured with the chosen measurement points, but it is plausible that this eddy is present considering the gradient between the lower two points. Note that the measured maximum is not necessary the maximum velocity in reality. If the maximum velocity needs to be determined a higher resolution of measurement points around the center of the jet is needed. The CFD calculations showed a jet which attached to the bottom, therefore it is likely that the maximum velocity will be found a bit under the center of the opening at $z = 0.1$ meter. This will be discussed further when comparing the point measurements to the PIV measurements.

Further downstream of the gate, at 0.3 meter, the jet is clearly attaching to the bottom. Furthermore a high amount of return flow in the eddy above the jet can be observed. Continuing to 0.8 meter from the gate the shear between the eddy near the bottom and the return flow above the jet result in a increasingly equally spread flow pattern. At 4.8 meter downstream of the gate the flow has almost reached a uniform flow distribution, concluded from the fact that there are no large gradients in the velocity profile. A quick check can be performed by averaging the velocity over the measured points and comparing this to the discharge through the flume divided by the wet cross-section, see Equation 5.2. With $Q = 0.045 m^3/s$ and $h = 0.3$ meter this results in 0.3 m/s, which agrees very well with the average of the measured velocities, 0.3 m/s.

$$\frac{Q}{A} \approx U_{x,average} \tag{5.2}$$

Where:

$Q$ = the discharge $[m^3/s]$
$A$ = the wet cross-section of the flume $[m^2]$
$U_{x,average}$ = the average measured flow velocity $[m/s]$

Figure 5.2 displays the flow velocity over the width of the flume without ship 0.1 meter downstream of the gate. The EMS was set at a height of 0.125 meter, which is in the center of the opening in the gate. The magnitude of the velocities agree with the CFD calculations, see Figure 3.3 in Chapter 3. The velocity profile is symmetrical. Peculiar is however, that the measured velocities near the walls are higher than the velocity in the center.

The wall causes friction and thus deceleration of the fluid, therefore it is expected that the velocity has its maximum in the middle of the flume. The explanation for the measured velocity profile has to be found in the behaviour of the jet and the surrounding eddies. The jet attaches to the bottom and does this more easily in the center of the flume, because here is no friction from the walls. For velocities measured at one height in a single cross-section this implies higher velocities near the wall, because the jet maintains its original direction and velocities longer near the wall. This can be proven by measuring a whole grid of points after the entrance instead of just a few lines which however was not part of the measurement program. The above situation has definitely a three-dimensional effect therefore the following question arises: "Is the two-dimensional schematisation still valid?" In this research it is assumed that the two-dimensional schematisation is still valid because the difference in flow velocity over the width is not significant, about 9% of the maximum velocity.

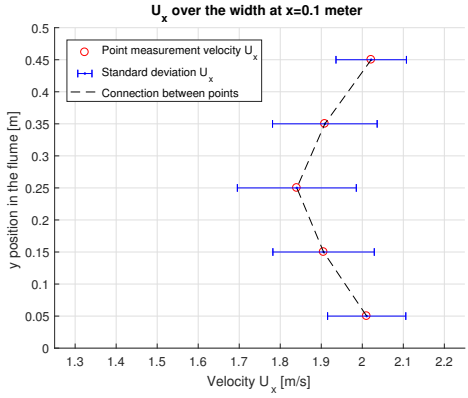


Figure 5.2: Point measurements without ship, over the width, 0.1 meter downstream of the gate

### 5.2.2. WITH SHIP

Figure 5.3 displays the measured velocities with ship in the flume. The velocity profiles over the depth are similar to the velocity profiles measured without ship in the flume. A clear jet 0.1 meter downstream of the gate and a nearly reached uniform flow at 4.8 meter after the gate. Just after the stern of the ship 1.2 meter downstream of the gate a typical wall jet is found, see Subsection 2.3.4. This is a result of the jet being forced under the ship and was also observed with the CFD calculation.

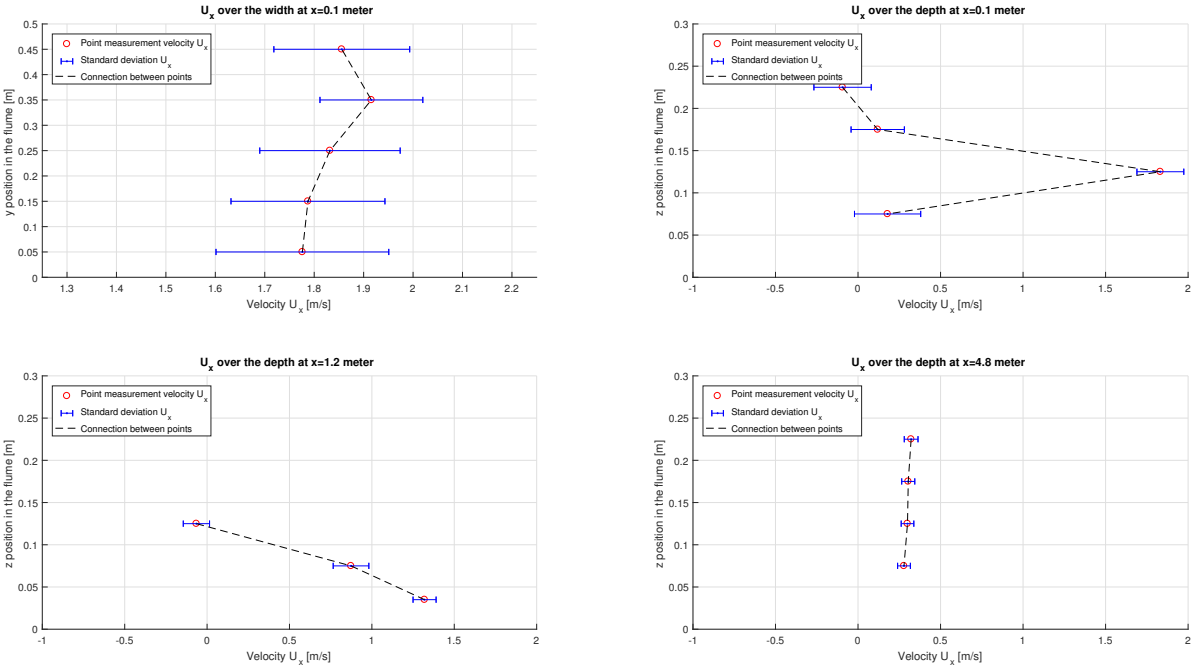


Figure 5.3: Point measurements with ship over the depth and width at 0.1, 1.2 and 4.8 meter downstream of the gate

Considering the measurement over the width of the flume between the gate and the ship, see the upper left plot in figure 5.3, the following can be noticed, the jet is not equally spread over the width of the flume but attaches to one of the walls. This means that the maximum velocity is not exactly in the center of the flume. This is not necessarily a problem but needs to be taken into account since the PIV measurements will be performed in the center of the flume. A number of reasons can be thought of regarding why the jet tends to attach to the wall:

1. The flow already attaches to the wall upstream of the gate, resulting in an unevenly distributed flow through the gate.
2. The tolerance between the ship and the wall is larger on one side providing a way with less resistance and thus a tendency for the jet to attach to that side.

The first point will be improved by inserting another perforated box at the start of the flume. This ensures an evenly distributed flow upstream of the flume. The second point can only be improved by carefully placing the ship in its position, but will always be dependent on the accuracy on which the ship can be installed. Another possibility is that the jet does not attach to the wall at all but oscillates over the width of the lock. This can be tested by checking if there are any significant fluctuations of the flow velocity over time. One measurement series with the coordinates $x, y, z = (10, 35, 12.5)$ cm is studied, this is the measurement series that displays the maximum in the upper left graph in Figure 5.3. The measurement signal, its the average and standard deviation are displayed in Figure 5.4. There are fluctuations in the signal but no clear indication of the maximum velocity in the jet shifting over the width of the opening, because the signal steadily fluctuates around the average. If, for example, the velocity decreased for a longer amount of time the maximum velocity in the jet would likely have shifted over the width of the opening. The differences in flow velocity over the width are relatively small and there is no indication of strong fluctuations over the width. Therefore it is assumed that the two-dimensional schematisation of the flow is still valid.

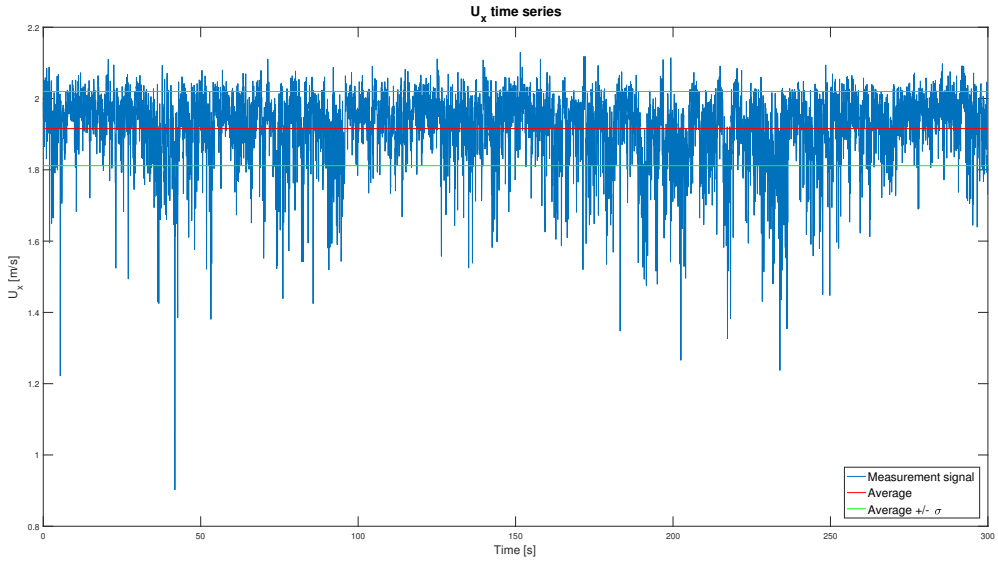


Figure 5.4: Time series of the velocity measurement with the coordinates $x, y, z = (10, 35, 12.5)$ cm

### 5.2.3. WATER SURFACE SLOPE

To get an indication of the water surface slope that is reached in equilibrium state the difference in water level between wave height meter two and three is analysed. An average water level difference is taken over all the measurements without ship. The average water level difference without ship in the flume was found to be 0.9 millimeter (higher downstream water level). The distance between wave height meter two and wave height meter three is 3.4 meter, resulting in a slope of $2.6 \cdot 10^{-4}$. This compares well to the slope calculated in Subsection 4.1.3 which was $2.2 \cdot 10^{-4}$. When the measured discharge and water level are used in combination with Equation 4.1 and 4.2 the comparison is even better. With a measured discharge of $Q = 45$ l/s and water level of $h_2 = 0.29$ meter the slope is $2.7 \cdot 10^{-4}$. The difference between the hand calculation with the measured value and the measured slope is only 3.8% of the measured slope. With this information it can be assumed that the applied roughness of the flume is correct.

## 5.3. FORCE MEASUREMENTS

The flow measurements discussed in the previous section give a clear understanding of the flow in the flume. The jet behaves as expected when compared to the two-dimensional CFD calculations in the sense that it attaches to the bottom and then spreads over the full depth. Furthermore, due to the point measurements the fluctuations over the width are known and their geometrical origin is prevented as much as possible. With this knowledge taken into account the force measurements were performed.

In Appendix E the results of the force measurements are tabulated. As a reminder, a positive force means that the force is directed away from the gate, see Section 4.3. For the normative position of the ship a force of 46 Newton was measured, see Figure 5.5, 5.6 and 5.7. This compares really well to the 48 Newton that was calculated with CFD. In the plots with dimensionless numbers the force $F_x$ is made dimensionless by dividing it by the momentum flux flowing through the gate. The momentum flux is defined as $\rho\frac{Q^2}{A_g}$, with $Q$ being the discharge through the gate and $A_g$ the area of the opening.

### 5.3.1. RELATION BETWEEN THE FORCE AND THE KEEL CLEARANCE

The relation found between the keel clearance and the longitudinal force on the ship is displayed in Figure 5.5. The left graph displays the measured values and the corresponding standard deviation. In the right graph the values on both axis are made dimensionless. To make $k_c$ dimensionless it is divided by the average water depth around the ship measured with wave height meters three and four.

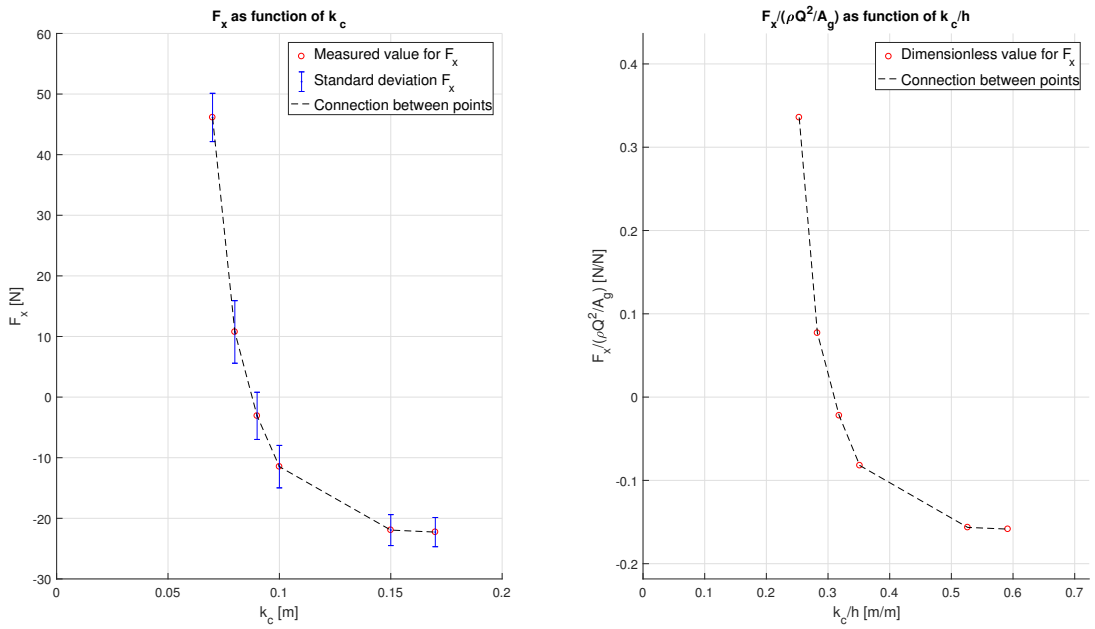


Figure 5.5: Relation between the keel clearance and the longitudinal force on the ship

The physical processes that dominate the relation between the force and the keel clearance will be explained here and were already introduced in Section 2.2. The positive force is mainly induced by the impingement of the jet against the bow and the water level difference over the ship resulting from friction along the ship and the flume. The negative force results from the high flow velocities in front of the ship which decrease the water level compared to the water level behind the ship. The keel clearance for which the highest positive force is measured is the normative position, which can be expected since the influence of the impinging jet is strongest here. From this point increasing the keel clearance results in a decrease of the positive force. Three regimes can be distinguished which can be coupled to the position of the opening in the gate:

1. The bottom of the ship is entirely below the opening in the gate, i.e. the keel clearance ranges from 0.07 up to 0.1 meter. In this regime the force decreases significantly with a small increase of keel clearance. This is caused by a strong decrease in both the jet and the friction force. While the force due to

the velocities in front of the ship remain nearly constant. The jet force decreases because the impingement area reduces. The friction force decreases because the available wet cross-section under the ship increases.

2. The bottom of the ship is on the same level as the opening in the gate, i.e. the keel clearance range from 0.1 up to 0.15 meter. In this regime an increase in keel clearance will result in a higher negative force but with a smaller slope then then in regime one. The slope is smaller because the effect of the jet which is the cause for all three components gets smaller when the ship is on the same height as the opening.
3. The bottom of the ship is entirely above the opening in the gate, i.e. the keel clearance range from 0.15 up to 0.17 meter. In this regime the effect of the impinging jet is almost negligible, after all the jet was found to attach to the bottom and therefore has very little impact on the ship. In other words the gradient in the relation between the force and the keel clearance is almost zero since the jet goes almost fully under the ship and does no longer influence the force significantly. The water level difference over the ship caused by the high velocities in front of the ship are dominating, therefore a negative force is measured.

On the basis of the calculated standard deviations in the force signal something can be said about the fluctuations in the force over time. In general the fluctuations decrease when the ship has a larger keel clearance. Which make sense since the influence of the turbulent jet gets increasingly smaller. The largest fluctuations can be observed at a keel clearance of 0.1 meter. This is when the bottom of the ship is at the same height as the lower side of the opening.

### 5.3.2. RELATION BETWEEN THE FORCE AND THE DISTANCE TO THE GATE

The relation found between the distance from the gate and the longitudinal force on the ship is displayed in Figure 5.6. The left graph displays the measured values and the corresponding standard deviation. In the right graph the values on both axis are made dimensionless. To make $X_{bow}$ dimensionless it is divided by the minimum allowable $X_{bow}$, i.e. the $X_{bow}$ for the normative situation.

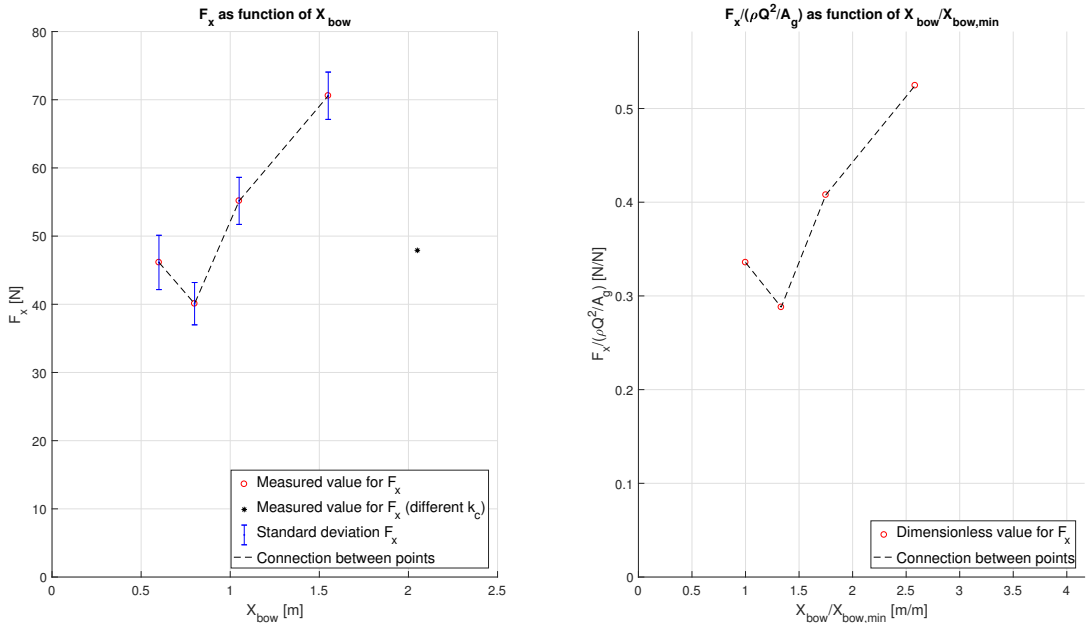


Figure 5.6: Relation between the distance from the gate and the longitudinal force on the ship

The relation that was found between the force and the distance from the gate differs significantly from the expectations. It was expected that the force on the ship would decrease with increasing distance from the gate, since the jet would spread out and thus have a lower impact on the ship. When considering the starting point in normative position 0.6 meter from the gate and the second point 0.8 meter from the gate, this is also the behaviour that follows from the measurements. However, when the ship is positioned even further away the force seems to increase significantly. The force seems to be very strongly influenced by the water

level difference over the ship which increased with an increasing distance from the gate. The measurement 2.05 meter from the gate could not be performed with the normative keel clearance of 0.07 meter because the setup in front of the ship became so high that the ship would overflow. This measurement was therefore performed with a higher keel clearance of 0.085 meter, significantly reducing the force on the ship. The measurement point is indicated with a black star in the left graph. This measurement point is not performed under the same conditions as the other measurements therefore it will be left out of consideration, the other measurements are successful and will be analysed further. The increase in water level difference over the ship and thus the force on the ship can be explained by means of a momentum balance over the bow of the ship.

The following physical process needs to be remembered from Section 2.1.2: a deceleration in the fluid velocity will result in a water level rise. Since the flow is continuously decelerating over the length of the flume the water level will rise. This effect mainly takes place because the ship is blocking the flow, otherwise the water surface would tend towards the equilibrium slope, which can be observed in a flume where no ship is present. The point is that due to the ship blocking the flow and the presence of enough space between the gate and the ship for the water to decelerate the water level in front of the ship will get increasingly higher with a larger distance from the gate. The water level difference over the ship ($\triangle h_s$) is a large contributor to the force, i.e. $F \propto \triangle h_s^2$ based on the hydrostatic pressure in a water column see Equation 2.2 in Subsection 2.1.2. A slight increase in water level in front of the ship results therefore in a large increase in the positive force. The initial decrease in positive force between 0.6 and 0.8 meter from the gate can be explained by means of the tendency of the jet towards the bottom. When the ship is still close to the gate the increase of water level in front of the ship is not yet significant. In this regime the force due to the impinging jet dominates and this force decreases with a larger distance from the gate.

To summarise, there are likely two processes resulting in the curve displayed in Figure 5.6. Close to the gate the impinging jet is dominating the resulting force. This effect decreases as the ship is placed further from the gate. Further from the gate the setup caused by flow deceleration is dominant. This effect increases as the ship is placed further from the gate, at least within the measured range. This will be discussed further in Section 6.4.3.

### 5.3.3. RELATION BETWEEN THE FORCE AND THE WATER LEVEL DIFFERENCE

The relation for the water level difference over the gate ($\triangle h$) and the longitudinal force on the ship is displayed in the left graph of Figure 5.7. In the same figure on the right the relation between the discharge ($Q$) and the force can be found. Both are displayed since $\triangle h$ and $Q$ are strongly related, in the sense that the water level difference over the gate is dependent on the discharge.

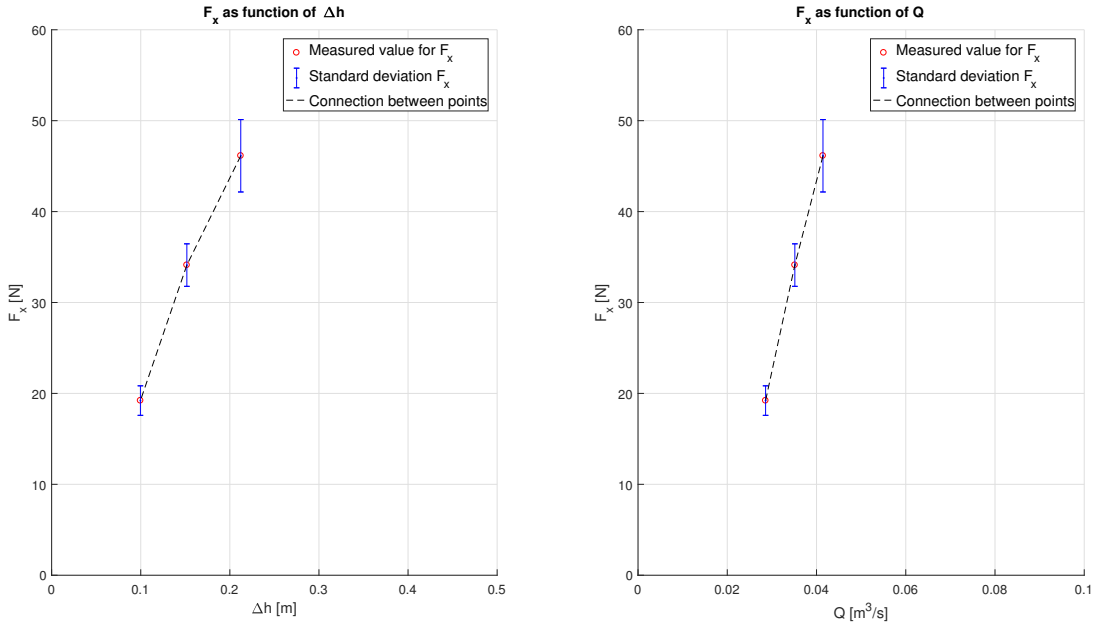


Figure 5.7: Relation between the water level difference/discharge and the longitudinal force on the ship

As explained in Subsection 4.7.2 a linear relation is expected between the force on the ship and the water level difference over the gate. This is in reasonable agreement with the measurements, when looking at the trend of the line. However $F_x \neq 0$ for $\triangle h = 0$ therefore the relation is not linear. This can be explained by the fact that the reasoning for a linear relation only considers the impingement force and not the friction force. The friction force will also decrease with a decreasing water level difference over the gate, making a parabolic relation more likely. The same can be said concerning the the relation between the discharge and the force on the ship. Since the relation appears to be non linear more points on the curve would have been referred, especially close to $\triangle h = 0$.

What can be concluded from both plots is that the fluctuations in force decrease as the water level difference decreases. This is a direct result of the lower flow velocities in the flume with a smaller water level difference. When the water level difference is high the speed at which the water is forced through the door increases and so do the turbulent fluctuations, which result in higher fluctuations in the force measurements.

## 5.4. TWO-DIMENSIONAL FLOW PATTERN MEASURED WITH PIV

In this section the necessary steps are described that lead to the needed results from the PIV measurements. The PIV measurement method was performed on two different cases, the first case is without the ship in the flume and the second case is with the ship in the normative position. For both situations four measurements where performed with different *dt* values, see Subsection 4.8.2. Considering the displacement of particles between two frames the measurements with a *dt* of 1.6 ms was found to be most optimal. This measurement series for the case without ship and the case with ship will be further processed.

After the determination of the optimal *dt*, bad frame pairs with too much bubbles, shaded areas or reflection were selected and neglected during processing. These frames will otherwise negatively influence the average since unrealistic velocity fields will be generated with the bad images. For both measurement series about 30 frame pairs where found to be affected significantly by the negative influences mentioned earlier. These frames where neglected during processing. This is an acceptable amount since it is only a very small percentage of the total amount of frame pairs, which was 1500.

Once the bad frames are selected to be neglected a mask can be defined. This mask basically gives the range in which the instantaneous velocity field will be determined. The boundaries for the mask are mostly determined by physical boundaries like the edge of the window and the bottom of the water surface stabilisation tool. The mask for the case with no ship was defined from the center of the gate till 0.6 meter downstream and from 0.02 meter above the bottom till 0.22 meter above the bottom. The mask with ship is a bit smaller due to the bow of the ship and a shadow zone under the ship. The mask for the case with ship was defined from the center of the gate till 0.55 meter downstream and from 0.03 meter above the bottom till 0.22 meter above the bottom.

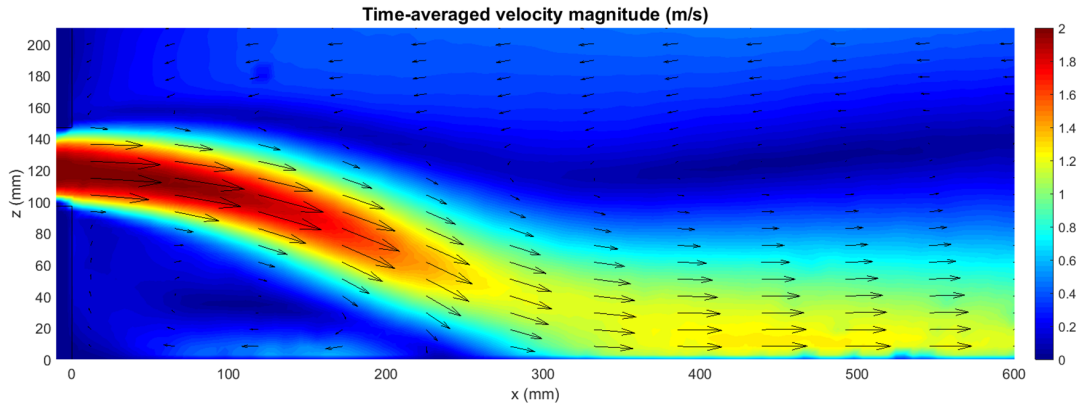


Figure 5.8: Velocity magnitudes found with the PIV measurement without ship

The remaining frame pairs bordered by the mask can be processed with the cross-correlation procedure. Ev-

ery pair results in a single vector plot with an amount of correct vectors and a few outliers. These outliers are incorrect vectors resulting from loss of seeding particles between frames or heterogeneous distribution of the particles. These outliers are inevitable, even with optimised parameters and excellent PIV images. For every vector the global average, current average and local median velocity are determined and compared to each other. If there is a large deviation the vector is defined as an outlier and thus an incorrect vector. The outliers are replaced by a vector interpolated between the neighbouring vectors. The resulting vectors are smoothed and filtered to create the final velocity vector plot, which is an average over the measured time. The resulting $U_x$ velocities for the measurement without ship are displayed in Figure 5.8 and the results for the measurement with ship in Figure 5.9.

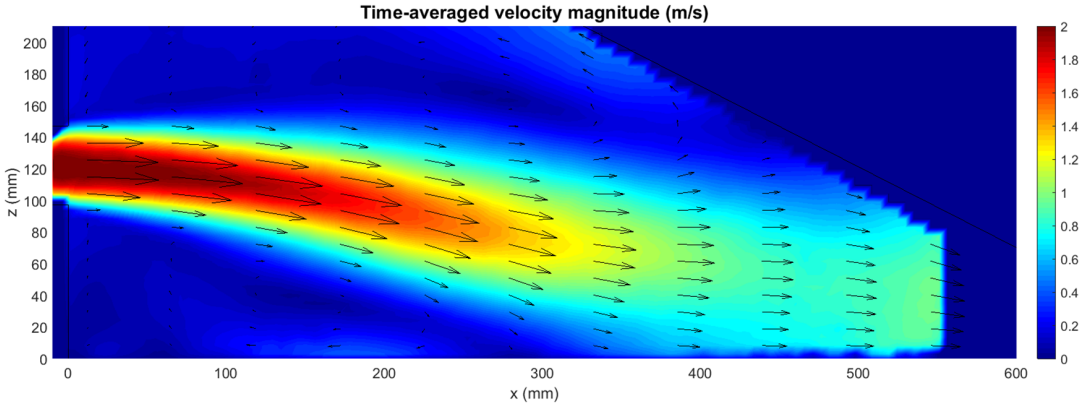


Figure 5.9: Velocity magnitudes found with the PIV measurement with ship

The velocity field found with PIV for the situation without ship looks very similar to what was found with the CFD calculations. The jet attaches to the bottom and the recirculation above the jet is larger then under the jet. Comparing the flow without ship to the flow with ship the following can be noticed: the jet deflects stronger towards the bottom when there is no ship present. In the case without ship the core of the velocity profile deflects with a sharp angle towards the bottom while in the case with ship the deflection is more gradual. The explanation can be found in the presence of the ship itself. The ship counteracts the deflection towards the bottom by blocking the eddy above the jet. It functions like the object which deflects the jet researched in Miozzi et al. (2010) see Subsection 2.3.5. However, since the flow needs to go under the ship the jet will still tend towards the bottom anyway.

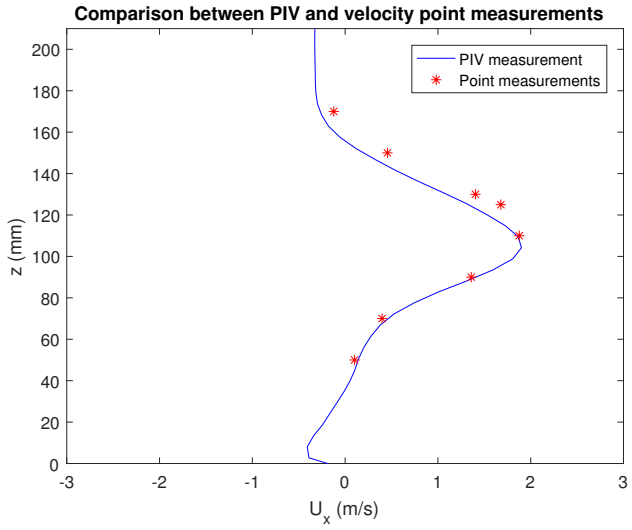


Figure 5.10: Comparison between the PIV measurement and the velocity point measurements

In Figure 5.10 the PIV velocity profile measured at 0.1 meter from the gate is compared to the additional point measurements that were performed. The agreements are clear, in the sense that there is not a very big difference between the tow measurement methods. The same shape of the velocity profile is found as well as the same maximum. A difference can be noticed in the upper part of the velocity profile, i.e. above the gate opening. Here the velocities found with the point measurements are slightly higher then the velocities found with PIV. The reason for this is that the measurement layer of the EMS is larger for higher fluctuations in the flow field, see Subsection 4.4.2. Higher fluctuations in the upper part of the jet can be expected due to the deflection towards the bottom and interaction with the upper eddy, resulting in more turbulence. The bigger measurement layer results in a slight overestimation of the velocities since the velocities near the center of the jet are bigger.

## 5.5. CONCLUSIONS CONSIDERING THE MEASUREMENT RESULTS

The velocity point measurements over the depth capture the same behaviour of the jet as the CFD calculations show. The initial behaviour of the jet can be described as a clear jet just after the gate, with the maximum just a bit under the center of the opening. This means that the jet starts attaching to the bottom almost immediately. Then later on in the flume the jet gradually spreads over the full depth. At the measurement location 4.8 meter downstream of the gate the flow is nearly uniform, which justifies the location of the reference wave height meter 5.1 meter downstream of the gate. The velocity point measurements over the width reveal some differences between the situation with ship and the situation without ship. For the situation without ship higher velocities are found near the walls of the flume. This is likely an effect caused by the jet attaching to the bottom more easily in the center of the flume. Since the differences in velocity are only 9% the two-dimensional flow assumption is still valid. For the situation with ship a non-symmetrical velocity profile is found. However by analysing one measurement signal over time a strong fluctuation of the maximum velocity is excluded. Furthermore, the measured water surface slope is compared to the calculated slope, concluding that the assumed roughness is correct.

The force measured for the normative situation is 46 Newton, which compares well to the 48 Newton that was found with the CFD calculation. As displayed in Figure 5.5 an increase of the keel clearance results in a decrease in the positive force. This corresponds to the expectations since the main contributor of the positive force is the jet, which has less influence on the ship when it is placed higher in the water. The relation between $X_{bow}$ and the force on the ship is shown in Figure 5.6. First a decrease is measured indicating a reduction of the positive force due to a lower effect of the jet. However if the ship is placed even further from the gate another effect dominates the force. This effect is the increase in water level in front of the ship when the jet loses momentum due to spreading of the jet. The results of variations in water level difference over the gate are displayed in Figure 5.7. As expected the force on the ship decreases for a lower water level difference. This decrease is however not completely linear since the force is determined by both the jet impingement and friction.

The PIV measurement with a $dt$ of 1.6 ms was processed resulting in a two-dimensional flow pattern without ship and a two-dimensional flow pattern with ship. Both results compare well to CFD and the EMS point measurements. Comparing the flow without ship to the flow with ship revealed that the deflection of the jet towards the bottom is stronger when no ship is present. The explanation for this is found in the fact that the ship limits the size of the upper eddy and therefore creating an under pressure. This under pressure deflects the jet upward, resulting a more centered jet.

# 6

# Analysis and Discussion

In this chapter the results from the measurements will be compared with Lockfill and interpreted using the theory presented in Chapter 2. First an explanation is given about the method used to compare Lockfill to the performed measurements. A direct comparison is not possible since the measurements were performed with a constant discharge throughout the flume and Lockfill considers a filling cycle of the lock, which means discharge decrease over the length of the lock. Therefore the Lockfill equations are adapted to ensure the same conditions as the scale tests. This can be realised by removing the discharge decrease from the equations, basically assuming that the lock is infinitely long. This does not influence the other force components.

The analysis of the equations shows that the force on the ship is mainly determined by the momentum flux in front of the bow of the ship. The momentum flux in front of the bow follows from the behaviour of the jet. The behaviour of the jet covers the spreading and the direction of the jet, which follows from the tendency of the jet to attach to a boundary. As mentioned in Chapter 5 the presence of the ship does influence the behaviour of the jet and thus the momentum flux. This will be analysed extensively by determining the momentum flux from the velocity profiles in front of the bow.

Once it is clear how the jet behaves and how the momentum flux in front of the ship can be found with the velocity profile in the jet, the forces on the ship in normative position, determined with different methods can be discussed. It is concluded that the force on the ship can be predicted well with Lockfill, provided that the right angle of the jet is taken into account. Besides the normative position the performance of Lockfill is analysed for variations in keel clearance, the ship's distance from the gate and discharge through the gate.

## 6.1. Translation from the measurement conditions to Lockfill

The results of the force measurements will be compared to the results Lockfill would give for the same situation. To make a comparison with Lockfill, the terms representing the decrease in discharge over the length of the lock must be extracted from the equations, since this effect is not present during the scale tests. The effect of the discharge decrease is deeply embedded into the equations, therefore a new set of equations will be derived, see Appendix F. These equations will represent the calculation method Lockfill is using but do not include the discharge decrease. Analysing the equations presented in Appendix F, it can be noticed that most of the parameters are known from the chosen geometrical dimensions, however there are a few which are more difficult to determine. These parameters are: the angle of the jet with respect to the horizontal $\alpha$, the Nikuradse roughness of both the ship and the flume walls and the momentum flux in the jet just in front of the bow $S_b$. As these parameters have not yet been introduced, additional explanation can be found in the following paragraphs

Since the flow is not solved in Lockfill but schematized using a parametrization of the jet, the angle of the jet for Lockfill calculations is often determined by means of a CFD analysis. To perform this analysis the geometry tested in Lockfill is also made in a CFD environment and the flow is studied to determine an angle or a range of angles for the jet. In this study PIV measurements were performed which give an accurate representation of the jet flow. These can therefore be used to determine the angle of the jet for the ship in normative

position. An assumption has to be made about the angle of the jet for other positions of the ship, since these were not measured with PIV.

The roughness of the flume walls and model ship influence the forces quite significantly. In Subsection 4.1.3 a prediction was made about the water surface slope in the flume, which is also related to the roughness of the flume walls. A Manning roughness of 0.014 $s/m^{\frac{1}{3}}$ was assumed for the glass walls. In Subsection 5.2.3 the calculated water surface slope is compared to the measured water surface slope. Since the calculated water surface slope compares very well to the measured slope it is likely that the assumed roughness is at least in the correct order of magnitude. Lockfill uses a Nikuradse roughness description of the ships hull and the walls of the lock. Therefore literature was consulted to rewrite the Manning roughness into Nikuradse roughness. According to Jayaratne (2010) the Manning roughness and Nikuradse roughness have an approximate relation as in Equation 6.1.

$$n \approx \frac{k_s^{\frac{1}{6}}}{26} \tag{6.1}$$

Where:

$n$ = the Manning's roughness $[s/m^{\frac{1}{3}}]$
$k_s$ = the Nikuradse surface roughness $[m]$

Using Equation 6.1 the Nikuradse friction coefficient of the flume walls can be determined, $k_I = 0.0023$ meter. The roughness of the model ship hull can be found similarly. The Manning roughness of the ship is assumed to be 0.02 $s/m^{\frac{1}{3}}$ (Chow 1959). Which comes down to a Nikuradse roughness of $k_{II} = 0.0198$ meter. The assumed roughness for both the ship and the flume seem quite high, considering the materials are wood and glass which are not known to have a high friction interaction with the fluid. Any results should be checked for overestimation of the friction forces.

The overestimation of the friction coefficient can be cause by the fact that other processes are included into the friction calculation. A couple of these processes will be discussed here. First of all the flow velocities along the ship are assumed to be uniform which is in reality not the case. Higher velocities are expected at the bottom of the ship due to the jet impinging against the bow and thereafter attaching to the hull of the ship. The impinging jet becomes a wall jet, with the hull of the ship being the wall, this effect is already introduced in Subsection 2.3.4. Due to the wall jet, higher velocities at the hull of the ship are expected, therefore increasing the friction force. Another possibility is that the jet does not fully attach to the hull, but rather releases due to the angle from the bow to the bottom of the ship. This effect is called flow separation and causes a momentum loss and thus a force against the ship. If this occurs it is indirectly taken into account by the overestimated friction coefficient.

To determine the force on the ship the momentum flux in the jet, just in front of the bow of the ship, must be calculated. In a uniform flow the momentum flux in the jet can be found with $S = \rho UQ$. However, since the discharge is not constant in the jet, the momentum flux can be calculated with the velocity profile at the location of interest. Given a velocity profile $U(z)$ over the height $z$, the momentum flux in the x-direction $S_x$ can be determined using Equation 6.2.

$$S_x = \rho w_l \int_{z_b}^{z_t} U(z)^2 \mathrm{d}z \tag{6.2}$$

Where:

$S_x$ = the momentum flux in the x-direction $[kgm/s^2]$
$w_l$ = the width of the flume (lock) $[m]$
$U(z)$ = the velocity over the height of the lock $[m/s]$
$z_b$ = the bottom of the jet (defined where the velocity becomes 0 m/s) [-]
$z_t$ = the top of the jet (defined where the velocity becomes 0 m/s) [-]

It is assumed that the velocity profile in the center of the flume is representative for the entire width. In reality the velocity is not uniform over the width as explained in Section 5.2, however the deviations from the center velocity are small. The interest lies in the momentum flux in the jet, therefore only the positive velocities

are considered in the calculation. In Section 6.2 the momentum flux development in the jet will be studied, both for the Lockfill approach and the PIV measurements. Comparing the measurements with the Lockfill schematisation will provide insight into possible improvements of the Lockfill schematisation. Comparing the two PIV measurements, with and without ship, will give a better understanding of the influence of the ship on the flow.

## 6.2. ANALYSIS OF THE FLOW IN FRONT OF THE SHIP

As explained in Section 6.1 an essential part of calculating the forces on the ship via the Lockfill approach is finding a correct value for the momentum flux in front of the bow of the ship. Two different methods which can be used to determine the velocities in front of the bow will be compared to each other. The first method considers the approach that is implemented in Lockfill, which is based on a parametrization of the filling jet. The second method is fully based on the velocity measurements with PIV. Comparing the different methods will be done in three steps:

1. Determine the cross-sectional velocity profiles over the length of the Lock. The Lockfill velocity profiles are based on a theoretical parametrization of the jet (Vrijburcht et al. 1988).
2. Integrate the velocity over the cross-sectional area of the jet to find the positive discharge in the jet. The variation of the discharge in the jet over the length of the lock influences the momentum flux at each location in the lock.
3. Combine the velocity profile and the discharge, making it possible to understand the momentum flux at each cross-section in the lock.

### 6.2.1. VELOCITY PROFILES OVER THE LENGTH OF THE LOCK

The $U_x$ velocity profiles measured with PIV are displayed in Figure 6.1 and Figure 6.2. The color scaling is adjusted in such a way that the transition from positive to negative velocities is clearly visible. The positive velocities (yellow and red), represent the filling jet and thus the part that determines the force on the ship. It is important to realise that the jet is defined as all positive velocities, this includes the positive velocities in the eddies. The recirculation is defined as the negative velocities (blue), i.e. the negative velocities in the eddies.

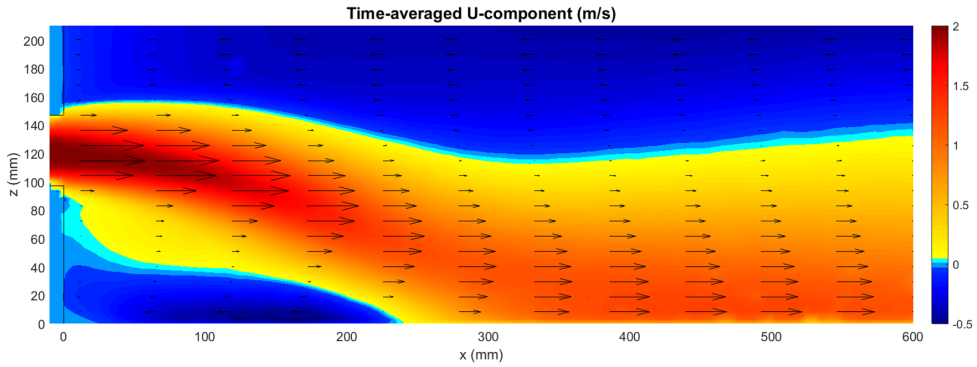


Figure 6.1: U-component of the velocity found with the PIV measurement without ship

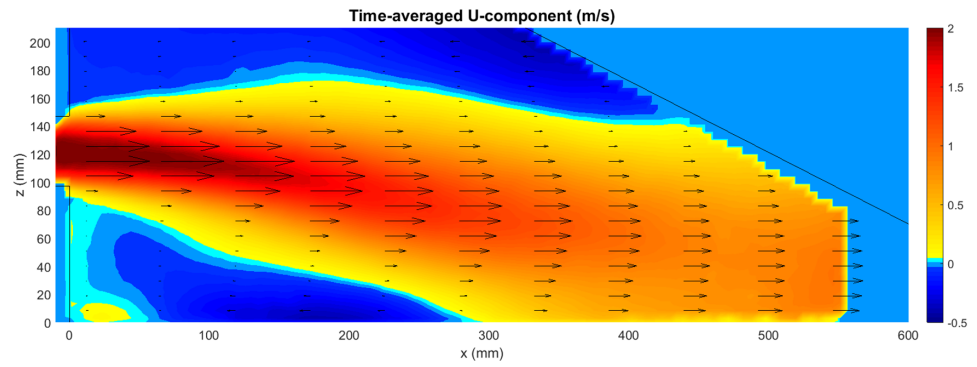


Figure 6.2: U-component of the velocity found with the PIV measurement with ship

There are some big differences noticeable between the jet without ship and the jet with ship, which are especially clear with the current representation. First of all the jet without ship attaches stronger to the bottom, meaning that the point of attachment is closer to the gate, this was already addressed in Section 5.4. Secondly the jet with ship spreads over a bigger portion of the water depth, which is of course a result of the first effect. It is however clear that the jet without ship does not spread upwards at all before it is attached to the bottom. Lastly, stronger velocities near the bottom are observed in the jet without ship. This corresponds to what is expected based on literature considering a wall jet, see Subsection 2.3.4.

The velocity profiles obtained with the Lockfill schematisation are given in Figure 6.3. Since the angle at which the jet enters the flume influences the Lockfill jet schematisation and thus the velocity profile significantly, three different cases will be considered. The first case considers an angle of $\alpha = 0°$ and thus assumes that the jet does not attach to a boundary. The second case is based on an angle estimated from the PIV measurement with ship in the flume. The angle is estimated by following the direction of the jet which results in $\alpha = -8°$. The third case is based on an angle estimated form the PIV measurements without ship in the flume. The angle is found with a straight line between the center of the opening in the gate and the point where the jet is considered to be fully attached to the bottom at $x = 6$ meter, this results in $\alpha = -13°$.

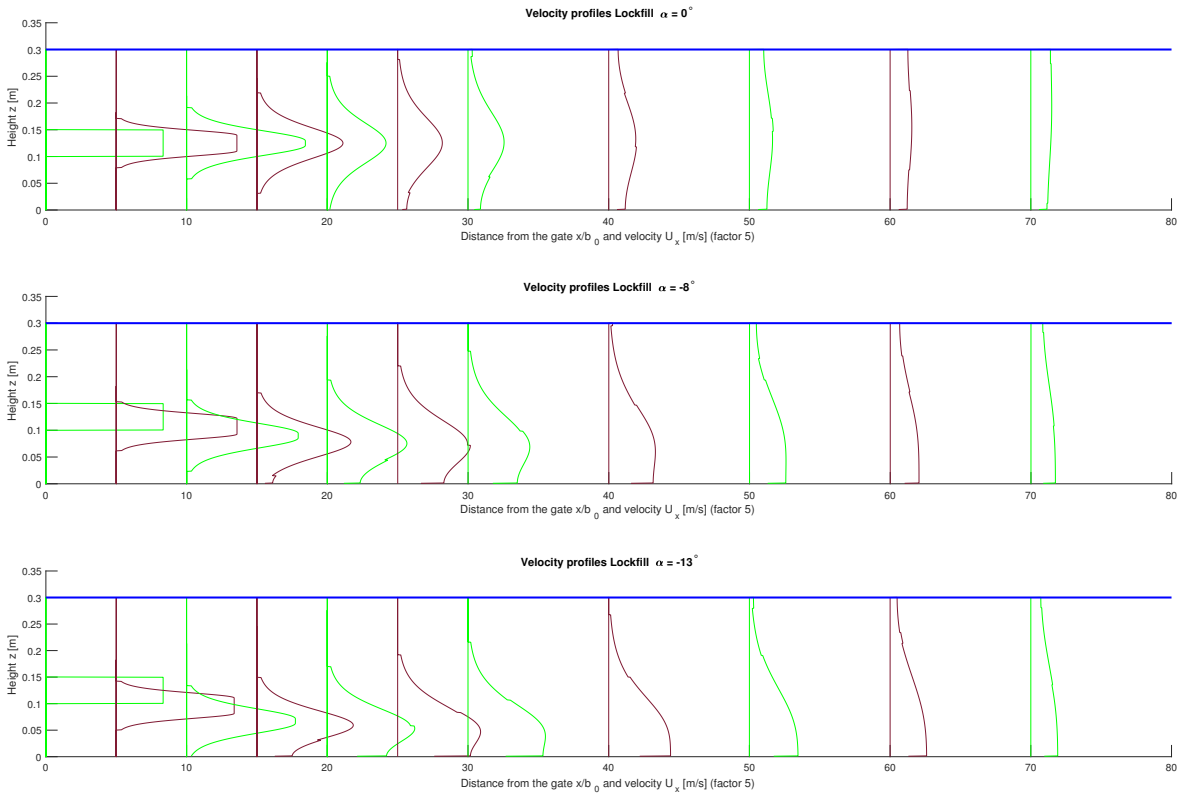


Figure 6.3: Velocity profiles with the Lockfill schematisation, jet angles: $\alpha = 0°$, $\alpha = -8°$ and $\alpha = -13°$ (velocities scaled with a factor 5)

To clearly present the profiles, the velocities are multiplied by a factor 5. A water depth of 0.3 meter is taken into account and the rest of the parameters are chosen to be identical to the normative scale test. It is clear that when no angle of the jet is manually implemented the jet behaves as a free jet. When an angle is implemented, attachment to a boundary can be artificially simulated. A higher negative angle means a stronger attachment to the bottom, i.e. attachment to the bottom at a smaller distance from the gate. Only the positive velocities are calculated in the Lockfill approach. Where the velocities are indicated to be zero, the return flow of the eddies is present as explained in Section 2.3. The positive area of the eddies is part of the jet schematisation. The size and location of the eddies influence the discharge in the jet. In conclusion, Lockfill assumes a certain spreading of the jet and includes the entertainment of water from the eddies surrounding the jet. Doing so, it includes the positive half of the recirculation zones in the jet schematisation. It does however neglect the return flow of these recirculations.

### 6.2.2. DISCHARGE IN THE JET

Figure 6.4 displays the discharge in the jet over the length of the flume. Just after entering the lock the jet will entrain water from the surrounding eddies as explained in Section 2.3. These eddies can be observed in both the PIV measurements and the Lockfill calculations. The discharge in the jet will increase until the jet starts yielding water back to the surrounding the eddies. The location in the flume where this will happen depends on the size of the eddies and the size of the eddies depends on the geometry of the lock. Note that the Lockfill schematisation does not include the presence of a ship, therefore entrainment can occur at the position where the ship is present in reality. First the Lockfill case will be analysed separately and then a comparison is made with the PIV measurements.

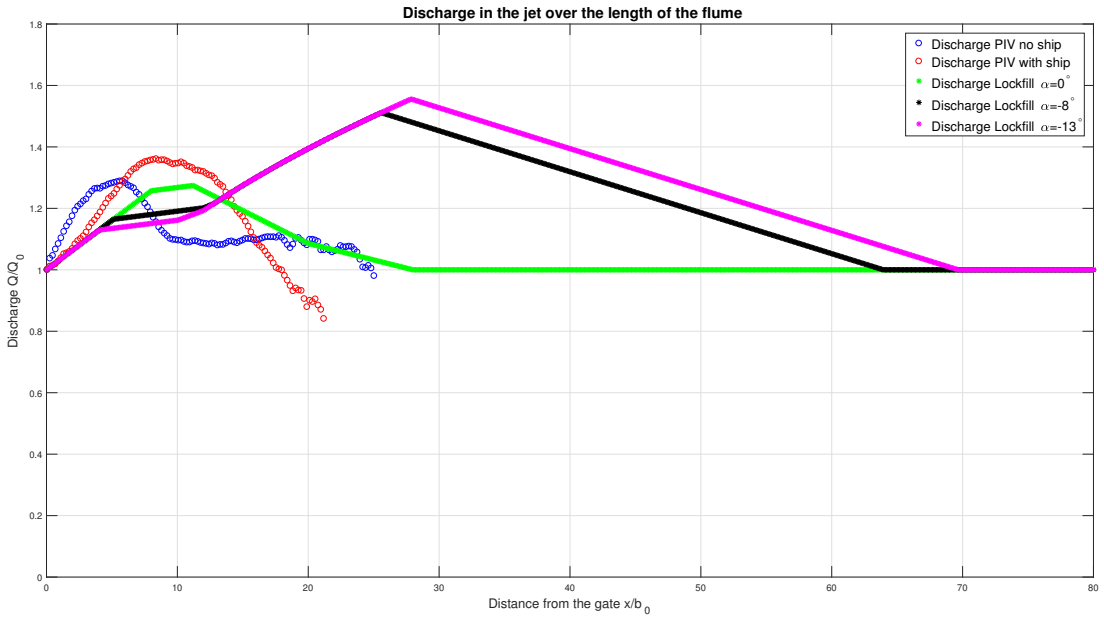


Figure 6.4: The positive discharge in the jet for the Lockfill schematisation and PIV (location of the ship $x/b_0 = 24$)

When no angle is implemented in the Lockfill calculation, the jet will behave as a free jet with reflection to the bottom and the water surface. Water is extracted from the first half of the eddies and yielded back in the second half. The line towards the maximum is not straight since the eddy under the jet is a bit smaller than the eddy above the jet. This is a result of the jet not entering in the center of the water body but a bit closer to the bottom. The entertainment from the lower eddy therefore stops earlier hence the change in slope. The same can be observed in the region where the slope is negative, at the point where the slope changes the lower eddy stops and therefore less discharge is yielded from the jet to the eddies. Once the eddies are no longer present the discharge is equal to the starting discharge.

In Lockfill, when the jet enters under a negative angle and the jet attaches to the bottom, the upper eddy will be much larger than the lower eddy, see Figure 6.3. The distance over which the jet will entrain water will therefore become larger as well. The discharge in the Lockfill calculations with a negative jet angle can be split into four regions starting at the gate. In the first region both the eddy under the jet and the eddy above the jet feed the jet with water, resulting in a steep increase of discharge, up until $x/b_0 \approx 5$. In the second region water is yielded back to the smaller eddy under the jet while the upper eddy still provides water, resulting in a less steep increase of the discharge, until $x/b_0 \approx 10$. In the third region the lower eddy is no longer present and only the upper eddy influences the discharge, this continues until the discharge reaches its maximum. At this point the upper eddy will stop providing water to the jet and the fourth region will start. In the fourth region the jet will return the water entrained from the upper eddy until the discharge is the same as the starting discharge. Note that a higher negative angle will have two effects. One, the lower eddy will become smaller moving the starting and ending position of region two towards the gate. Two, the upper eddy will become larger, increasing the maximum discharge and moving region four further from the gate. These zones and angle dependency can be recognised in the slopes of the lines in Figure 6.4.

For the discharge determined from the PIV measurements a similar trend of increasing and decreasing discharge can be observed. For the case without ship the increase is however faster, indicating that the maximum amount of water is entrained over a shorter distance. Furthermore, the discharge in the jet for the case without ship does not directly return to the starting discharge, but remains at approximately $Q/Q_0 = 1.1$ for some distance. This means that there is a residual water entrainment once the jet is attached to the bottom. As expected the additional discharge will be returned to the upper eddy gradually once the jet starts spreading over the total water depth. It is however interesting to notice that initially the discharge remains nearly constant once the jet is attached to the wall.

For the case with a ship a larger maximum increase of discharge can be observed, this can be explained by the fact that the jet remains more centered compared to the case without ship, see Figure 6.2. Due to the fact that the jet remains more centered the lower eddy is longer and does therefore provide a large distance over which water can be entrained. Note that the discharge decreases further than the initial discharge, which should not be the case since mass balance demands the same amount of water passes under the ship as through the gate. Two explanations can be thought of when trying to account for this, most likely each mentioned explanation will partly cause the total discharge loss observed in the measurement. The small residual discharge along the sides of the ship can partly justify the discharge loss and due to the jet reaching the boundaries the mask chosen for the PIV processing can account for a bit of discharge loss, see Section 5.4.

### 6.2.3. MOMENTUM FLUX IN THE JET

In Figure 6.5 the calculated momentum flux in the x-direction is displayed for each case. Note that this is the momentum flux in the jet and the jet is defined as all the positive velocities. The momentum flux is made dimensionless with the flux of momentum through the gate ($S_0$).

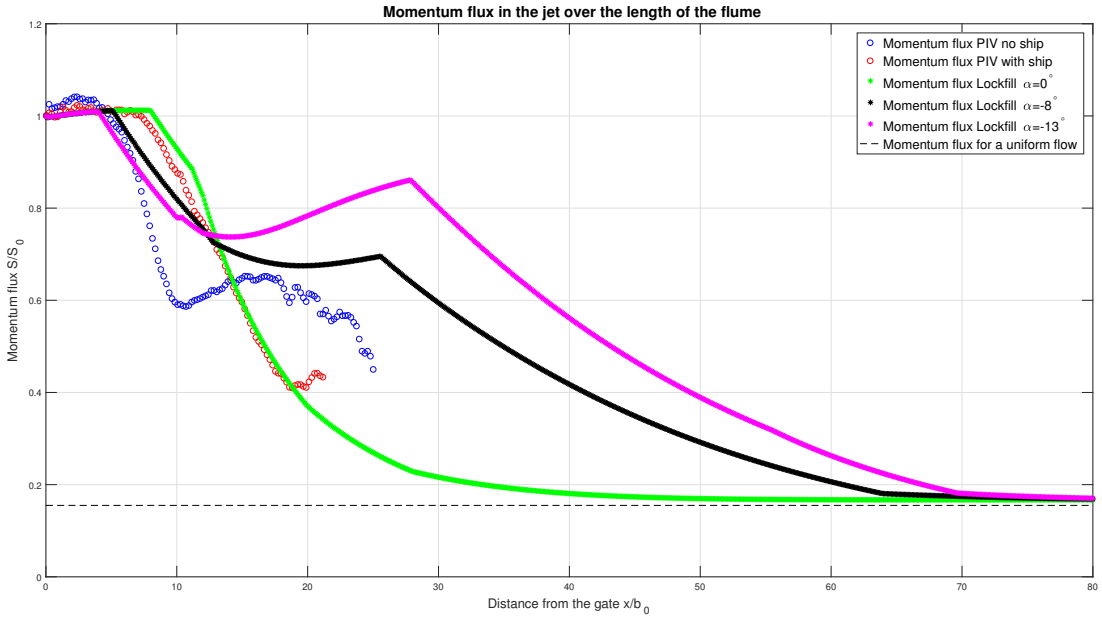


Figure 6.5: The positive momentum flux in the jet for the Lockfill schematisation and PIV measurements

In order to make a conversion to the real calculated values possible the $S_0$ for each case is given in Table 6.1. These values are not the same since the PIV measurements and the Lockfill schematisation have a different velocity profile through the opening, while the discharge through the opening is the same for every case, $Q_0 = 41.5$ l/s. The distance is made dimensionless with half the gate height $b_0$, which is equal to 0.025 meter.

The momentum flux in the jet is both dependent on the discharge in the jet and the velocity of the jet. Furthermore when considering the momentum flux in a specific direction, the direction of the jet is also of interest.

Four different processes need to be taken into account when analysing the results displayed in Figure 6.5:

1. The increase of total discharge in the jet due to the entertainment of water from the surrounding eddies, more discharge in the jet gives a higher momentum flux.
2. The decrease of total discharge in the jet as a result of the jet losing water to the eddies, lower discharge gives a lower momentum flux.
3. Spreading of the velocity over the height and width of the flume, lower velocities result in a lower momentum flux.
4. Direction of the jet with respect to the x-axis (horizontal). The momentum flux in Figure 6.5 is the momentum flux in the x-direction, therefore a higher deviation of the jet with the horizontal gives a lower momentum flux in that direction.

Table 6.1: $S_0$ values for the different cases presented in Figure 6.5

| Case for the momentum flux calculation | $S_0$ $[kgm/s^2]$ |
|---|---|
| Momentum flux PIV no ship | 67.4 |
| Momentum flux PIV with ship | 69.9 |
| Momentum flux Lockfill $\alpha = 0°$ | 74.1 |
| Momentum flux Lockfill $\alpha = -8°$ | 74.1 |
| Momentum flux Lockfill $\alpha = -13°$ | 74.1 |

Just downstream of the gate the momentum flux in the jet will remain approximately constant because the discharge increases while the jet decelerates due to spreading. In the case of the PIV measurements a slight increase of momentum flux can be observed at $x/b_0 < 5$ because the entertainment that increases the discharge in the jet is stronger than the loss of velocity due to spreading of the jet. The increase of discharge was observed to be faster than that following from the Lockfill schematisation, see Figure 6.4. In the case of the jets with a low angle with respect to the x-axis the constant region lasts longer. This can be explained by the fourth effect mentioned earlier, a larger angle with respect to the horizontal results in more momentum loss in the x-direction. Furthermore in Figure 6.4 it can be seen that the region in which the jet entrains water is longer and therefore maintains a larger distance of constant momentum flux. To highlight this the momentum flux derived from the PIV with and without ship can be compared to each other. It is clear that the line representing the case without ship decreases earlier and faster than the case with ship. This is a direct result of the larger angle of the jet in the case without ship. A jet that attaches to a boundary will therefore lose momentum more quickly than a jet which remains centered. The same can be observed in the lines plotted with the Lockfill schematisation of the jet.

Once the entertainment of water from the surrounding eddies stops the jet will quickly lose momentum. This can be observed for all the different cases and processes two and three are the main cause of this. As discussed earlier the location on which the loss of momentum flux starts depends on the angle of the jet. There is a big difference noticeable between the case with ship and the case without ship, therefore the inclusion of the ship in the calculation has a significant influence on the estimation of the momentum flux in front of the bow.

Considering the Lockfill jet without angle, the momentum flux keeps decreasing until the jet is fully spread over the depth. At this point a uniform flow is established, resulting in a constant momentum flux. However when the jet is known to have an angle the discharge will keep increasing as displayed in Figure 6.4. This means that at the point where process four is no longer in effect, the jet is aligned with the horizontal, the momentum flux will start increasing again. The momentum increase due to the entrainment of water being stronger then the momentum decrease due to spreading. Unfortunately the range of the PIV was limited therefore this process is not captured entirely. However the trend of an increasing momentum flux can be observed in the PIV results and the second decrease in the results from PIV without ship.

In general the trends measured with PIV are similar to the trends from the Lockfill schematisation, however the values deviate quite significantly. For the case without ship this is caused by the fact that the discharge in the jet decreases between $x/b_0 = 5$ and $x/b_0 = 10$ indicating a stronger influence of the lower eddy then accounted for in the Lockfill approach. The momentum flux in the case with ship is most similar to the jet without angle. The exact cause of this can most likely be explained by the ship blocking the flow, thus avoiding

the occurrence of the larger upper eddy observed with the case without ship, therefore preventing the jet from strongly attaching to the bottom. Consequently in this case a schematisation without angle in the jet would give more accurate results when calculating the forces on the ship.

## 6.3. CALCULATION OF THE FORCE ON THE SHIP USING THE MEASURED FLOW

A momentum balance calculation based on the measured velocities can be made to validate whether or not the measured force on the ship can be reproduced using the measured flow. To perform this calculation both the velocity profile and water level upstream and downstream of the ship must be known. For the ship in normative position the required information is available, therefore this calculation will consider the ship to be in its normative position. In front of the bow of the ship, 0.10 meter downstream of the gate, both the average water level and a full velocity profile are measured. The velocity is measured with PIV and the water level with wave height meter three, see Figure 4.9. At a position downstream of the ship 5.1 meter from the gate, wave height meter two was positioned to measure the water level. From the lower right plot of Figure 5.3 can be concluded that the velocity is almost uniform over the depth, therefore an uniform velocity is assumed at 5.1 meter downstream of the gate. With the information of both the velocity profiles and the water levels Equation 6.3 can be used to determine the force on the ship. The position in the flume upstream of the ship is denoted with the subscript $a$ and the position in the flume downstream of the ship with subscript $b$.

$$F_{ship} = S_a + \frac{1}{2}\rho g h_a^2 - \rho\frac{Q^2}{A_b} - \frac{1}{2}\rho g h_b^2 \tag{6.3}$$

Where:

$F_{ship}$ = the resulting force on the ship $[N]$
$S_a$ = the momentum flux in the jet in front of the ship calculated from PIV $[N]$
$h_a$ = the water level at position a $[m]$
$Q$ = the discharge $[m^3/s]$
$A_b$ = the wet cross-sectional area at location b (width of the flume times the water level) $[m^2]$
$h_b$ = the water level at position b $[m]$

The momentum flux in front of the bow can be determined with Equation 6.2 and is found to be $S_a = 70.5$ Newton. Furthermore, $h_a = 0.28$ meter, $h_b = 0.29$ meter, $Q = 0.041\ m^3/s$ and $A_b = 0.15\ m^2$. This results in a total force $F_{ship} = 45$ Newton. This is a slight underestimation of the total measured force for the ship in normative position, which is 46 Newton.

## 6.4. VALIDATION OF LOCKFILL WITH THE MEASURED FORCES

The results from the force measurements will be compared to the results Lockfill would give for the same situations. To make a comparison with Lockfill, the terms representing the decrease of discharge over the length of the lock are extracted from the equations, since this effect is not present during the scale tests, see Appendix F. The three variables for which force measurements were performed, $k_s$, $X_{bow}$ and $Q$ will be treated separately. But first the normative position of the ship will be discussed extensively because for this situation the most information is available.

The Lockfill calculation requires the input of a lot of parameters. Some of these are geometrical dimensions of the scale model covered in Chapter 4. The friction coefficients are elaborated in Section 6.1. The discharge through the gate is usually calculated based on a water level difference over the gate and a loss coefficient. However, for the purpose of comparing to the measurements the measured discharge is used. The water level in the lock is based on the measured reference water level measured in the flume (wave height meter two). Now the determined force mainly comes down to the momentum flux in front of the bow and the position of the ship, which is the main interest of this research. When determining the momentum discharge in the jet an angle of the jet with the horizontal can be taken into account. To cover the extremes of a jet attaching to the bottom $\alpha = 0°$ and $\alpha = -13°$ are taken into account.

### 6.4.1. THE LONGITUDINAL FORCE ON THE SHIP WHEN IN NORMATIVE POSITION

For the normative situation not only force measurements but also PIV measurements and a CFD calculation are available. Therefore additional comparisons can be made. The $X_{bow}$ for the ship in normative position is

0.6 meter. With the known angle of the bow and a water level of approximately 0.3 meter, the position where the bow and the water level intersect can be determined, which is 0.15 meter downstream of the gate. This is the location downstream of the lock where the momentum flux needs to be determined according to the Lockfill calculation method. Therefore for each case the momentum flux determined from the velocity profile at 0.15 meter from the gate is used. These values can be determined from the graph in Figure 6.5.

In Table 6.2 the results are displayed. The relative error is defined as $\frac{F_{x,method}-F_{x,measured}}{F_{x,measured}}$, by definition this results in a relative error of 0% for the measured force. Both PIV and CFD predict the force well as long as the presence of the ship is taken into account, the errors are less than +4%. However, when the presence of the ship is not taken into account, see PIV without ship, the force prediction is way off, with a relative error of 35%. This emphasizes the influence that the ship has on the flow and consequently the momentum flux in front of the ship. The Lockfill prediction with $\alpha = 0°$ is also quite accurate with an error less then 5%. The Lockfill prediction with $\alpha = -13°$ is less accurate, which can be expected since this angle is to large considering it is determined from the PIV without ship.

Table 6.2: The momentum flux in front of the bow $S$ and the resulting longitudinal force on the ship $F_x$ for different methods

| Method of determining $S$ | $S$ at $x = 0.15$ meter $[kgm/s^2]$ | Calculated force [N] | Relative error |
|---|---|---|---|
| Measured with force sensors | - | 46.2 | 0% |
| PIV with ship | 70.1 | 47.9 | +3.7% |
| PIV without ship | 63.7 | 62.3 | +35% |
| CFD model | - | 47.9 | +3.7% |
| Lockfill $\alpha = -13°$ (without ship) | 63.8 | 50.1 | +8.4% |
| Lockfill $\alpha = 0°$ (free jet) | 69.9 | 48.4 | +4.8% |

It is clear that a lower momentum flux results in a higher positive force. This might seem counter intuitive but is actually correct since the water level has generally a higher influence on the force than the impact of the jet itself. A lower momentum flux means a higher water level in front of the ship and thus a higher positive force. The force prediction following from Lockfill is dependent on the assumed angle of the jet, which both influences the momentum flux and the impact of the jet on the ship. But the assumed angle has no influence on the friction force or the force against the stern of the ship.

### 6.4.2. THE LONGITUDINAL FORCE AS FUNCTION OF THE KEEL CLEARANCE

Varying $k_c$ will change a few parameters in the momentum balance resulting in a different force on the ship. The friction force will decrease because there is more space available under the ship and the jet impact is less resulting in a lower positive force. Furthermore, both the hydrostatic pressure against the bow and the hydrostatic pressure against the stern will decrease, however the magnitude of this decrease is identical. In total the positive force will therefore decrease leading to the results displayed in Figure 6.6.

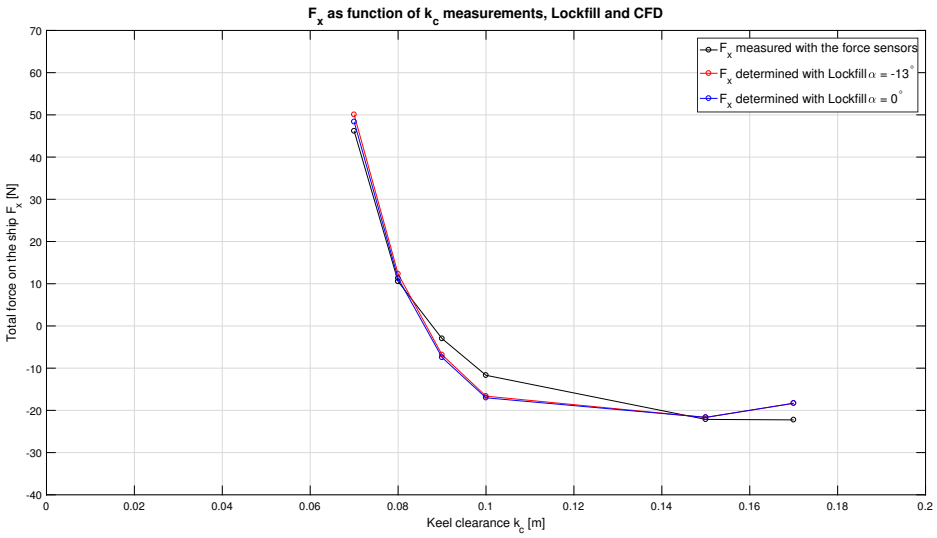


Figure 6.6: Longitudinal force as function of the keel clearance of the ship, comparing measurements with the Lockfill calculation method

Important to note is that the ship stays in the same longitudinal position with respect to the gate. This means that the location of the cross-section where the momentum flux must be determined does not change. However, the flow field is expected to change since the blockage of the ship changes with the change in $k_s$. In Lockfill this can be accounted for by changing the angle of the jet and the spreading of the jet. In this analysis this is not performed since these changes are very case specific. This can however be a reason for the difference between the measured force and the force determined with Lockfill for higher keel clearances.

In general Lockfill compares very well to the measurements and only starts deviating once the keel clearance increases significantly. Like mentioned before it should be taken into account that the jet is assumed to remain the same for each variation in keel clearance, because there are no flow field measurements available for situations other than the normative position. When the keel clearance increases it is however expected that the jet will tend more towards the situation measured with the PIV without ship and therefore increasing the negative jet angle. This is also why the Lockfill calculation with $\alpha = -13°$ starts to perform slightly better when the keel clearance is high.

### 6.4.3. THE LONGITUDINAL FORCE AS FUNCTION OF THE DISTANCE FROM THE GATE

Figure 6.7 displays the forces as function of the distance between the ship and the gate. Since the position of the ship in longitudinal direction changes, the location of the momentum flux in front of the bow also changes. This has a significant effect on the momentum balance over the bow of the ship. Increasing the distance between the gate and the ship will allow the jet to spread over the full water depth in the flume. A more spread jet means lower velocities and thus a lower momentum flux, see Figure 6.5. The lower momentum flux results in a higher positive force because the water level difference over the bow becomes positive, i.e. $h_1 - h_2 > 0$, whereas in general $h_1 - h_2 < 0$ applies. With $h_1$ being the water depth in front of the bow and $h_2$ being the water depth just after the bow, see Figure B.1 in Appendix B.

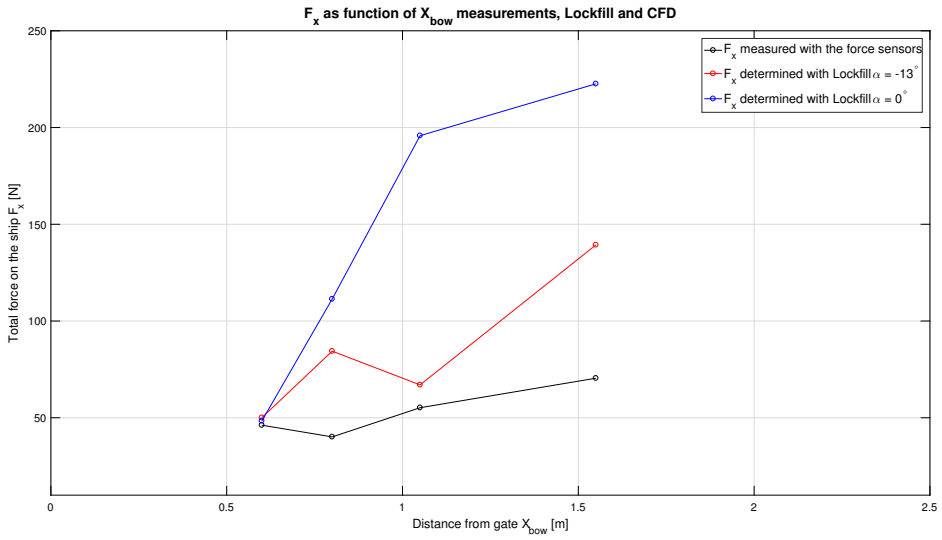


Figure 6.7: Longitudinal force as function of the distance between the gate and the bow of the ship, comparing measurements with the Lockfill calculation method

Considering the momentum flux curves in Figure 6.5 it is no surprise that the forces for a jet with $\alpha = 0°$ overestimate the measurements significantly, since the momentum flux decreases fast to the constant value of a fully spread jet. With the information that the jet attaches to the bottom and thus a negative angle is expected, a better prediction can be realised. When $\alpha = -13°$ the agreement with the measurements is already better. However, the increase and decrease of force are still overestimated and are not in the right longitudinal position. No solid judgement can be made about why the measurements do not correspond to the Lockfill calculation method without detailed information about the flow field in front of the ship. In a future study CFD or PIV can be used to find the flow field for the situations where the ship is positioned further downstream in the lock.

It is likely that the Lockfill jet schematisation does not correspond to the reality. Speculating about the jet that occurs in realty will result in the following: between $X_{bow} = 0.6$ meter and $X_{bow} = 0.8$ meter the momentum flux in the jet will increase due to entertainment while the velocity decrease due to spreading remains limited. Then between $X_{bow} = 0.8$ meter and $X_{bow} = 1.05$ meter the velocity will decrease, decreasing the momentum flux and thus increasing the force. This last effect is however overestimated in Lockfill and can be explained by the jet being attached to the bottom in reality. When the jet remains attached to the bottom the flow will spread less resulting in a higher momentum flux and thus a lower positive force, due to a lower water level difference over the ship. Furthermore the attachment of the jet to the bottom will decrease the force on the ship even further since there is less impingement against the bow, i.e. the jet can go more freely under the ship.

### 6.4.4. THE LONGITUDINAL FORCE AS FUNCTION OF THE DISCHARGE

Decreasing the water level difference over the gate and subsequently the discharge through the gate will also decrease the discharge in the flume. Decreasing the discharge in the flume will reduce both the friction force and the direct force of the jet against the bow. Furthermore, the momentum flux in front of the bow is decreased, by the decrease in discharge and the lower velocities through the gate. In total a significant decrease in longitudinal force on the ship is expected.

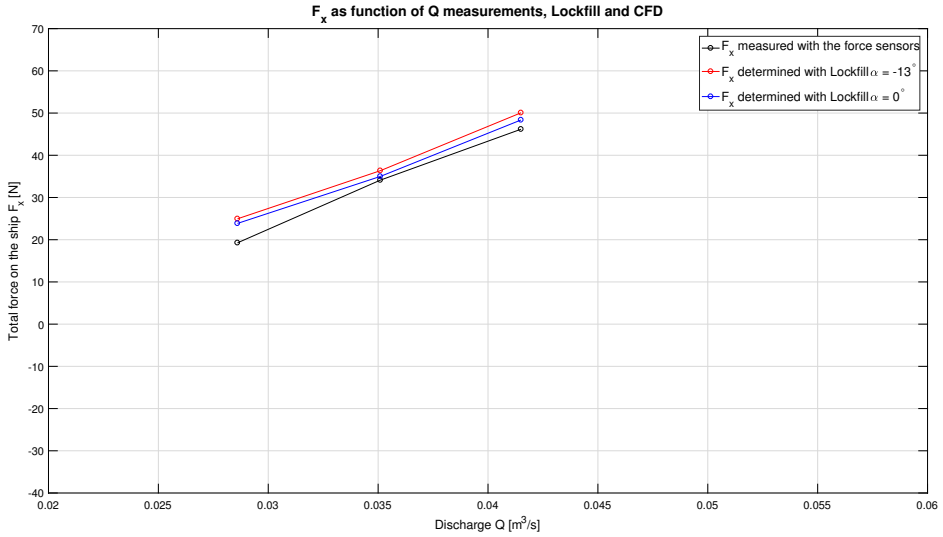


Figure 6.8: Longitudinal force as a function of the discharge through the gate, comparing measurements with the Lockfill calculation method

The agreement between the measured force on the ship and the calculated values with Lockfill in Figure 6.8 is relatively good. The nearly linear relationship between the force and the discharge is represented well and the forces are only overestimated by a small margin. For a very low discharge the difference is more pronounced. This can be the result of a change in jet behaviour. Unfortunately this was not measured within this study.

## 6.5. POSSIBLE CONSEQUENCES OF THIS ANALYSIS CONCERNING LOCKFILL

From the measurement in normative position follows that Lockfill performs really well when the ship is placed close to the gate. The same follows from the measurements where the keel clearance or water level difference are varied. However, when the ship is placed further downstream of the gate significant differences can be observed with respect to the measurements. The cause of this can be found in the schematisation of the jet in Lockfill. When the ship is placed close to the gate the jet does not have a large distance over which it can change, therefore the correct schematisation is not of major importance and the Lockfill schematisation suffices. However when the ship is placed further downstream the assumptions of the Lockfill jet schematisation seems to be off. This results in a wrong prediction of the momentum flux in front of the bow and thus an incorrect force. Considering that the force is overestimated with Lockfill it is expected that a lower momentum flux is predicted than in realty occurs. The cause of the underestimation of the momentum flux

is likely to be that the Lockfill schematisation does not include the attachment of the jet to the bottom. When the jet stays attached to the bottom the spreading over the height is limited, therefore the momentum flux in the jet remains high. When this attachment is included the force on the ship will be reduced since the momentum flux in front of the ship is higher, therefore resulting in a lower water level difference over the ship. Furthermore the impingement surface of the jet is lower, also reducing the positive force on the ship.

It is recommended to ensure that the jet schematisation in Lockfill is correct especially when the ship is placed further from the gate because the difference in the force prediction can be significant, see Figure 6.7. What should however be taken into account is that the overestimation will be less in reality since the decrease in discharge over the length of the lock, which was neglected for the purpose of the comparison with the measurements, reduces the effect of the jet on the force. Ideally the Lockfill schematisation can be adjusted to include the attachment of the jet to the bottom.

From the analysis in this study follows that a correct prediction of the momentum flux results in a correct force prediction with Lockfill. Furthermore, the effect of the ship in the normative position on the flow was analysed. It was found that the attachment to the bottom was less for the situation with ship. This resulted in a jet that actually compares well with the free jet assumed in Lockfill, see Figure 6.5. This is however just one situation and it can not yet be guaranteed that this is the case for every position of the ship.

## 6.6. CONCLUSIONS CONSIDERING THE ANALYSIS

It was found that an important contributor to the force on the ship is the momentum flux in the jet in front of the ship. The momentum flux can be determined from the positive velocity profile just in front of the bow of the ship.

Using the PIV measurements and the EMS point measurements a momentum balance could be made over the ship. This momentum balance can predict the force on the ship accurately, making sure that the force can be calculated using the measured flow.

Comparing the PIV measurements to the Lockfill jet schematisation revealed that the Lockfill schematisation predicts the momentum flux in the jet well close to the gate. However, further from the gate the prediction can deviate significantly from the measurements. This is caused by the fact that a jet angle is assumed in Lockfill which has a significant influence on the downstream momentum flux. The angle mainly influences the size of the eddies, larger eddies result in more water entrainment and thus a higher momentum flux. Furthermore the continuous attachment of the jet to the bottom is not included in Lockfill, resulting in an underestimation of the momentum flux at the bow of the ship when placed at some distance from the door.

The forces on the ship when in normative position were calculated with the Lockfill approach for several different methods of determining the momentum flux. Both CFD and PIV predicted the force very accurately when compared to the measurements. The Lockfill schematisation of the jet also performed well with errors from 4.8% up to 8.4% depending on the assumed angle.

When the keel clearance is increased Lockfill maintains a good performance. The same can be said about a decrease in discharge through the gate. However, when the distance between the gate and the ship is increased the forces found with Lockfill deviates significantly from the measured forces. It is concluded that the deviation is mainly caused due to schematisation of the jet, which does not correspond to what occurs in reality. This corresponds to what was found with the flow measurements.

# 7

# CONCLUSIONS AND RECOMMENDATIONS

In this chapter the final conclusions and recommendations of the report are discussed. The conclusions are based on the findings in this study and will provide an answer to the research questions. The recommendations consist of suggestions for further research and improvements for the software model Lockfill. All the scale model measurement results are made available at http://researchdata.4tu.nl.

## 7.1. CONCLUSIONS

Several approaches are available when calculating forces on a ship in a lock. CFD can be used to solve the flow and can predict the forces on the ship based on the flow. This method requires high computation power, expertise and time. By using a parameterization of the fluid flow a program like Lockfill can determine the forces faster while still maintaining sufficient accuracy, provided that the fluid motion is schematised correctly. This study is conducted to validate and improve the schematisation, with the main point of interest being the influence of the presence of the ship on the fluid behaviour.

The main goal of this research was to establish an understanding of the interaction between the jet flow and a ship in the lock. This includes both the effect of the ship on the flow and the resulting forces on the ship due to the flow. The following main research question was formulated:

*"To what extend does a ship in a lock influence the flow pattern in front of the ship and how does the position of the ship influence the longitudinal forces on the ship?"*

To answer this main question, the following sub questions are explored:

1. *"How are the longitudinal forces on the ship determined in Lockfill?"*
2. *"What differences can be noticed when looking at the flow pattern in the lock, with and without a ship in the lock and can this be quantified by means of the momentum flux in the jet?"*
3. *"How do the forces determined with Lockfill and the scale model measurements compare to each other?"*

The three sub questions will be answered in the following subsections. The answer to the main research question follows from the conclusions regarding the sub questions.

### 7.1.1. LOCKFILL CALCULATION METHOD

The calculation method that Lockfill uses was analysed in depth. The most important concluding remarks considering this calculation method will be mentioned here.

- The calculation method is based on the conservation laws of mass and momentum, while determining the flow using a schematisation of the filling jet.
- It is assumed that the ship does not influence the jet flow in front of the ship. The schematisation of the jet can however be adjusted, for example based on a CFD study or scale model. This adjustment is realised by changing the angle of the jet with respect to the horizontal and the spreading angle of the jet. In doing this the attachment of the jet to a boundary can be schematized.
- The effect of the eddies on the jet is accounted for by a formula describing entrainment of water into the jet. The water is later on yielded back in the form of a return flow.

### 7.1.2. FLOW PATTERN IN THE LOCK

The flow in the lock was quantified by means of CFD calculations, EMS point measurements and PIV measurements. The findings regarding the flow in the lock are presented here.

- The EMS point measurements revealed vertical flow profiles that qualitatively correspond to the CFD calculations. The flow attaches to the bottom and then spreads gradually over the entire water depth. Some variations over the width were measured, however these were relatively small and therefore assumed to be of minor importance, allowing to limit the measurements with PIV to the centerline.
- The PIV measurements confirmed the attachment to the bottom and compare really well to the EMS point measurements.
- PIV measurements were performed with and without the ship. It was found that the presence of the ship reduces the deflection towards the bottom. The reason for the reduced deflection is the interference of the ship's bow with the upper eddy limiting the fluid motion, resulting in a reduction of pressure and therefore a translation of the jet in the upward direction.
- A quantitative analysis of the flow based on the PIV measurements was performed. The momentum flux in the jet without ship decreased faster as a result of the stronger attachment to the bottom. A higher maximum discharge is established in the jet for the situation with a ship present, this is a consequence of more entrainment because the lower eddy is larger.
- Using the momentum flux determined with the PIV flow field and the measured flow velocities further downstream a momentum balance was made to reproduce the measured forces with the measured flow. A good agreement was found between the force based on the flow and the force recorded by the force sensors.

### 7.1.3. MEASURED FORCES COMPARED TO LOCKFILL FORCES

For the ship in normative position the longitudinal force on the ship was determined with a number of different methods. The force was measured using force sensors and determined using CFD. Furthermore the force was calculated with the Lockfill calculation method including the Lockfill jet schematisation and with the Lockfill calculation method but based on the momentum flux from the PIV measurements. The conclusions regarding the normative position of the ship will be discussed here.

- The momentum flux in front of the bow of the ship is important for determining the force on the ship correctly. A higher momentum flux means a lower force, because the water level difference over the bow is less. Consequently, a lower momentum flux means a higher force.
- The CFD calculation and PIV measurement with ship predict the force well with respect to the measurements. Lockfill also performed well, with a minor dependency on the chosen jet angle.
- The force predicted with the PIV measurements without ship differed significantly from the force predicted with the PIV measurements with ship, emphasising a strong effect of the presence of the ship on the flow field and thus the force on the ship.

Force measurements were performed for variations in keel clearance, distance between the gate and the ship and water level difference over the gate. The following conclusions can be formulated regarding the different positions of the ship.

- An increase in keel clearance results in a decrease in the positive longitudinal force. At higher keel clearances the force becomes negative and at some point nearly constant. Lockfill predicts the forces reasonably well with a larger deviation at higher keel clearances.
- An increase in distance from the gate results in an increase of the force because the momentum flux in the jet decreases over the length of the lock. This effect is overestimated by the Lockfill schematisation resulting in a significant overestimation of the force. The prediction can be improved by implementing an angle of the jet but will still differ significantly from the measurements. The reason for this is that the jet stays more attached to the bottom in reality maintaining a higher momentum flux.
- A decrease in water level difference over the gate and thus a decrease in discharge through the gate results in a decrease of the longitudinal force. Lockfill predicts this decrease well but the forces are overestimated slightly.

Lockfill predicts the forces on the ship well as long as the momentum flux in front of the bow is calculated accurately. Since the momentum flux depends on the schematisation of the jet this comes down to an accurate force prediction when the jet is schematised correctly.

## 7.2. RECOMMENDATIONS

The recommendations consist of suggestions for future research, both covering the limitations of this study and suggestions for further research due to the new findings. Furthermore possible improvements for Lockfill will be given.

### 7.2.1. FURTHER RESEARCH

Variations in the shape of the ship or gate were not considered. These will however have an influence on the jet in the lock and are therefore interesting to consider in a future study. The bow shape is especially important regarding the flow between the gate and the ship, since the shape of the bow will likely influence the upper eddy. For example the straight bow of an inland ship will have a different effect on the jet than the pushing barge bow that is considered in the present study. Considering the gate, variations in the position of the opening with respect to the downstream water level are relevant, because this will influence the tendency of the jet towards a certain boundary.

Only two situations could be measured with PIV, therefore information is lacking regarding the flow fields for other positions of the ship. To fully understand the forces that were found for the non-normative positions of the ship, flow fields are required. These flow fields can be measured using PIV or calculated with CFD, assuming that the CFD model is validated with the already performed PIV measurements. The situations for which the ship is positioned further from the gate would be most interesting to measure, because for these situations the Lockfill predictions were inaccurate. In the present study this was presumed to be due to a strong attachment of the jet to the bottom which is not accounted for in the Lockfill schematisation. This explanation is likely correct but can only be proven by additional measurements.

A nearly two-dimensional approach was used for the measurement setup. The reality is not two-dimensional, therefore some fluctuations over the width were observed in the velocity point measurements. The fluctuations were relatively small and therefore disregarded. This is however a limitation in this research and further investigation into the behaviour of the jet over the width is recommended. This may eventually even lead to a three-dimensional schematisation of the jet in Lockfill.

The friction force had to be estimated based on the materials used in the scale tests. Although the assumed friction coefficient was validated with the measured free water surface slope, the friction coefficient is still regarded as one of the bigger uncertainties. For future measurements a more accurate estimation of the friction coefficient is recommended.

In the present study CFD is used in preparation of the scale model tests. Comparing the PIV measurements with the CFD model calculations has not been done because it had limited influence on the results of this study. However, a comparison will give insight into the ability of CFD to reproduce the measured flow, which can be very useful for further research. If CFD can correctly predict the velocities, a flow field can be generated for each position of the ship for which no flow field is known yet. Besides the flow field also the forces on the ship and the momentum flux as function of the x-coordinate can be determined using CFD, since the normative condition showed good agreement between the CFD calculation and the measurement.

### 7.2.2. IMPROVING LOCKFILL

The most important suggestion for an improvement of Lockfill following from this study is the schematisation of the filling jet. Preferably it should be improved in such a way that the momentum flux in front of the bow of the ship is determined accurately for every position of the ship in the lock. Since it is only possible to use a parameterization of the jet in Lockfill and there are so many different variables influencing the jet, the schematisation will likely never be perfect. However, by including the tendency of the jet to attach to a certain boundary, i.e. the Coanda effect, a big improvement will be made. The next step can be to also include the influence of the ship on the jet, as found in this study. Another possibility is to leave the jet schematisation as it is and always use CFD or scale model measurements to adjust the parameters of the jet in such a way that they match the specific case that needs to be calculated. For this to work, it should be tested if every needed situation can be modeled with the adjustable parameters, since this was not analysed in the present study.

# REFERENCES


Anderson, J. (1995), *Computational Fluid Dynamics*, McGraw-Hill, New York.

Barrass, B. (2004), *Ship Design and Performance for Masters and Mates*, Elsevier Butterworth-Heinemann, Oxford.

Chanson, H. (2004), *The Hydraulics of Open Channel Flow: An Introduction*, Elsevier Butterworth-Heinemann, Oxford.

Chow, V. (1959), *Open-Channel Hydraulics*, McGraw-Hill, New York.

De Loor, A. (2012), 'Forces on sea-going vessels in navigation locks', Technical report, Deltares, Delft .

Deltares (2016), 'Lockfill, user and technical manual', Technical report, Deltares, Delft .

Jayaratne, R. (2010), 'Hydraulic roughness - links between manning's coefficient, nikuradse's equivalent sand roughness and bed grain size', *The School of Computing and Technology 5th Annual Conference, University of East London,* pp. 27–32.

Miozzi, M., Lalli, F. & Romano, G. (2010), 'Experimental investigation of a free-surface turbulent jet with coanda effect', *Springer-Verlag* .

O'Mahoney, T., De Loor, A. & Rietveld, M. (2015), 'Stroming door (rinket)schuiven, Validatie van CFD-berekeningen voor stroming in een sluis', Technical report, Deltares, Delft .

Rajaratnam, N. (1976), *Turbulent Jets*, Elsevier Science, Amsterdam.

Rijkswaterstaat (2000), *Ontwerp van schutsluizen*, Drukkerij Feiko Stevens, Emmeloord.

Rijkswaterstaat (2011), *Richtlijnen Vaarwegen 2011*, Delft.

Samson, A. (1972), 'THE FLOW OF LIQUID FROM A JET THROUGH A COMPRESSIBLE POROUS LAYER. PART II: THE IMPINGEMENT OF A PLANE FREE TURBULENT JET ON A FLAT IMPERVIOUS SURFACE', *The Journal of The Textile Institute,* **63**(9), 502–514.

Schwarz, W. H. & Cosart, W. P. (1960), 'The two-dimensional turbulent wall-jet', *Department of Chemical Engineering, Stanford University, Palo Alto, California,* pp. 481–495.

Shimada, N., Hibara, H., Ishibashi, Y., Sumida, M. & Sudo, K. (2004), 'Analysis of submerged water jets by visualization method', *Journal of Visualization,* **7**(4), 281–289.

Van der Ven, P. (2015), 'Memo lockfill ontwikkelingen december 2015', Technical report, Deltares, Delft .

Van der Ven, P., Van Velzen, G., O'Mahoney, T. & De Loor, A. (2015), 'Comparison of scale model measurements and 3d cfd simulations of loss coefficients and flow patterns for lock levelling systems', *SMART RIVERS,* **105**.

Van Rijn, L. (2011), *Principles of fluid flow and surface waves in rivers, estuaries, seas and oceans*, Aqua Publications, The Netherlands.

Van Velzen, G. & Dos Santos Nogueira, H. (2015), 'Stroming door (rinket)schuiven, modelonderzoek', Technical report, Deltares, Delft .

Vrijburcht, A. (1988), 'Het vulproces van een schutsluis met een langsvulsysteem, verslag berekeningen', Technical report, Rijkswaterstaat, Waterloopkundig Laboratorium, Delft .

Vrijburcht, A., Zhong-ging, J., Gilding, B. H., Bolt, E. & Van Kleef, E. A. (1988), 'Langskracht op een schip door de vulstraal in een sluis', Technical report, Rijkswaterstaat, Waterloopkundig Laboratorium, Delft .

# A

# CONSERVATION OF MASS AND MOMENTUM

This appendix is a supplement to Section 2.1 and contains the derivation of the mass balance and momentum balance. For an extensive coverage of the subject the reader is referred to Van Rijn (2011).

## A.1. DERIVATION OF THE MASS BALANCE

Considering an elementary control volume which is open on all sides. The dimensions of the control volume are given by $\Delta x * \Delta y * \Delta z$. The mass flow into minus the mass flow out of the volume in the positive $x$ direction is given by $\rho U \Delta y \Delta z - \rho U \Delta y \Delta z + \frac{\delta(\rho \Delta y \Delta z)}{\delta x} \Delta x$. In the same way a formulation can be made for the $y$ and $z$ direction. Adding the different directions yields a total balance which should be equal to zero. Dividing by the volume of the element and assuming constant density gives Equation A.1, which is called the continuity Equation.

$$\frac{\delta U}{\delta x} + \frac{\delta V}{\delta y} + \frac{\delta W}{\delta z} = 0 \tag{A.1}$$

Simplifying further by considering only one direction and reintroducing the density of the fluid $\rho$ will give the Equation as presented in subsection 2.1.1.

## A.2. DERIVATION OF THE 2D MOMENTUM BALANCE

The mass per unit of time with velocity $U$ passing through a small section with height $dz$ can be expressed by, $Mass = \rho U dz$. In order to find an expression for the momentum through this small section, the mass should be multiplied by the acceleration or the velocity per unit of time. Resulting in Equation A.2, when integrated over the depth, with a section height of h.

$$Momentum = \rho h U^2 \tag{A.2}$$

When considering a balance between two sections not only the mass flow needs to be considered, but also the force due to hydrostatic pressure at both sections and sources and sinks for forces between the sections. The formulation for hydrostatic pressure is as in Equation A.3, with h the water depth.

$$Pressure = \frac{1}{2} \rho g h^2 \tag{A.3}$$

Taking the different components into account the balance between two sections, 1 and 2, can be made using Equation A.4.

$$P_1 - P_2 + M_1 - M_2 - F = 0 \tag{A.4}$$

Where:

$P$ = the force due to pressure at the section defined in the subscript $[N]$
$F$ = a force sink, for example friction $[N]$
$M$ = the force due to mass transport at the section defined in the subscript $[N]$

# B

# DERIVATION OF THE LOCKFILL FORMULATIONS

This appendix is a supplement to section 2.2. It provides the reader a more technical in depth explanation of the calculation approach in Lockfill, by reproducing the derivation of the force equations. Not every derivation step will be presented, for more information the reader is referred to Vrijburcht (1988) or De Loor (2012).

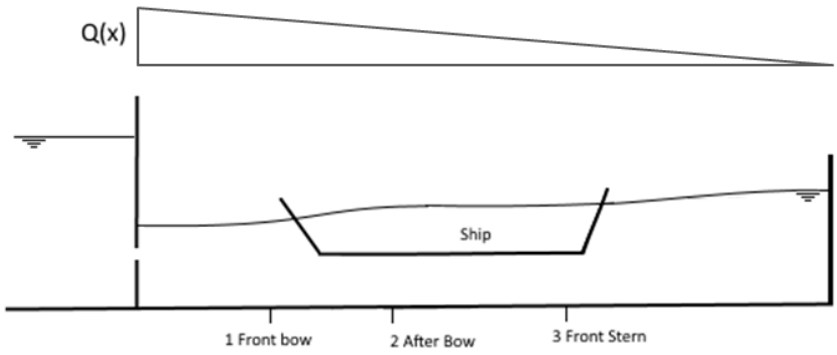


Figure B.1: Locations for the momentum balance in Lockfill and the decrease of the discharge in horizontal direction

## B.1. MOMENTUM BALANCE AT THE BOW OF THE SHIP

The momentum balance Equation B.1 can be formulated between point 1 and point 2. In Figure B.1 the location of these points is visualised.

$$\frac{1}{2}\rho g h_1^2 w_l - (\frac{1}{2}\rho g h_2^2 w_l - \frac{1}{2}\rho g d_s^2 w_s) - F_b + \rho Q_1 U_1 cos(\alpha) - \rho Q_1 U_2 = 0 \tag{B.1}$$

Where:

$h$ = the depth at the location defined in the subscript $[m]$
$w_l$ = the width of the lock $[m]$
$d_s$ = the depth of the ship $[m]$
$w_s$ = the width of the ship $[m]$
$F_b$ = the force on the bow of the ship $[m]$
$Q$ = the discharge at the location defined in the subscript $[m^3/s]$
$U$ = the velocity at the location defined in the subscript $[m/s]$

Using the continuity law, Equation B.2 and Equation B.3 can be formulated. In Figure B.1 the decrease of the discharge over the length of the lock is schematised.

$$Q_1 = \frac{l_l - x_b}{l_l} Q_0 \tag{B.2}$$

$$(h_2 w_l - d_s w_s) U_2 = Q_1 \tag{B.3}$$

Where:

$l_l$ = the length of the lock $[m]$
$x_b$ = the distance between the gate and the ship $[m]$
$Q$ = the discharge at the location defined in the subscript (0 is at the gate) $[m^3/s]$

The force on the bow of the ship contains a term for the hydrostatic pressure (first term in Equation B.4) and a term for the deviation of the hydrostatic pressure due to the filling jet (second term in Equation B.4). The second term is a formulation for pressure increase due to an impinging jet on an inclined plate. Both the angle of the bow of the ship and the angle of the jet with the horizontal are taken into account.

$$F_b = \frac{1}{2}\rho g (h_1 - h_2 + d_s)^2 w_s + C_1 C_2 \rho Q_1 U_1 sin(\alpha + \beta) sin(\beta) \tag{B.4}$$

Where:

$C_1$ = a coefficient for the decrease in pressure due to the flow along the bow [-]
$C_2$ = a coefficient for the amount of momentum of the jet that actually hits the bow of the ship [-]
$\alpha$ = the angle of the jet with the horizontal [°]
$\beta$ = the angle of the bow with the horizontal [°]

Combining Equation B.1, B.2, B.3 and B.4 results in an expression for the difference in water level between cross-section 1 and 2, see Equation B.5. For simplification it is assumed that the difference in water level is very small compared to the water depth in the lock. Notice that the left part is the effect of the mean flow induced by the jet, while the right part is the effect of the jet itself.

$$h_1 - h_2 = \frac{-Q_1 U_1 cos(\alpha) + \frac{Q_1^2}{h_1 w_l - d_s w_s}}{g(w_l h_1 - w_s d_s)} + \frac{C_1 C_2 Q_1 U_1 sin(\alpha + \beta) sin(\beta)}{g(w_l h_1 - w_s d_s)} \tag{B.5}$$

The formulation for the direct force of the filling jet against the bow originates from the expression for the force of a jet against a perpendicular plate $\rho UQ$. This assumes that the total velocity momentum in the x direction is deflected and converted into a force on the plate. How the angles of the bow and the jet influence the force is not explained in Vrijburcht (1988). This can however be explained using geometry laws, see Figure B.2. Starting with a filling jet vector with a known force $F$, the force perpendicular to the plate can be determined with $F_p = F * sin(\alpha + \beta)$. The red angle is proven to be equal to $\beta$, because helpline 1 is parallel to the bow of the ship. The purple angle is equal to $\beta$ as well. This can be proven using $purpleangle + b = 90°$, $a + b = 90°$ and $a = \beta$. Now follows $F_x = F_p * sin(\beta)$. Combining the two operations results in the equation given in Vrijburcht (1988), $F_x = \rho UQ sin(\alpha + \beta) sin(\beta)$.

## B.2. MOMENTUM BALANCE ALONG THE HULL OF THE SHIP

Equation B.6 can be found for the momentum balance between point 2 and 3. Including the friction along the hull $F_{hf}$ and the friction along the walls of the lock $F_{lf}$. These friction forces are determined using Chézy and Stickler and White-Colebrook, assuming an equal distribution of the flow over the available wet cross-section. Furthermore, the Nikuradse-roughness of the ship and the lock walls needs to be known or estimated. A coefficient $C_3$ is introduced to compensate for the fact that the flow is not instantaneously fully developed after the bow.

$$\frac{1}{2}\rho g h_2^2 w_l - \frac{1}{2}\rho g d_s^2 w_s - \frac{1}{2}\rho g h_3^2 w_l + \frac{1}{2}\rho g d_s^2 w_s - \rho g d_s l_s \frac{h_2 - h_3}{l_s} - F_{hf} - F_{lf} + \rho Q_2 U_2 - \rho Q_3 U_3 = 0 \tag{B.6}$$

Where:

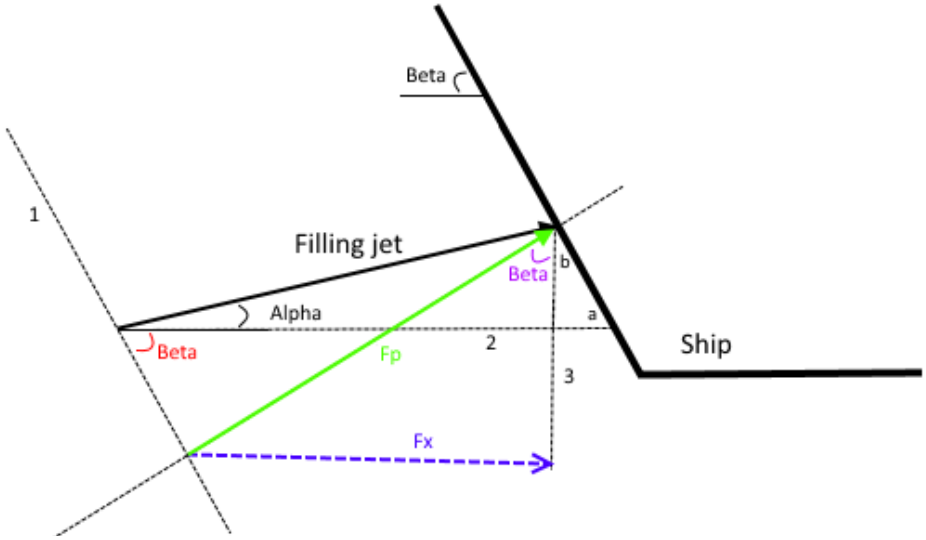


Figure B.2: Geometrical proof of $F_x$ against the bow

$h$ = the depth at the location defined in the subscript $[m]$
$Q$ = the discharge at the location defined in the subscript $[m^3/s]$
$v$ = the velocity at the location defined in the subscript $[m/s]$
$l_s$ = the length of the ship $[m]$

Assuming the difference in water level is relatively small compared to the water depth in the lock, Equation B.7 can be found. The local discharge can be expressed in the initial discharge $Q_0$ using conservation of mass and the assumption that the discharge decreases linearly over the length of the lock.

$$h_2 - h_3 = \frac{-Q^2}{g(h_2 w_l - d_s w_s)^2} \frac{(2l_l - 2x_b - l_s)l_s}{l_l^2} + \frac{F_{hf} + F_{lf}}{\rho g(h_2 w_l - w_s d_s)} \tag{B.7}$$

Now Equation B.8 can be formulated for the total force on the hull of the ship. Here the first term originates from the force induced due to the water level difference between the bow and the stern and the second term is the direct friction force of the water flow along the hull.

$$F_h = \rho g(h_2 - h_3) d_s w_s + F_{hf} \tag{B.8}$$

## B.3. HYDROSTATIC FORCE AGAINST THE STERN OF THE SHIP

It is assumed that the flow separates at the stern of the ship. This implies that a hydrostatic force is present at this location, see Equation B.9.

$$F_s = \frac{1}{2}\rho g w_s d_s^2 \tag{B.9}$$

## B.4. TOTAL FORCE ON THE SHIP CATEGORISED BY FORCING MECHANISM

The next step is to combine the different forces $F_b$, $F_h$ and $F_s$, using Equations B.4, B.8 and B.9. For the water level differences Equations B.5 and B.7 are used. For the local water depths that did not yet cancel out of the equations an average water depth $h_l$ is introduced. This assumes that the water level differences are relatively small compared to the depth. The final step is to split the total force equation into separate equations which are categorised by forcing mechanism. These are the equations that are used for the Lockfill calculations. A distinction is made between:

1. The force resulting from the momentum over the length of the lock ($F_{md}$), Equation B.10.
2. The direct force from the filling jet on the bow of the ship ($F_{fj}$), Equation B.11.

3. The friction between the water flow and the hull, wall and chamber floor ($F_f$), Equation B.12.

$$F_{md} = \rho(\frac{d_s w_s}{h_l w_l - d_s w_s})(-Q\frac{l_l x_b}{l_l}U_1 cos(\alpha) + \frac{Q^2}{h_l w_l - d_s w_s}(\frac{l_l - x_b - l_s}{l_l})^2) \tag{B.10}$$

$$F_{fj} = \rho(\frac{h_l w_l}{h_l w_l - d_s w_s})(C_1 C_2 Q\frac{l_l - x_b}{l_l}U_1 sin(\alpha+\beta)sin(\beta)) \tag{B.11}$$

$$F_f = (\frac{d_s w_s}{h_l w_l - d_s w_s})F_{lf} + (\frac{d_l w_l}{h_l w_l - d_s w_s})F_{hf} \tag{B.12}$$

The force due to the decrease of momentum has a lot of different components. To give more insight into what these components are Equation B.10 can be split into into two separate equations. Giving Equation B.13 for the component resulting from the decrease of momentum over the bow and Equation B.14 for the component resulting from the decrease of momentum over the hull. The first term in Equation B.13 is a result of the direct flow induced due to the filling jet and the second term originates from the mean flow.

$$F_{md12} = \rho(\frac{d_s w_s}{h_l w_l - d_s w_s})(-Q\frac{l_l x_b}{l_l}U_1 cos(\alpha) + \frac{Q^2}{h_l w_l - d_s w_s}(\frac{l_l - x_b}{l_l})^2) \tag{B.13}$$

$$F_{md23} = \rho(\frac{d_s w_s}{h_l w_l - d_s w_s})(-\frac{(2l_l - 2x_b - l_s)l_s}{l_l^2}Q^2) \tag{B.14}$$

# C

# DETAILS ABOUT THE CFD MODEL

This appendix is a supplement to section 3.5. To keep the main text clear and without to much unnecessary detail, some more detailed information about the settings of the CFD model can be found here.

## C.1. MESH

Besides the trimmed cell mesher the prism layer mesher is used to create a finer grid along the boundaries of solid structures. This mesh operation creates smaller cells near a solid surface, which then get increasingly larger until they have the same size as the surrounding cells. The intention of the refinement in the prism layer is to calculate the boundary flow more accurately. The velocity gradients are often higher near a boundary and thus more cells are required.

Table C.1: Local refinements in the CFD mesh

| Location | Percentage of base size x direction | Percentage of base size y direction |
|---|---|---|
| Atmosphere | 100 | 100 |
| Water level downstream of the gate | 20 | 20 |
| Water surrounding the ship | 10 | 10 |
| Water surrounding the gate | 2.5 | 2.5 |
| Around the water surface | 25 | 2.5 |
| Gate opening | 1 | 1 |

In Table C.1 the local refinements in the mesh for each location are given. The refinements are expressed in percentages of the base size, with the base size being 0.25 meter. In case of an overlapping refinement the refinement with the finer mesh is normative. This results in the mesh presented in Figure 3.2 in Subsection 3.5.1, only the area of interest is displayed to ensure a clear image.

## C.2. BOUNDARY CONDITIONS

Table C.2 displays the selected boundary conditions for the domain. A no-slip wall induces that the calculation obeys the law of the wall, which states that the relative fluid velocity tangential to the wall is zero. In a free and stationary flow this will result in a logarithmic velocity profile.

Table C.2: Boundary conditions for each boundary in the domain

| Location | Type of boundary condition |
|---|---|
| Upper edge | Pressure outlet |
| Upstream inlet | Stagnation inlet |
| Downstream outlet | Pressure outlet |
| Bottom | No-slip wall |
| Sides of the flume | No-slip wall |
| Ship and lock door | No-slip wall |

# D

# IMAGES OF THE SCALE MODEL TEST SETUP

In this appendix some images of the scale model test setup are included. These images were made during the scale tests. The purpose of these images is to get a better idea of the measurement setup and the used materials.

(a) Pump one, used to regulate the discharge

(b) Pump two, used to create a steady discharge

Figure D.1: The two pumps used to realise the discharge in the flume

(a) Perforated boxes to stabilise the water flow at the entrance of the flume

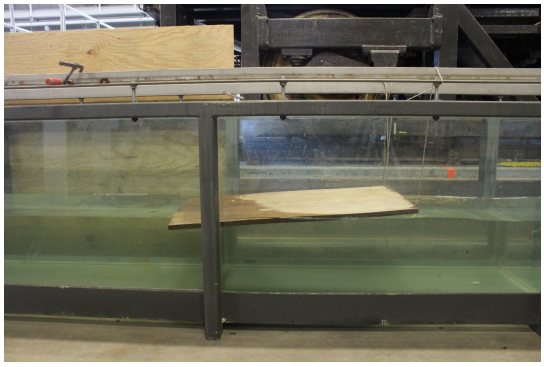

(b) Plate on the water surface to prevent reflecting waves near the end of the flume

Figure D.2: Structures to regulate the hydrodynamic conditions

(a) Overview of the PIV setup

(b) Camera position for the PIV measurements

Figure D.3: Some photo's concerning the PIV setup

(a) For the case without ship

(b) For the case with ship

Figure D.4: The water surface stabilisation structures

# E

# TABLES WITH RESULTS FROM THE FORCE MEASUREMENTS

The results from the force measurements are displayed in the figures in Section 5.3. However for a complete overview and for the purpose of presenting the exact values the results will also be tabulated in this appendix. The results for variations in keel clearance are displayed in Table E.1, the results for variations in distance between the gate and the ship are displayed in Table E.2 and the results for variations in water level difference are displayed in Table E.3. All the measurement results are made available at http://researchdata.4tu.nl, the DOI of the dataset is 10.4121/uuid:0aff8af7-9baa-40be-8f4f-45bed1b31062.

Table E.1: Forces and discharge measured for variations in keel clearance

| Keel clearance $k_c$ [m] | Measured force $F_x$ [N] | Discharge through the gate $Q$ [$m^3/s$] |
|---|---|---|
| 0.07 | 46.2 | 41.5 |
| 0.08 | 10.5 | 41.8 |
| 0.09 | -3.0 | 41.8 |
| 0.10 | -11.7 | 41.8 |
| 0.15 | -22.1 | 41.9 |
| 0.17 | -22.3 | 41.9 |

Table E.2: Forces and discharge measured for variations in distance between the gate and the ship

| Distance $X_{bow}$ [m] | Measured force $F_x$ [N] | Discharge through the gate $Q$ [$m^3/s$] |
|---|---|---|
| 0.6 | 46.2 | 41.5 |
| 0.8 | 40.1 | 41.7 |
| 1.05 | 55.2 | 41.1 |
| 1.55 | 70.4 | 41.2 |

Table E.3: Forces and discharge measured for variations in water level difference over the gate

| Water level difference $\triangle h$ [m] | Measured force $F_x$ [N] | Discharge through the gate $Q$ [$m^3/s$] |
|---|---|---|
| 0.20 | 46.2 | 41.5 |
| 0.15 | 34.1 | 35.1 |
| 0.10 | 19.3 | 28.6 |

# F

# LOCKFILL FORMULATIONS WITHOUT DECREASE OF THE DISCHARGE OVER THE LENGTH OF THE LOCK

This appendix is a supplement to Chapter 6. Because the measurements were performed under stationary conditions the discharge does not change over time nor over the length of the lock. To make a comparison with Lockfill possible the terms in the equations of Lockfill that represent the decrease of discharge over the length of the lock need to be removed. Mathematically this can be realised by taking an infinite length for the lock chamber, $l_l = \infty$. The terms that consider the length of the lock will then drop out of the equations making a comparison with the measurements possible. Furthermore, to meet the requirement of mass balance the discharge in every section of the lock must be the same. Most of the equations are already provided in Appendix B, however for a complete overview each equation needed for the comparison with the measurements will be given in this appendix.

Like in Appendix B the momentum is calculated at three positions: In front of the bow, after the bow and at the stern. For the current derivation Equation F.1 holds, meaning that the discharge remains constant.

$$Q = Q_0 = Q_1 = Q_2 = Q_3 \tag{F.1}$$

Where:

$Q$ = the constant discharge downstream of the gate $[m^3/s]$

The force against the bow can be described with Equation F.2 and the water level difference over the bow with Equation F.3. The momentum flux in front of the ship $S_b$, is in Lockfill determined by a parameterized schematisation of the jet. In general the following expression holds $S_b = \rho U Q$. The coefficient $C_2$ is defined as the cross-sectional area of the ship blocking the jet divided by the total cross-sectional area of the jet at the bow.

$$F_b = \frac{1}{2}\rho g(h_1 - h_2 + d_s)^2 w_s + C_1 C_2 S_b sin(\alpha+\beta) sin(\beta) \tag{F.2}$$

$$h_1 - h_2 = \frac{-\frac{S_b}{\rho} cos(\alpha) + \frac{Q^2}{h_l w_l - d_s w_s}}{g(w_l h_l - w_s d_s)} + \frac{C_1 C_2 \frac{S_b}{\rho} sin(\alpha+\beta) sin(\beta)}{g(w_l h_l - w_s d_s)} \tag{F.3}$$

Where:

$S_b$ = the momentum flux in the jet just in front of the bow $[kgm/s^2]$

The force on the hull of the ship can be calculated using Equation F.4 and the water level difference over the hull with Equation F.5.

$$F_h = \rho g(h_2 - h_3) d_s w_s + F_{hf} \tag{F.4}$$

$$h_2 - h_3 = \frac{F_{hf} + F_{lf}}{\rho g(h_l w_l - w_s d_s)} \tag{F.5}$$

The friction terms can be calculated with Equations F.6, F.7, F.8 and F.9. The coefficient $C_3$ represents the measure of the boundary layer development. A value of 1 meaning a fully develop boundary layer and a value of 0 meaning no boundary layer. The default setting is $C_3 = 1$.

$$F_{hf} = C_3 \rho g (\frac{Q}{h_l w_l - d_s w_s})^2 \frac{(w_s + 2d_s) l_s}{C^2} (\frac{k_{II}}{k_I})^{\frac{1}{4}} \tag{F.6}$$

$$F_{lf} = C_3 \rho g (\frac{Q}{h_l w_l - d_s w_s})^2 \frac{(w_l + 2h_l) l_s}{C^2} \tag{F.7}$$

$$C = 18 log(\frac{12R}{k_I}) \tag{F.8}$$

$$R = \frac{h_l w_l - d_s w_s}{(\frac{k_{II}}{k_I})^{\frac{1}{4}} * (w_s + 2d_s) + (w_l + 2h_l)} \tag{F.9}$$

Where:

$C_3$ = a measure for boundary layer development [-]
$k_I$ = the Nikuradse roughness of the lock [-]
$k_{II}$ = the Nikuradse roughness of the ship [-]

Hydrostatic pressure is assumed against the stern of the ship, see Equation F.10.

$$F_s = \frac{1}{2} \rho g w_s d_s^2 \tag{F.10}$$